PhD Program in Translational and Molecular Medicine

University of Milano-Bicocca
Department of Medicine and Surgery

MLL rearranged infant acute lymphoblastic leukemia: unravelling the functional role of the RNA-binding protein Musashi-2 (MSI2) and identifying novel therapeutic strategies

Coordinator: Prof. Francesco Mantegazza

Tutor: Dott. Giovanni Cazzaniga

Co-Tutor: Dott.ssa Michela Bardini

Candidate: Luigia Valsecchi

Matr: 863283

XXXV cycle

Academic Year
2021/2022

TABLE OF CONTENTS

CHAPTER 1

GENERAL INTRUDUCTION

Childhood Leukemia

Leukemias are a group of malignant disorders of the blood and bone marrow characterized by a differentiation arrest and a monoclonal expansion of one hematopoietic stem cell (HSC). This cell (leukemic blast) is blocked in a stage of differentiation, starts to proliferate in an uncontrolled way and its progeny takes over the normal hematopoietic stem cells. It follows that the normal hematopoiesis and the homeostasis is compromised[1]. Leukemia is the commonest childhood cancer.

Clinical Aspects, Classification and Incidence

At the onset of the disease, principal clinical signs and symptoms are nonspecific like: anemia, thrombocytopenia and neutropenia lead to pallor, fatigue, petechiae, bruising, bleeding, and fever. Following, the extramedullary infiltration of the leukemic blast into other organs (primarily blood, spleen, liver) can cause lymphadenopathy, hepatomegaly and splenomegaly. Headache, vomiting, and lethargy are indicators of central nervous system (CNS) metastasis[2].

Diagnosis of these patients is based initially on morphological and histological analysis of bone morrow (BM) and peripheral blood (PB) samples, followed by more specific cytogenetic and molecular analysis, that allow to discriminate between different Leukemia subgroups and to select the correct therapeutic strategy[3].

Leukemia can be divided in different subgroup with specific biological and clinical feature and the classification of these groups depends on the onset, the evolution, the stage of tumor cells differentiation and the rate of disease progression[3].

The First distinction is between **acute** and **chronic** leukemias and it is related to the natural development and outcome of the disease without treatment. Indeed, in the chronic leukemia the disease onset is late, generally asymptomatic and the course of the disease slower; instead, in the acute leukemia the disease onset is sudden with acute symptoms and the development is very rapid with poor outcome.

Leukemia is also classified according to the "lineage" of the leukemic blast into **lymphoid** leukemia or **myeloid** leukemia. Therefore, the four most common types of leukemia are: **chronic myeloid leukemia (CML)**, **acute myeloid leukemia (AML)**, **chronic lymphocytic leukemia (CLL)**, and **acute lymphoblastic leukemia (ALL)**[4]. CLL and ALL are in turn subdivided into **B-** or **T-** CLL/ALL, depending on whether they are B or T lymphocytes, respectively.

In addition, the French–American–British (FAB) cell-classification system, adopted in the mid-1970s, classified the AML in eight groups (M0-M7) and the ALL in three groups (L1-L3) based on morphological and phenotypic features of the leukemic cells.

The chronic forms of leukemia (CML and CLL) occur mainly in the elderly patients, instead the AML is present mainly in adult patients

and the ALL is the most frequent type of tumor occurring in childhood.

Childhood leukemia with the rearrangement of the MLL gene on chromosome 11q23, the topic of my thesis, does not completely fit into this classification and therefore represents a sort of exception, since leukemic blasts express surface markers belonging to both lymphoid and myeloid "lineages". For this reason, it is defined as **bi-phenotypic leukemia** or **mixed "lineage**".

Pathogenesis and Etiology

Like other type of cancers, the onset of leukemia results from cumulative combination of several factors: etiological factors, inherited susceptibility and exposure to internal/external environmental factors. Regarding genetic factors, some congenital genetic abnormalities and genetic syndromes presenting an intrinsic genomic instability have been linked to predisposition to childhood ALL including Down's syndrome (constitutive chromosome 21 trisomy), Fanconi anemia (FA), germline mutations in p53, PAX5 and ETV6, and polymorphic variants in specific genes including ARID5B, CEBPE, GATA3 and IKZF1[5,6].

Regarding environmental risk-factors, it has been clearly established that the ionizing radiations is related to the development of CML, AML and ALL in a dose-dependent manner; for the other candidates (i.e. cytotoxic drugs, pesticides, consumption of alcohol and tobacco

and non-ionizing electromagnetic fields) only mild associations have been demonstrated[7]. Finally, in the past century, the infections were considered as a pathogenetic mechanism for the development of childhood leukemia.

Acute Lymphoblastic Leukemia in Children: Incidence, Cytogenetic and Molecular Basis

Acute lymphoblastic leukemia (ALL) is a heterogeneous hematological disease characterized by clonal proliferation of immature lymphoid cells. It is the most frequent malignancy among pediatric patients under the age of 15 years, with a peak of incidence in children aged 2-5 year and about 40 new cases per million per year in Italy. ALL occurs in the 80% of all de novo leukemia cases during childhood, while it is less frequent in adults representing only 20% of leukemic types in old age. The absolute number of new diagnoses of ALL per year in Italy is 350-400. (https://www.airc.it)

The cell of origin of this disease can be the B lymphocyte, 80% of the cases, or the T lymphocyte, in the remaining 20%. (https://www.aiom.it)

Genetic or chromosomal abnormalities, such as aneuploidy, chromosome translocations and/or deletions, but also point mutations, occur very frequently in ALL and can be identified in over 80% of the patients. These genetic alterations represent the cause of leukemic transformation of the cell of origin (HSC or committed

progenitors) by modifying cellular functions. The identification of these alterations is important to confirm the diagnosis and to predict the patients' prognosis. The genetic aberrations can be either numerical or structural[8].

Reciprocal translocations are the most common cytogenetic mutation of childhood leukemias and are caused by a break and exchange of genetic material between two chromosomes leading to the expression of a fusion gene. The majority of these mutations is well characterized both clinically and molecularly and has a causative role in leukemogenesis.

These genetic mutations (translocations, hyperdiploid and hypodiploid karyotypes) are important in leukemia initiation, but alone are not enough to generate a full leukemic phenotype, indicating that cooperating oncogenic lesions are required. Indeed, the "two hits model" proposed by Mel Graves based on the idea that the natural history of the onset and progression of leukemia includes two distinct and successive phases. The initiating event normally happens *in utero* and is involved in the neoplastic transformation of the HSC cells ("first Hit"); but it is not enough to develop the clinical leukemia because it's necessary a secondary (or several) post-natal mutation ("second Hit")[9]. Exceptions to this model are the MLL-fusions, in which the MLL rearrangement is by itself sufficient to rapidly induce leukemia. Indeed, this highly aggressive leukemia

shows a very short disease latency and presents few somatic mutations[10].

Infant Acute Lymphoblastic Leukemia with MLL Rearrangement

The ALL with onset in the first year of life is a high-risk, rare but very aggressive subtype of leukemia with an incidence of 10-11 new cases per year in Italy. Infant ALL has the worst outcome of all others pediatric leukemias, with event free survival (EFS) rates of ~20%–40% compared to EFS rate of ~80% in children older than one year of age. Additionally, infant ALL patients with age < 3 months at diagnosis, WBC count > 100,000/ μL or the t(4;11) translocation have an EFS rate of only ~5%[11,12].

Clinical Aspects and Incidence

Patients with MLLr ALL typically present hyperleukocytosis, early onset, aggressive clinical characteristics at diagnosis including high white cell count and extramedullary involvement with frequent involvement of the central nervous system (CNS) and poor prognosis due to high incidence of relapse[13].

About 80% of infant patients show the rearrangement of the histone-lysine N-methyltransferase 2A (KMT2A) gene, also known as MLL (mixed lineage leukemia), on the short arm of chromosome 11 (11q21). The incidence of MLL rearranged leukemia is strictly age-related because affects more than 80% of newly diagnosed ALL in infants (< 1 year of age), 5–6% of pediatric cases and 15% of adult cases. In infants, the median age of diagnosis is 4 months, whereas in

adults, incidence increases with age, with a median age at diagnosis occurring between 38 and 43 years[14].

Pathogenesis and Etiology

In addition to spontaneously arising leukemia, it has been discovered that Topoisomerase II inhibitors (such as etoposide) are associated with development of MLLr ALL in therapy-related cases. Topoisomerase II is an enzyme essential for the unfolding of supercoiled DNA during chromatin remodeling processes and for the repair of DNA double strand breaks. The inhibitors induce the formation of a stable ternary complex with the enzyme and DNA and, therefore the double-strand breaks are most likely to be repaired by non-homologous end joining system.

Interestingly, studies investigating the exposures of patients' parents to bioflavonoids found in foods and herbal compounds suggested that these could inhibit the topoisomerase II and promote rearrangement of the MLL locus.

Additionally, it seems that also ionizing radiations could activate some proteases, independently of topoisomerase II, which in turn can cleave the MLL gene[15].

Biological and Molecular Features

The MLLr ALL patients typically express the pan-leukocyte CD19 antigen and the stem cell marker CD34; in addition, the leukemic blast has a very immature pro-B immunophenotype characterized by absence of CD10, CD20 and CD24 (antigens typical of more mature lymphocyte), lack of mature immunoglobulins and intermediate expression of CD45. Moreover, MLLr blast cells simultaneously co-express lymphoid and myeloid-associated antigens such as CD13, CD15, CD33, and CD65. This peculiarity confers to leukemia a biphenotypic or '**Mixed Linage'** feature and gives the name to the gene MLL (Mix Lineage Leukemia)[14,15].

MLLr is not only associated to BCP-ALL, but also to AML. The lineage specificity of resulting leukemia is related to the partners of MLL in the rearrangement. Indeed, MLL has many known gene translocation partners, the most common are AFF1 (AF4), MLLT3 (AF9), and MLLT1 (ENL); other less common fusion partners are AF10 and AF6. The MLL::AF4 fusion protein generated from the translocation t(4;11) represents overall the most common translocation (being found in ~ 50% and 75% of infants and adult MLLr leukemia, respectively) and it is almost exclusively associated to a BCP-ALL phenotype. AF4 interacts with cyclin-dependent kinases promoting transcriptional elongation and with SL1 (selectivity factor 1) implicated in direct recruitment of RNA polymerase II to the targets. The MLL::AF9 protein, derived from the translocation t(9;11), is mostly associated

to myeloid leukemias; while the MLL::ENL protein, derived from the translocation t(11;19) rearrangement is found in both lymphoid and myeloid leukemias[13].

Infant ALL with t(4;11) is characterized by a lineage plasticity with a propensity to undergo spontaneous myeloid **lineage switch** at relapse or during treatment. The intrinsic ability of the blast cells to switch lineage can be the results of a mechanism of therapy escape (under the pressure of a targeted CD19 CAR-T therapy for example) and may be due to the fact that the cell of origin in which the leukemia originally arose is an early stem cell-like precursor retaining leukemia potential to differentiate towards both myeloid and lymphoid lineages.

Sticking evidences have demonstrated that several chromosome translocations commonly found in pediatric leukemia occur in utero. The first evidence comes from the observation of the clonal relationship (concordance) of leukemia occurring in monochorionic twin pairs. The second evidence comes from the retrospective screening of genomic DNA breakpoint sequence assessed in neonatal blood spots (GUTHRIE CARDS) demonstrating that the pre-leukemic clone was already present at birth.

Studies conducted in identical twin patients affected by ALL have clearly demonstrated that they shared a MLL rearrangement with the same breakpoints with a concordance of almost 100%. This clinical phenomenon was first recorded in 1882 and then explained in 1975

by Boyse and Clarkson, which suggested that the fusion originates in one fetus and then metastasizes to the other through the shared placental blood circulation. The retrospective Polymerase chain reaction (PCR) analysis of neonatal blood-spot has indeed confirmed the prenatal origin (in uterus) of many leukemias, including MLL rearranged infant leukemia, TEL::AML1+ ALL and AML1::ETO+ AML. The E2A::PBX1 fusion generated by the t(1;19) is an exception because might arise predominantly postnatally in BCP cells and most neonatal blood spots are indeed negative for E2A::PBX fusion sequences. These findings have subsequently been confirmed by other studies using clonotypic IGH sequences in blood spots further reinforcing the hypothesis that the pre-leukemic clone arises before birth[16-19].

These studies have provided great insights into the peculiar characteristics of MLLr ALL in infants. First, postnatal latency of disease onset is short by definition, with a diagnosis after a few days or months of birth compared with other BCP-ALL in older children, who typically develop the disease later on after birth, and the latency could be protracted for several years. Second, in monochorionic twins with infant ALL the concordance rate is close to 100% compared to a concordance rate of 5–10% in older children (Figure 1). The main explanation of these features is that in MLLr infant ALL the MLL-fusion gene is sufficient itself to cause leukemia, while the other translocations require additional, postnatal genetic hits to

induce leukemia. Therefore, MLLr infant ALL seems to be an exception to the classical "two-hits hypothesis" by Mel Greaves[9].

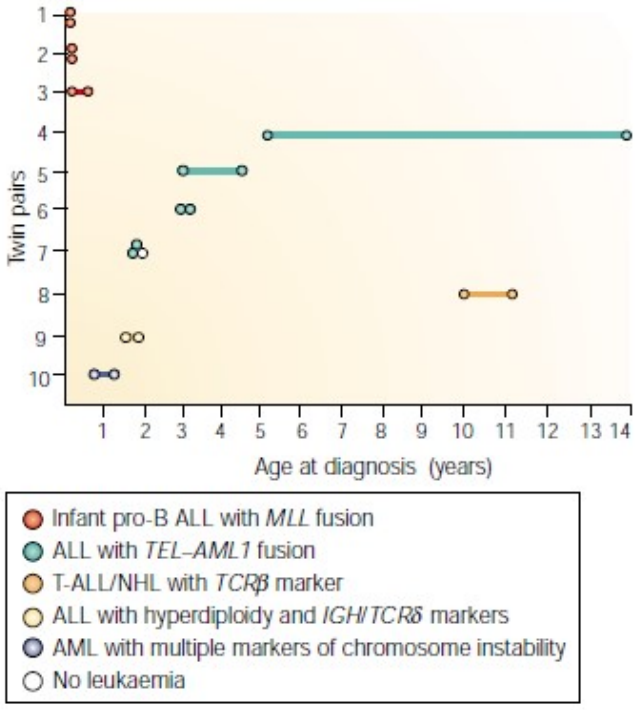

Figure 1: Concordant acute leukemia in identical twins share identical (clonotypic) genomic rearrangements. (Adopted from: Nat Rev Cancer, 2003; Mel F Greaves): A summary of twin pairs who are concordant for acute leukemia and have been analyzed for molecular markers of clonality. The colored circles indicate the age at diagnosis for each twin pair (numbered 1–10). The subtype of leukemia for each twin pair and the molecular markers used to show clonality are given in the key. Set 7 were triplets; two monozygotic twins in this set had acute lymphoblastic leukemia (ALL), the third triplet was dizygotic and healthy. In all of these 10 pairs of twins, the leukemic cells shared one or more unique or clonotypic

molecular markers, which is indicative of a single-cell origin in one twin, followed by 'metastasis' through the shared placenta to the other twin in utero.

Another important characteristic of MLLr ALL is that it originates in fetal hematopoietic stem and progenitor cells, which are present only in fetal life and absent in postnatal life[20]. This type of cells is characterized by a specific molecular program and transcriptional pathways with a prominent proliferative and oncogenic nature that persists in infant ALL blasts[21]. Rice et al, created a model by engineering the primary human fetal liver hematopoietic cells with CRISPR-Cas9 gene editing to produce a t(4;11)/MLL::AF4 translocation and therefore replicates the fetal-specific gene expression programs. These engineered cells gave arise a potent infant-like leukemia in vivo with also secondary organs infiltration, including CNS, and recapitulated the molecular phenotype of MLLr infant ALL. Then, by using this model, the authors demonstrated that the fetal-specific gene expression programs are maintained in MLL::AF4 infant-ALL but not in MLL::AF4 childhood-ALL[22].

MLL Gene and Protein Structure

The MLL gene is also termed ALL1, HRX and HTRX and is involved in reciprocal chromosome translocations in children and adults with acute lymphoblastic leukemia (ALL) or acute myeloid leukemia (AML)[23].

The MLL gene structure was first described by both Tkachuk et al. and Gu et al. The first one in 1992 demonstrated that the gene, involved in recurring 11q23 leukemic translocations in children under the age of 1 year, coded for a large protein that was a Human homolog of Drosophila trithorax and was involved in homeotic gene regulation[24]. The second one better characterized the MLL gene structure and identified chimeric transcripts produced in cells with the t(4;11) chromosome translocation[25].

When MLL was deleted in heterozygosity (+/-) in mice in embryonic stem cells, mice displayed a delay in growth, hematopoietic abnormalities, bidirectional homeotic transformations of the axial skeleton and sternal malformations; when the deletion was homozygous (-/-), it was lethal. These studies demonstrated that MLL gene has a role in embryonic development and hematopoiesis[26].

MLL gene was also renamed KMT2A to reflect its lysine methyltransferase function, and to avoid confusion with the clinical term mixed lineage leukemia. KMT2A has a wide range of targets, including regulators of hematopoietic cell proliferation and differentiation Meis homeobox 1 (MEIS1) and the homeobox A (HOXA) gene cluster. MLL is a gene of 90kb formed by 37 exons[27] and encodes for a large (431-kDa, 3968 ammino acid), multi-domain nuclear protein expressed in hematopoietic cells including stem and progenitor population.

As regards to the MLL structure, from N- to C- terminus, the protein is composed of three **AT-hook motifs**, binding to AT-rich DNA sequences, followed by two speckled nuclear localization motifs (**SNL1** and **SNL2**) and two repression domains (**RD1** and **RD2**), the first of which (RD1) also contains a CxxC domain. CxxC zinc-finger motif is homologous to DNA methyltransferase 1 (DMT), which methylates cytosine residues of DNA and recruit HPC2 and the transcriptional co-repressor CtBP34. RD2 recruits the histone deacetylases HDAC1 and HDAC2. In the middle part of MLL there are four plant homeodomain (**PHD**) fingers, which mediate protein–protein interactions; in particular, the third PHD finger interacts with the cyclophilin CYP33, which is important for negative regulation of MLL target genes. Further downstream, after the two-cleavage site (**CS1** and **CS2**), there is the **transcriptional activation** domain that recruits CREB-binding protein (CBP), a histone acetyltransferase that activates gene expression. The *C*-terminal portion contains a **SET** (Suppressor of variegation 3–9, enhancer of zeste, trithorax) domain, homologous to that of *Drosophila* trithorax and responsible for methylation of H3K4. These latter four domains (PHD finger, bromodomain, activation domain, and SET domain) are all lost in most MLL fusion proteins[28]. (Figure 2a)

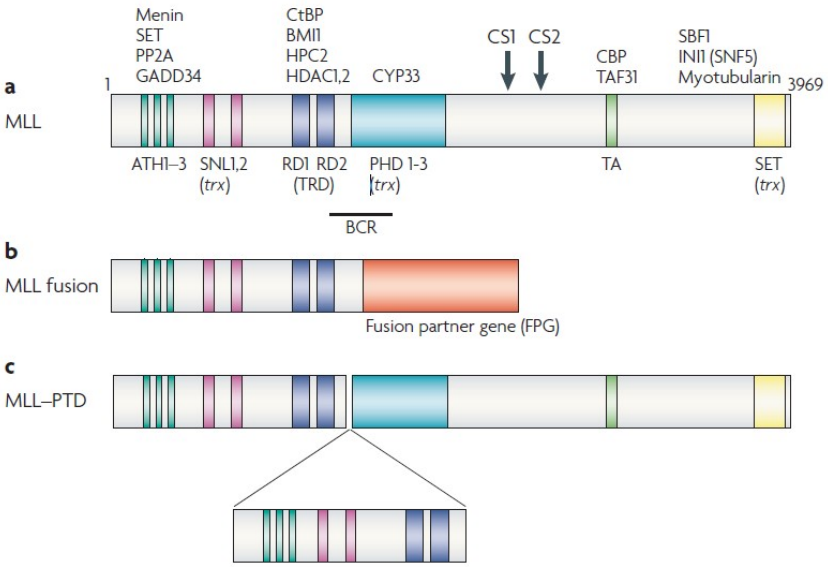

Figure 2: Schematic representation of the MLL wild-type and MLL rearrangements. (Adopted from: NatRevCancer, 2007; Krivtsov AV, Armstrong SA)

MLL is post-transcriptionally regulated by the taspase-1 enzyme, which cleaves MLL into two subunits: the 320-kDa *N*-terminal fragment (MLL^N) and the 180-kDa *C*-terminal fragment (MLL^C). MLL^N contains all domains except the transcriptional activation domain and the SET domain. MLL^N and MLL^C subunits reassociate into the MLL^N-MLL^C dimer and take part to the formation of a multiprotein complex that regulates chromatin modification and gene expression[29].

MLL Rearrangements and Biological Functions

As previously mentioned, KMT2A rearrangements is present in 6% of new B-ALL diagnoses, including 70% of infant ALL cases, 4–14% of new AML diagnoses, including 35–50% of infant AML, and 4–8% of new T-ALL diagnoses[14]. MLL is involved in numerous genomic lesions that cause the acute leukemia, including reciprocal chromosomal translocations, internal tandem duplications, internal deletions and amplifications. MLL translocations (Figure 2b) are the most common genomic lesions and are a consequence of DNA double strand break repair failure in developing hematopoietic cells, this results in the generation of fusion genes leading to the expression of fusion protein with aberrant functions. MLL fusion breakpoints are typically located within the 8.3 kb breakpoint cluster region spans exons 8-13 that contains topoisomerase II cleavage sites. The fusion proteins maintain the N-terminus part of MLL with the non-specific DNA and protein-binding capacity, while the regulatory bromodomain, repression domain, PHD domains and the H3K4 methyltransferase activity are partially or entirely lost. As a result of gene rearrangement, the MLL fusion complex associates with other histone writers, resulting in an aberrant H3K79me patterns which maintain an open conformation of the chromatin. For this reason, MLL fusions still positively regulate the transcription of HOXA cluster genes.

A total of 135 different MLL translocations have been identified across B-ALL, T-ALL and AML so far. MLL translocation can be classified into four groups according to the function of the fusion partner gene. The first group is characterized by fusions with the **nuclear DNA-binding proteins** AF4, AF9, AF10, ENL and ELL and accounts for most of MLL rearranged leukemias (80%). MLL::AF4 is most frequently fusion protein found in early B-cell ALL in infants and adults. A second group includes **cytoplasmic proteins** such as GAS7, EEN, AF1p or Eps15, AF6 and AFX, which may possess coiled-coil oligomerization domains that are important for their transformation potential. The third small group of partners includes **septins** (SEPT2, SEPT5, SEPT6, SEPT9 and SEPT11), which are cytoplasmic proteins involved in cell-cycle control, vesicle trafficking and compartmentalization of the plasma membrane, although their physiological significance remains largely unknown. A fourth group includes **histone acetyltransferases** p300 and CBP52–54. MLL fusions with these proteins retain histone acetyltransferase activity of either CBP or p300.

Another type of MLL rearrangement is the partial tandem duplication (MLL–PTD), which is a result of internal tandem duplication of select exons 55–57. However, this rearrangement is less frequent, and it can be found in 4-7% of AML patients[28]. (Figure 2c)

Deletion of KMT2A alone is not sufficient for leukemic transformation, but rare cases of 3' KMT2A deletions have been reported in ALL, in particular in T-ALL cases.

MLL protein is involved in epigenetic regulation of defined developmental genes[30]; indeed it has a histone methyl transferase activity at the histone3-Lysine4 (H3K4) residue[31]. It mediates the passage of chromatin from a closed and compact conformation (heterochromatin) to an open and loose form (euchromatin) which allows the assembly of the transcription initiation complex. The SET domain methylates lysine 4 of histone H3 (H3K4) and gives the mark for the starting of RNA transcription by the RNA polymerase II and in consequence for the transcriptional activation of Homeobox (HOX) and other genes during development[32].

The RNA polymerase II is not able to proceed with transcription of genes without specific methylation marks on the histone core; In particular, the histone H3 lysine 4 (H3K4) methylation in the promoter gives the mark for the starting of transcription, the histone H3 lysine 36 (H3K36) methylation for the extension and the histone H3 lysine 79 (H3K79) methylation across promoter and open reading frame regions for the maintenance of the transcription[28,33].

MLL forms a nuclear complex with others different proteins with distinct functions. MLL binds the DNA directly through the AT-hook domains and this binding with DNA may also be influenced by interactions with other DNA-binding proteins such as Menin. The

tumor-suppressor Menin (encoded by MEN1) acts as a co-factor for MLL, as it binds to MLL through an RXRFP motif to form the MLL-Menin complex, which binds to the HOXA9 promoter in order to positive regulate HOXA9 expression. MLL can also interact with multiple proteins that suppress gene expression, such as histone deacetylase 1 (HDAC1) and HDAC2, CYP33, PcG proteins PC2 and CTBP34[28].

In MLL translocations the domain that mediates H3K4 methylation (SET domain) is lost, but the expression of HOX and other genes is increased. This happens because also the MLL fusion partners are involved in transcriptional control and transcriptional elongation. For example, one fusion partner is ELL, an elongation factor that binds the RNA polymerase II and several other proteins. Another example is that in MLL fusions Menin allows the recruitment of LEDGF (lens epithelium derived growth factor, alternative name PSIP1), which is a histone reader with a PWWP domain that recognizes H3K36 di/trimethylation; Consequently, the PWWP domain replaces the function of the Menin/AT-hook region[34].

The most common MLL fusion partners AF4, AF9 and ENL contain C-terminal transcriptional activation domains. In MLL fusion, ENL and AF9 lose their amino-terminus highly conserved YEATS domain, a histone reader that recognizes acetylated H3 and in some cases other histone modifications and that has affinity to H3K9ac[35]. Instead ENL and AF9 maintain the ability to interact with AF4 that in turn binds

the positive elongation factor b (P-TEFb), a protein part of the super elongation complex (SEC). P-TEFb is a dimer formed by cyclin dependent kinase 9(CDK9) and one of two cyclin T versions (CYCT1 or CYCT2). Active CDK9 phosphorylates RNA Polymerase II and favors the elongation of transcription by release of transcriptional initiation complex from stalling points. Since the P-TEFb interaction domain is localized in the N-terminus of AF4, it is lost in MLL::AF4 positive cells, and AF4 cannot directly interact with P-TEFb. However, the C-terminal domain of AF4 binds to ENL and to its YEATS domain[34]. (Figure 3)

In addition, AF10 recruits the methyltransferase DOT1L which promotes methylation of histone H3 lysine 79 (H3K79) on the HOXA9 promoter. Furthermore, AF9 and AF4 directly bind DOT1L and ENL is found in nuclear complexes with AF4 and AF10 associated with DOT1L[36]. Therefore, the recruitment of these complexes to MLL fusion protein target genes results in an increase of H3K79 methylation, that compensates the loss of H3K4 methyltransferase activity and causes the upregulation of transcription of these target genes[37].

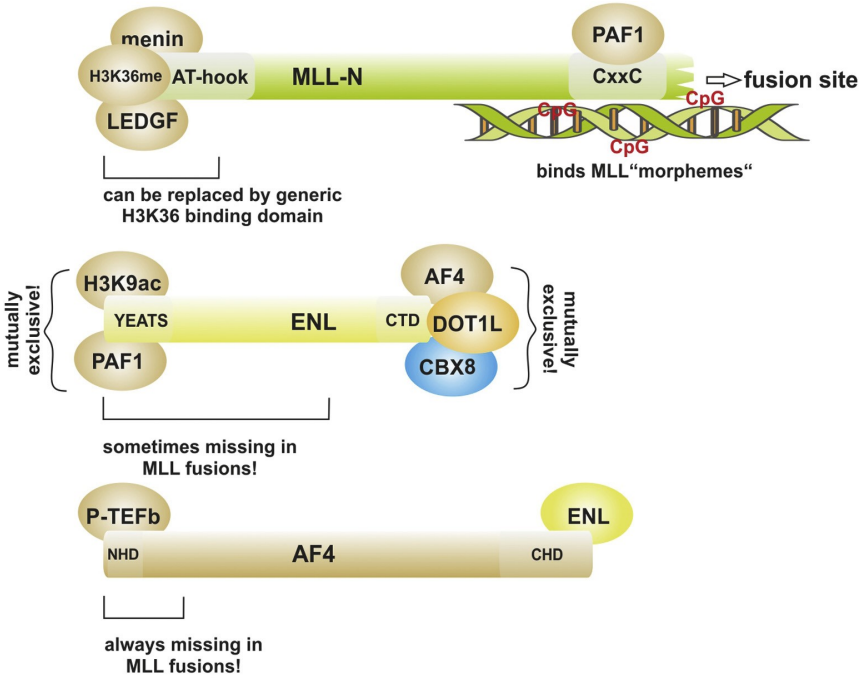

Figure 3: Interactome of MLL-N, ENL, and AF4 showing the crucial partners for localization and functional interaction with the transcriptional machinery. (Adopted from: Elsevier, 2020; Robert K. Slany)

Other important proteins of the MLL complex are the Members of the Bromodomain and Extra-Terminal (BET) family of epigenetic adaptors (including BRD2, BRD3 and BRD4), which recognize specific acetylated lysine residues of the histone core though their Bromodomains and mediate the assembly and the recruitment of the super-elongation complex (SEC) to promote the transcription. in particular BRD4 is a mediator of transcriptional elongation by recruiting pTEFb which in turn actives the RNA Polymerase II[38]. (Figure 4)

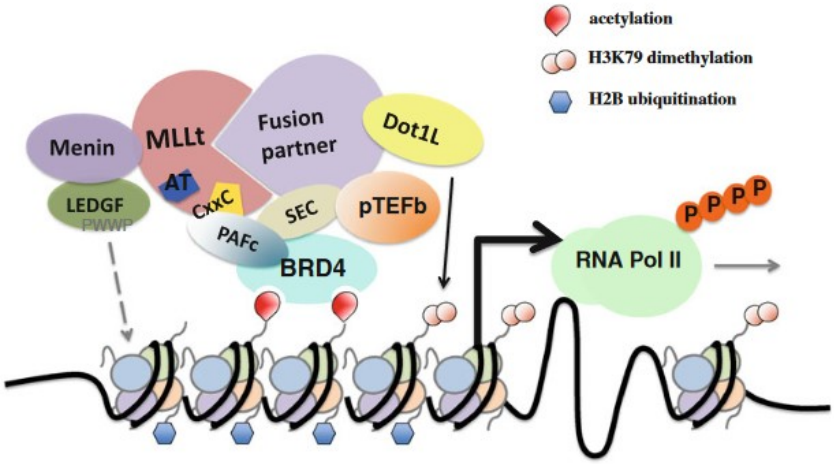

Figure 4: Interactome of most common MLL fusion complexes. (Adopted from: Int J Ematol, 2012; Yue Zhang)

In conclusion, the aberrant epigenetic regulation is thought to be the main mechanism leading to MLL leukemogenesis, therefore the MLLr infant ALL might be considered the paradigmatic example of an epigenetic disease.

Therefore, a possible strategy to treat MLLr ALL is to target the proteins of the MLL fusion complex, either directly or indirectly. Indeed, several groups have developed inhibitors for MLL–MEN1 or MLL–LEDGF interactions, DOT1L, HDAC or BET proteins (BRD4)[39], or the SET domain of MLL and MLL::AF4[40].

Treatment of Infants with MLL Rearranged Acute Lymphoblastic Leukemia

Clinical Trials

Given the peculiarity and aggressiveness of the disease, infant patients are enrolled in a dedicated protocols. In particular, infant ALL specific clinical trials are conducted by three large collaborative groups: the Interfant Study Group, the Children's Oncology Group (COG) and the Japanese Pediatric Leukemia/Lymphoma Study Group (JPLSG). More in detail, The Children's Oncology Group is formed by two US pediatric cooperative trial groups: the Children's Cancer Group (CCG) and the Pediatric Oncology Group (POG)[41].

In Europe, the Interfant protocol ("International Collaborative Treatment Protocol for infants under one year with acute lymphoblastic or biphenotypic leukemia")[42] combined classic drugs used in the treatment of ALL with other drugs typically used in myeloid leukemia. The Interfant-99 protocol (ClinicalTrials.gov NCT00015873) was the first treatment protocol of this collaborative group that consisted of all major European study groups and several study groups and large pediatric oncology centers outside Europe. At the interim analysis in May 2004, the overall outcome of the Interfant-99 protocol was comparable to that of the most favorable historical control series with sufficient patients' numbers (BFM, CCG) and better than previous results from other study groups. The second

one is the Interfant-06 (ClinicalTrials.gov NCT00550992) that started in January 2006 and was concluded in 2017. Interfant-06 based on results of Interfant-99, stratified patients into low risk (MLL germline), high risk (MLL rearranged and age <6 months and WBC>300x10^9/l at diagnosis and/or poor day 8 prednisone response) and medium risk (all other cases). However, since clinical monitoring relative to the total 20 years of enrollment did not show any substantial improvement in the outcome of MLLr ALL infants patients[43], from 2017 to 2022 such patients were enrolled in the phase 3 clinical protocol common to all affected pediatric patients (AIEOP-BFM ALL 2017, www.clinicaltrialsregister.eu EudraCT 2016-001935-12). Now a third Interfant protocol, the Interfan-2021 (ClinicalTrials.gov NCT05327894), is started with the purpose of improving the outcome of MLLr ALL in infants; in this protocol all patients receive Blinatumomab in the first phase of induction and then are randomized.

In US, three infant-specific CCG (107, 1883 and 1953) and three infant-specific POG (8398+8493, 9107 and 9407) followed one another from 1984 to 2000 without improvement in the infant MLLr ALL outcome. The first COG, COG P9407, focused on reducing toxicity substituting and reducing the dose of steroid during induction, reinduction and continuation and substituting of the continuous with daily short daunorubicin infusions during induction and reinduction for all patients. The COG AALL0631 study (NCT00557193), that started in 2008 and was concluded in 2014, demonstrated for the

first time the safety and feasibility of adding the small molecule Fms-like tyrosine kinase 3 (FLT3) inhibitor, CEP-70, to postinduction chemotherapy[44]. The COG AALL15P1 (NCT02828358) started in 2016 tested the tolerability and safety of combining the Azacitidine, a demethylating agent to the postinduction chemotherapy. The COG AALL2121 Phase I (NCT05326516), started in 2022, will determine the safety and tolerability of the Menin inhibitor SNDX-5613 combined with standard chemotherapy backbone in infants with relapse/refractory MLLr leukemias. In the future COG ALL2122, Venetoclax and Blinatunumab will be incorporate into the standard chemotherapy backbone for infants with MLLr ALL.

The Japanese JILSG was the first group that study the effectiveness of risk-adapted therapy according to the presence or absence of MLL rearrangements. Two consecutive protocols, MLL96 and MLL98, from 1995 to 2001, demonstrated that the outcome was significantly better for infants with germline MLL compared to those with MLLr. The subsequent MLL03 aimed to anticipate in the early phase the HSCT to prevent early relapse. In conclusion, in the last JPLSG study, MLL10 opened in 2011, there was a new stratification system. In particular, MLL germline infants were classified low risk and treated with the MLL96/98 chemotherapy backbone; MLL rearranged infants >180 days of age with no CNS disease were intermediate risk and treated with intensive combination therapy without HSCT. MLL rearranged infants <180 days of age or with CNS disease were high risk and treated with intensive combination therapy with HSCT[45].

Immunotherapies

T-cell Chimeric Antigen Receptor is directed against the CD19 antigen (CD19 CAR-T) and Blinatumomab, a Bi-specific T-cell engagers (Bite) antibody, binds the CD19 antigen of the blast cells and the CD3 antigen of T-cells. The tolerability and efficacy of blinatumomab for children with relapsed/refractory B ALL, and, also, for infants with relapsed/refractory MLLr ALL was demonstrated in clinical trials[46,47]. For this reason, Blinatumomab was introduced as a frontline therapeutic agent in the new upcoming Interfant-21 clinical trial. About CAR-T cell therapy, the proportion of MLLr patients enrolled in clinical studies is limited and infants below the age of one were excluded due to low circulating blood volume, which provides challenges in the production process; in addition, Infants with MLLr ALL have high peripheral blast counts and can be clinically unstable during the intense early phases of therapy. A possible solution to overcome these limitations is the use of allogeneic T cells from healthy donors to be administered as 'off-the-shelf' CAR-T cells; UCART19 therapy is currently in clinical trials for adult and pediatric relapsed/refractory B-ALL[48]. However, a major limitation of this approach in infants is the occurrence of a lineage switch of the leukemic blasts, typically from ALL to AML phenotype (which may also occur spontaneously in some patients) following blinatumomab or CAR-T cell therapy. Indeed, loss of the CD19 cell surface protein and of all other B-lineage markers and acquisition of a myeloid phenotype causes relapse in infant patients[49]. The downregulation of

the CD19 surface antigen represents indeed a mechanism to escape therapy under the pressure of the CD19-directed targeting strategy.

Preclinical Studies for Targeted Therapies

In the last decades several approaches for targeted therapies have been conceived for the treatment of MLLr ALL aiming at ameliorating the outcome of this very young patients. Here follows a review of the more relevant pre-clinical studies using different inhibitor compounds[13,15] (Figure 5):

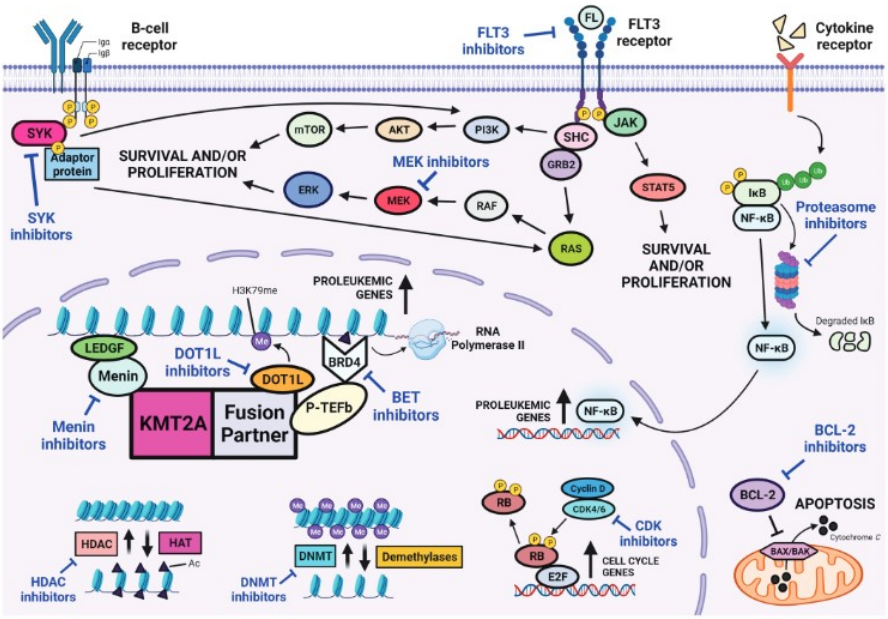

Figure 5: Targeted therapy strategies recently used in preclinical studies for the treatment of infants with MLL rearranged acute lymphoblastic leukemia. (Adopted from: Hematology, 2022; Kotecha RS)

FLT3 inhibitors

FMS-like tyrosine kinase 3 (FLT3) is a proto-oncogene expressed on the surface of hematopoietic progenitor cells, which plays a role in the normal development of hematopoietic stem cells, cell survival, proliferation, and differentiation and is overexpressed or constitutively active in infants MLLr ALL. FLT3 inhibitors increased chemotherapy-induced cytotoxicity and synergized with chemotherapy in a sequence-dependent manner in preclinical models[50]. In the COG AALL0631 phase III study, infants MLLr patients received either post-induction chemotherapy only or post-induction chemotherapy plus the FLT3 inhibitor lestaurtinib, but, unfortunately, the study demonstrated that the combination of lestaurtinib with standard chemotherapy did not improve EFS overall. However, the next-generation FLT3i such as gilteritinib and quizartinib are more potent and maybe could give better results[44].

MEK inhibitors

Mutations in RAS pathway are present in 24% of infant ALL patients with the t(4;11); in particular, of this 24%, 11% are mutations in NRAS and 14% are KRAS mutations[51]. Furthermore, RAS mutations are correlated with worse clinical outcome in this high-risk group. For this reason, the MEK Inhibitors could be promising for the treatment of infant MLLr ALL. Mark Kerstjens et al. demonstrated that RAS-mutant MLLr ALL cells were sensitive to MEK inhibitors MEK162,

Selumetinib and Trametinib. In RAS mutated cells MEK inhibitors reduced p-ERK levels, and induced apoptosis. In addition, MEK inhibition sensitized to prednisolone both the RAS-mutant and RAS-wildtype cells[52].

Histone deacetylase inhibitors (HDACi)

Several studies demonstrated the preclinical efficacy of histone deacetylase inhibitors. For example, P G Castro et al. demonstrated the in vivo efficacy of Panobinostat (LHB589) in a xenograft mouse model of MLL rearranged ALL. They observed that Panobinostat in monotherapy caused a prolong survival and a reducing overall disease burden in vivo by inducing acetylation of histone and by inhibiting the RNF20/RNF40/WAC E3 ligase complex and therefore the H2B ubiquitination[53]. In a more recent study, L. C. Cheung et al observed that Romidepsin increased the activity of cytarabine against MLLr ALL in vivo without toxicity. At molecular level, Romidespin enhanced the DNA double-strand break response of cytarabine. In addition, Romidepsin synergized also with daunorubicin, 4-hydroperoxycyclophosphamide, vincristine and dexamethasone in vitro; therefore, Romidespin could be combined with standard Interfant chemotherapy backbone[54]. These preclinical studies that demonstrated the efficacy of HDCA inhibitors gave the rationale for starting clinical studies. Indeed, the TINI study (NCT02553460), started in 2015 by St Jude Children's Research Hospital, tested the safety of Vorinostat, a histone deacetylase inhibitor and Bortezomib,

a proteasome inhibitor, in combination with the chemotherapy backbone of infant ALL.

De-methylating agents

Infant MLLr ALL shows an aberrant epigenetic profile with an overall global hypermethylated state and a hypermethylation profile of CpG islands on the promoters of crucial genes[55]. The CpG hypermethylation confers to chromatin a closed conformation, leading to the transcriptional silencing of selective tumor suppressor genes and is associated with high relapse risk[56]. Hypomethylating agents (HMA) such as cytosine analogs Azacytidine (AZA) or Decitabine (DEC), inhibit the function of DNA methyltransferases (DNMT) by incorporation into the DNA and prevent the methylation of cytosine during cell division. C Roof et al demonstrated that DEC had more effect than AZA in MLLr BCP ALL cell lines and synergized with cytarabine in vitro (but not in vivo), however the effect of the combination between Decitabine and chemotherapeutic drug differed between cell lines and cytostatic drugs; in vivo Decitabine delayed leukemia progression in MLLr xenograft models but did not eradicate ALL[57]. Also P. Schneider confirmed that decitabine was insufficient to prevent leukemia progression in vivo, mildly sensitized to conventional chemotherapy currently used for infant MLLr ALL patients and showed an additive or moderate synergistic effects in combination with other epigenetic-based or anticancer drugs (HDCAi

Panobinostat, Venetoclax, MEK inhibitor Pimasertib, and receptor tyrosine kinase Foretinib)[58].

Bromodomain inhibitors (BETi)

The bromodomain and extra terminal (BET) family of proteins, which includes BRD2, BRD3, and BRD4, is a family of chromatin adaptor proteins that recognize and bind to acetyl-lysine residues. These proteins recruit transcriptional coactivators components of the SEC, many of whom are MLL fusion partner, and promote the gene transcription. The inhibitor of BRD4, GSK1210151A (I-BET151), showed efficacy against MLL::AF9 AML cell lines, through the induction of early cell cycle arrest and apoptosis. In particular, I-BET151 acted by inhibiting the transcription of key genes BCL2, C-MYC and CDK6. In vivo, this compound caused a prolonged survival benefit in mouse models of murine MLL::AF9 AML and human MLL::AF4 AML[59]. About MLL::AF4 infant ALL, Bardini et al demonstrated that I-BET151 decreased the leukemic engraftment in a preclinical mouse model, sensitized glucocorticoid-resistant MLL rearranged cells to prednisolone in vitro and had a synergistic effect in combination with HDAC inhibitors in vitro and in vivo[39]. Despite early clinical trials showed promising results in particular in AML, other subsequentially studies discovered the development of resistance mechanisms to the BET inhibitors I-BET and JQ1 in human and mouse leukemia cells. The resistant cells were smaller, more homogenous, enriched for LSCs and with NF-κB pathway significantly

downregulated and TGF-β and Wnt/β-catenin pathways significantly upregulated. Therefore, there was a small proportion of LSCs in AML samples, which were transcriptionally primed or displayed an adaptative transcriptional plasticity to survive at BET inhibitors treatment and become the dominant[60,61].

DOT1L inhibitors (DOT1Li)

DOT1 like histone lysine methyltransferase (DOT1L) is a protein methyltransferase responsible for methylation of lysine on histone H3 (H3K79). DOT1L interacts with the MLL fusion partners like AF9, AF4 and ENL and enhances leukemogenic gene expression. Scott R. Daigle et al, synthesized and characterized the DOT1L inhibitor EPZ004777; then they observed that this compound inhibited H3K79 methylation, blocked MLL fusion target gene expression, reduced the proliferation and increased apoptosis selectively of MLLr cell lines. In vivo EPZ004777 administration had an antitumor efficacy in a mouse xenograft model of MLL leukemia without overt toxicity or severe hematopoietic side effects[62]. However, the poor pharmacokinetic properties of EPZ004777 precluded its clinical development; for this reason, the same group developed another DOT1L inhibitor EPZ-5676 (Pinometostat), which showed robust antiproliferative activity in MLLr leukemia mouse model[63]. Given the inhibition of tumor growth demonstrated by EPZ-5676 and its preclinical safety, EPZ-5676 entered in clinical trial for pediatric and adult acute and myeloid leukemias with MLL rearrangements (NCT02141828 and

NCT01684150). Unfortunately, the results of these clinical trials pointed out that EPZ-5676 had modest clinical activity and continuous long-term administration could lead to drug resistance; for this reason, the combination of EPZ-5676 with other antileukemia agents or the development of others DOT1L inhibitors with novel scaffolds and better pharmacokinetic properties is warranted[64,65].

Menin inhibitors

Menin interacts with the N-terminal portion of the MLL protein and is essential for leukemogenesis. Many small molecule inhibitors that disrupt the binding between MLL and Menin have been developed and have shown *in vitro* and *in vivo* impairment of leukemia growth and proliferation. MI-1 was the first small molecule inhibitor of the Menin-MLL fusion protein interaction; from MI-1 were developed MI-2 and MI-3, that inhibited the menin-MLL-AF9 interaction and downregulated the expression of MLL target genes critical for oncogenic transformation (MEIS1 and HOXA9). They also selectively blocked proliferation and induced both apoptosis and differentiation of MLLr leukemic cells[66]. Krivtsov et al. developed VTP50469 a new inhibitor of Menin-MLL interaction, selective, more potent, with improved pharmaceutical properties and orally bioavailable. VTP50469 (SNDX-50469) decreased the proliferation of MLLr AML and ALL cell line in vitro and improved survival in PDX models of MLLr leukemia by completely eradicating the leukemia cells in BM, PB and spleen[67]. Given the promising preclinical results of Menin inhibitors

St. Jude started in 2022 a clinical study COG AALL2121 Phase I, to determine the safety and tolerability of the Menin inhibitor SNDX-5613 in combination with standard chemotherapy backbone (adopted from Interfant trial) in infants with relapse/refractory MLLr leukemias (NCT05326516).

Proteasome inhibitors

In MLLr ALL proteasome inhibitors would regulate the expression of the MLL fusion protein. Indeed, unexpectedly, expression of some MLL-fusion products impacts leukemia, therefore, accumulation of high levels of endogenous MLL-fusion proteins by using proteasome inhibitors can represent a possible strategy to inhibit leukemia cell survival and proliferation. The proteasome inhibitor Bortezomib selectively reduced viability of MLLr ALL cell lines by inducing mitochondrial apoptosis and caused the recruitment of P-TEFb complex to promote transcriptional processivity along CDKN1B. In addition, bortezomib treatment was an effective agent against pro-B MLL::AF4 leukemia cells also in vivo. MLLr AML leukemia cell lines were similarly resistant to bortezomib as non-MLL cell lines. Unfortunately, pro-B MLL leukemia cells can acquire resistance to proteasome inhibition, that could be overcome by using Bortezomib in combination with other anti-cancer agents[68].

However, the clinical study in which Bortezomib was combined with Vorinostat in younger patients with Refractory or Relapsed MLL Rearranged Hematologic Malignancies (NCT02419755) was terminated

early because accrual goals were no longer feasible. Nevertheless, the TINI study (NCT02553460), started in 2015 by St Jude Children's Research Hospital and tested the safety of Vorinostat, and Bortezomib in combination with the chemotherapy backbone of infant ALL is currently active.

BCL-2 inhibitors

B-cell lymphoma 2 (BCL-2) family proteins regulate the intrinsic mitochondrial apoptosis pathway. BCL-2, BCL-X L and MCL-1 are anti-apoptotic BCL-2 family proteins, instead BCL-2 homology 3 (BH3) proteins BIM, BID, BAD, NOXA, PUMA, and HRK are pro-apoptotic proteins that favor cell death; BCL-2 is a key antiapoptotic regulator. It was observed that BCL-2 is high expressed in MLLr ALL and that MLL::AF4 fusion active the transcription of BCL-2 mRNA via ENL and DOT1L-mediated H3K79 methylation[69].

Navitoclax (ABT-263), bound and blocked BCL-2, BCL-XL, and BCL-W and had efficacy against CLL; however, phase I trials caused an on-target thrombocytopenia due to BCL-XL inhibition. Instead, the subsequential ABT-199 (Venetoclax) is a BH3 mimetic that specifically targets BCL-2 and with demonstrated efficacy in patients with CLL, and preclinical activities in AML, early T cell progenitor leukemia, Myc-driven B cell lymphomas and ALL[70]. MLL::AF4 cells resulted sensible to ABT-199 and the combination of ABT-199 with DOT1L inhibitors or standard induction type chemotherapeutic agents was synergistic in vitro. In addition, in vivo treatment with ABT-199 of

MLLr ALL xenograft models reduced tumor burden[69,71]. More recently, Anna Richter et al, investigated more in details pathways activated in MLLr B-ALL after Venetoclax treatment. In particular, they observed that Venetoclax exposure caused BCL-2 dephosphorylation, reduction of antiapoptotic pathway members BCL2, MCL1, and BCL-XL and BAX-mediated caspase activation. In addition, genes of the tumor necrosis factor signaling cascade were increased[72]. Another group demonstrated that the combination of the hypomethylating agent Azacytidine and Venetoclax was synergistic and produced a significant survival advantage in infant MLLr ALL xenograft models[73].

Given these promising pre-clinical results and the fact that Venetoclax is currently in clinic for adult AML in combination with standard chemotherapy and Azacytidine (VIALE-A trial NCT03069352)[74,75], the COG AALL2122 designed a phase I trial to incorporate Venetoclax into standard chemotherapy for infants with MLLr ALL.

Glucocorticoids Resistance

MLLr ALL is characterized by a specific gene expression profile with an upregulation and overexpression of the HOX cluster genes and their cofactor MEIS1. These genes are involved in controlling hematopoiesis of the early stem cells, and they are downregulated with differentiation. This gene expression signature has conferred drug resistance to chemotherapy agents and contributed to poor

outcome. Indeed, MLLr ALL is resistant to corticosteroids and L-asparaginase chemotherapy[76].

Since it is known that infant patients with MLLr ALL are typically resistant to glucocorticoids (GCs), in these years several studies tried to explain the biological mechanisms responsible for GC resistance.

The group of Ronald W Stam in 2009 demonstrated for the first time that MCL-1 (a member of BCL-2 family with antiapoptotic functions) was overespressed in infant patients with MLLr ALL resistant to prednisolone (LC50 values greater than 150 g/mL prednisolone) and was predictive for both the in vitro and in vivo prednisolone response. In addition, they demonstrated that the reduction of MCL-1 protein expression by Knock-down system moderately sensitized the MLLr leukemia cell lines to prednisolone in vitro[77]. Then, it has also been shown that pan-BCL-2 inhibitors such as gossypol and AT-101 can induce prednisolone sensitivity in MLLr infant ALL patients by increasing the levels of pro-apoptotic proteins (BIM, BID, BAD and NOXA), rather than by decreasing the levels of pro-survival proteins (BCL-2, BCL-X or MCL1)[78].

In addition, the group of R W Stam investigated better other resistance mechanism and discovered that S100A8 and S100A9 protein were overespressed in MLLr ALL resistant patients and bound the free-cytosolic Ca^{2+}, which, consequently, cannot go into the mitochondria and activate apoptosis. Therefore, they have found that overexpression of S100A8/A9 complex was associated with

prednisolone resistance and the inhibition of these proteins by the Src kinase inhibitor PP2 sensitized the resistant MLLr ALL cells to prednisolone in vitro[79].

In a subsequent study, the authors focused on another gene differentially expressed between prednisolone-resistant and prednisolone-sensitive MLLr infant ALL patient samples: ANXA2. Annexin A2 is a member of the annexin family of calcium-dependent phospholipid-binding proteins and is activated by phosphorylation at tyrosine 23 mediated by SRC Kinases which requires the adapter protein p11 (encoded by the S100A10 gene). In this study it has been shown that the reduction of both expression and activation of ANXA2 sensitized to Prednisolone[80].

Then, after generating a GC-resistance gene expression profile specific for MLLr infant ALL and showing that this signature deviated from GC-resistance signatures in non-infant pediatric precursor, JAP Spijkers-Hagelstein and colleagues used this gene signature in Connectivity Map analysis to identify agents that induce GC sensibility in these patients. The most promising compound is LY294002, a PI3K inhibitor, that caused a downregulation of FCGR1B and induced prednisolone sensitization specifically in MLLr ALL[81]

Importantly, Mousavian et al developed a co-expression network analysis for the detection of gene modules that are associated with GC resistance. Co-expression networks are a gene networks in which highly co-expressed genes are grouped into co-expression modules

(gene sets) for further analysis and in each module there are the key regulators ('hubs'). By applying this method, they found a single module associated with prednisolone resistance and confirmed the presence of genes already known to be associated with prednisolone resistance (like ANXA2 and S100) in this module. In addition, new candidate genes involved in GC resistance from this module may be investigated in further analysis (es: LGALS3, ITGB2, CEBPB, VCAN, NCF2…)[82]. In a following interesting study the same authors have investigated a differential co-expression and protein-protein interaction in GC-resistant versus GC- sensitive samples of MLLr infant ALL patients and reported some active protein modules associated with GC-resistance in infant MLLr ALL, including electron transport chain, proteasome, tRNA-aminoacyl biosynthesis and peroxisome signaling pathways[83].

Interestingly, Anne P. de Groot et al. overcome the resistance of MLLr ALL to GCSs by treating GC-resistant infant MLLr ALL in vivo with the small molecule inhibitor RK-20449, that caused a dual inhibition of FLT3 and SFK pathways. Moreover, MLLr ALL cells were completely eliminated combining Dexametasone with RK-20449 and ABT-199 because the resistant cells to RK-20449/dexamethasone combination treatment, were dependent on Bcl-2 for survival[84].

More recently, in a very recent paper Candelli et al analyzed the expression of a prednisone-dependent signature in diagnostic bone marrow and peripheral blood biopsies by single cell RNA-Sequencing

and divided the leukemic cells in resistant or sensitive to treatment; the quantification of these two groups of cells can be used to better predict the relapse and the GCs resistance in individual patients. In particular the cells associated with high relapse risk were resistant to GCs, less metabolically active, quiescent and dormant, had a smaller size, and a specific gene expression signature related to cell stemness, drug resistance and GCs response[85].

The RNA-binding Protein Musashi-2

Given the aggressiveness of MLLr infant leukemia and the failure of the current therapies (typically due to drug resistance and high incidence of relapse), the identification of therapeutic targets for the development of novel therapeutic strategies still remains nowadays an unmet need. The RNA-binding proteins (RBPs) may represent potentially attractive alternative (and less known) target for therapeutic intervention in human cancers. Indeed, in addition to the genetic mutations and translocations, also the posttranscriptional mechanisms regulated the expression of specific genes to cancer development through a set of tumor-associated RNA binding proteins.

The RNA-binding Proteins in Cancers and Leukemia

The gene expression in normal and cancer cells can be physiologically regulated in many different ways. This includes: the epigenetic regulation of chromatin structure, the transcriptional regulation through transcriptional factors, the post-transcriptional regulation of gene transcripts, the regulation of the translational machinery, and the post-translational modifications which regulates protein activity or degradation. The RBP acts as posttranscriptional regulators of specific mRNA translation into proteins. Indeed, RBPs bind to single-stranded RNA and form the functional ribonucleoprotein (RNP) complexes with other proteins, mRNAs and noncoding RNAs (ncRNAs). As posttranscriptional regulators, they contribute to all

RNA processing steps (including capping, splicing, polyadenylation, exportation, localization and translation)[86]. RBPs contain multiple functional binding sites for the mRNA, the most common are:

- RNA-binding domain (RBD, also known as RNP domain and RNA recognition motif, RRM);
- K-homology (KH) domain;
- RGG (Arg-Gly-Gly) box;
- Sm domain;
- DEAD/DEAH box;
- zinc finger (ZnF, mostly C-x8-X-x5-X-x3-H);
- double stranded RNA-binding domain (dsRBD);
- cold-shock domain;
- Pumilio/FBF (PUF or Pum-HD) domain;
- Piwi/Argonaute/Zwille (PAZ) domain.

The different combination of multiple RNA-binding domains and auxiliary functional domains, alternative splicing and post-translational modification confer the diversity between different RBPs[86]. To date, approximately 1542 different human RBPs have been identified in various types of cells[87].

The first step of posttranscriptional regulation in which the RBPs are involved is the alternative splicing. During this process, the spliceosome, a macromolecule complex consisting of five small nuclear ribonucleoproteins (snRNPs) and small nuclear RNAs, and

including the RBPs SF3B1, SRSF2, and U2AF1, removes introns from the pre-mRNA and ligates the remaining exons. Then, other RBPs export the mature mRNA out of the nucleus. When the mature mRNA is localized in the cytoplasm, some RBPs, as antigen R (HuR) and IGF2BP3, stabilize and protect it from rapid turnover; instead, other RBPs, like Musashi RNA-binding protein 2 (MSI2), regulate the translation of their mRNA targets[88].

RBPs regulate the expression of many oncogenes and tumor suppressors in different cancer types, including leukemia. For this reason, altered expression of RBPs can affect crucial step of tumorigenesis, such as proliferation, apoptosis, angiogenesis, senescence, and EMT/invasion/metastasis. Aberrant RBP activity and mutations correlate with leukemia progression and are associated with acquisition of resistance to therapies, minimal residual disease, and relapse. Therefore, novel approaches targeting or inhibiting RBPs could potentially improve outcomes of cancers and leukemia[89]. In this way, small-molecule drugs, inhibitors, therapeutic small peptides, and antisense oligonucleotides (ASOs) against different RBPS are currently being developed and applied in clinical trials[90].

The Musashi Family of RNA-binding Proteins

In the 1994 Makoto Nakamura and colleagues[91] identified, for the first time, a neural RNA binding protein (RBP) responsible for maintaining the asymmetric division of sensory organs precursor (SOP) in Drosophila: Musashi (MSI). In the normal asymmetric

division, the SOP cells generate a neuronal precursor (from which cell neuron and glial cell arise) and a non-neuronal precursor (from which a socket cell and a bristle shaft arise); but, when Msi is mutated, SOP cells produce two shafts and either one or two sockets in a single bristle. The gene name reflects similarity of this double-bristle phenotype to the image of the iconic Japanese Samurai Miyamoto Musashi, a great swordsman of the Eastern culture who used two blades in combat; therefore, the martial portrayals of the two-sword fighting style originated by Miyamoto Musashi gave the name to this gene[92-94].

The RBPs Musashi are highly conserved and are essential regulators of stem and progenitor cell differentiation because they post-transcriptionally regulate expression of genes such as NUMB a component of the Notch signaling cascade, that is a critical regulator of asymmetric cell division in cell progenitors[94]. In addition, further studies in Drosophila demonstrated that Msi has a role in development of spermatogenesis and germline stem cells[95].

In mammals, two members of the human MSI family have been identified: Musashi-1 (MSI1) in the chromosome 12q24.31 and its homologue Musashi-2 (MSI2) in the chromosome 17q22, they are RNA-binding proteins and share 90% of homology (75% homology at amino acid level, 85% similarity)[92]. MSI1 is highly expressed in the

nervous system, in particular in the undifferentiated neural stem and precursor cells, and also in solid tumors such as malignant glioma, medulloblastoma, esophageal squamous cell carcinoma and gastric cancer[96,97]. Instead, MSI2 is mainly expressed in the hematopoietic system where it has a role both in normal hematopoietic stem cells (HSCs) and in hematopoietic malignancies[98,99]. In 2003, the MSI2 gene was found in a fusion protein rearranged with HOXA9 in chronic myeloid leukemia (CML), showing its role in cancer[100]. It is important that both Musashi proteins are much more expressed in tumor cells rather than normal tissues and their expression is associated with low differentiation status, poor prognosis, lymphnode invasion, metastasis cancer invasion, drug resistance and more aggressive cancer phenotypes[94].

The MSI1 and MSI2 proteins are composed of 362 and 328 amino acids, respectively. In the N-terminal of both there are two RNA-recognition motifs, defined as **RRM1** and **RRM2**, that mediate the binding of Musashi to target RNAs at the 3'-end. The RRM1 of MSI1 protein contains 20–110 amino acid residues and RRM2 contains 109–186 amino acid residues. Alternatively, the RRM1 and RRM2 of MSI2 contain 21–111 and 110–187 amino acids, respectively. The Musashi RRMs are highly conserved across diverse species and have the typical structure of RNP-type RNA-binding domains with four-stranded antiparallel β-sheets and two α-helices. Musashi RNA-binding affinity and specificity are mainly determined by the RRM1; instead, the RRM2 enhances the binding affinity in combination with

RRM1. In addition, within RRM1 is a nuclear localization signal (**cNLS**), and at the C-terminal end of RRM2 is a peptide-like nuclear localization signal (**pNLS**); these NLSs are necessary for the nuclear import of MSI via interaction with the importin-α protein because Musashi proteins normally are in the cytoplasm enriched in polysome fractions, but, sometimes, they are in the nucleus. The MSI1 and MSI2 RRMs show high sequence homology, so their RRMs bind similar if not identical RNA target sequences[101].

By contrast, the C-terminal differs significantly in length and amino acid sequence, with only 56% identity between MSI1 and MSI2. In fact, in the C-terminal region of the Musashi-1 protein there are two main domains of protein interaction: a polyA-binding protein (**PABP**) domain and a LIN28-binding domain (**LD**), that are not present in the MSI2. The binding MSI1-PABP prevents the binding between PAPB and the Translation Initiation Factor, eIF4G (Eukaryotic Translation Initiation Factor 4 gamma), inhibiting the translation of several genes. The binding domains for PABP overlap with that for GLD2, a poly(A) polymerase involved in mRNA polyadenylation and translational activation. Therefore, MS1 alternatively represses translation when PABP is bound or activates translation in the presence of GLD2. While the interaction MSI1-LIN28 regulates the post transcriptional biogenesis of microRNAs (miRNA). (Figure 6)

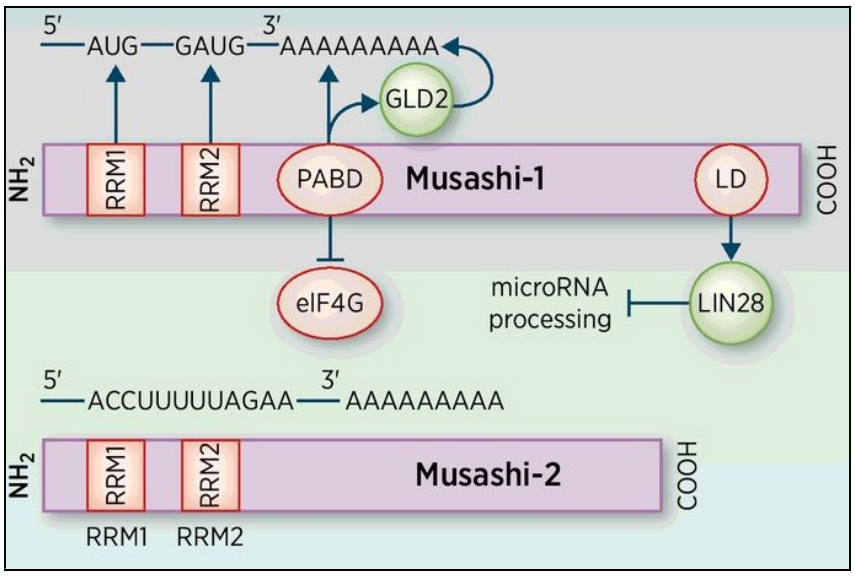

Figure 6 Schematic representation of Musashi-1 and Musashi-2 molecular interaction domains for binding to mRNA and interaction with other RNA-binding proteins. (Takes from: Clinical Cancer Research 2017; Alexander E. Kudinov)

Musashi-2 (MSI2): Structure and Regulation

The MSI2 gene encodes four protein isoforms (MSI2a, MSI2b, MSI2c, MSI2d). All of these four isoforms contain the two conserved RRMs but differ in the N-terminal or C-terminal amino acids.

MSI2 usually binds to ACCUUUUUAGAA motif or poly-U sequences, or UAG motifs of its mRNA targets and it may function as either a promoter or a repressor of protein translation[93].

MSI2 is expressed at higher level in most primitive cells, like long-term hematopoietic stem cells (LT-HSCs), short-term hematopoietic stem cells (ST-HSCs) and multipotent progenitors (MPPs), compared to progenitor cells, differentiated myeloid cells and lymphocytes[102]. Indeed, MSI2 acts as a critical regulator of hematopoietic stem cells, with MSI2 deletion leading to a decrease in hematopoietic stem cells[98]. MSI2 also regulates spermatogenesis and embryogenesis[95].

The canonical and full-length isoform MSI2a/MSI2v1 (NM_138962) has been most known, while only a few studies have focused on the functions of other MSI2 isoforms[103].

In the N-terminal region of the gene are located the two RRMs functional domains required to bind the mRNA targets, which are highly conserved between different isoforms and identical to RRMs found on MSI1 gene.

Two specific serine residues (namely S278 and S303) located on the C-terminal region of MSI2v1 (and homologous with those found on MSI1 gene, S312A and S337A) are critical sites regulating MSI2 function. The phosphorylation of these serines induces the polyadenylation-dependent translational activation of MSI2 direct targets. Therefore, the site-specific regulatory phosphorylation of the canonical MSI2 protein isoform is thought to be a mechanism to promote the translation of target mRNAs. In particular, MAP kinase and Ringo/CDK were found to be the kinases regulating MSI2 function via serine-specific phosphorylation.

In addition to the MSI2v1, an alternative spliced variant is also expressed in humans, the MSI2 variant 2 (MSI2v2/MSI2b) (NM_170721). The MSI2v2 protein is shorter, due to alternative splicing of an alternative exon 11 and it lacks the two regulatory serine residues present on MSI2v1 exon 12. MSI2v2 isoform also differs from MSI2v2 at the N-terminal (17 amino acid (MADLTSVLTSVMFSPSS) replacing the first 21 amino acids of MSI2v1 (MEANGSQGTSGSANDSQHDPG)), due to alternative splicing that replaces the first and second exon of MSI2v1 with an alternative exon 1. MSI2v1 and MSI2v2 are identical from the exon 3 to 10, but MSI2v2 isoform has a unique 13 amino contiguous C-terminal sequence (DYLPVSQDIIFIN) not found in MSI2v1[104]. (Figure 7)

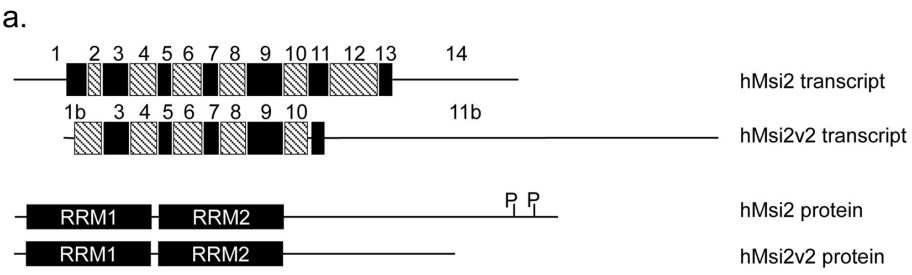

Figure 7: Schematic representation of the two transcript variants of the human MSI2 gene (full length hMSI2v1, long isoform and short hMSI2v2 isoform) (Adopted from: Scientific Reports 2017; Melanie C. MacNicol)

Although MSI2v1 and MSI2v2 targets are the same, the latter isoform is unable to activate the translation of those mRNA targets, due to the lack of the regulatory serine residues domain located at the C-terminal, thus representing a bona fide suppressive isoform.

In the majority of the organs, including the hematopoietic system, the canonical MSI2v1 is more expressed than the short MSI2v2 isoform, with the exception of brain and thyroid[104].

MSI2 expression is regulated by several transcriptional factors, as for example HOXA9. By binding to its upstream promoter, HOXA9 increases the expression of MSI2. This was seen both in HOXA9-NUP98 translocated blast crisis CML as well as in other leukemia[105]. MSI2 expression is also upregulated by receptor activator of NF-κB ligand (RANKL) during osteoclast differentiation[106]. In mouse spermatogonia cells, MSI2 expression is directly targeted and negatively regulated by MSI1 before nuclear translocation, suggesting the existence of a cross-regulatory activity between the two paralogue genes[107]. ETV4 promotes the transcription of MSI2 in lung adenocarcinoma, while KLF4 represses MSI2 transcription in pancreatic cancer cells.

MSI2 is also regulated post-transcriptionally, mainly by non-coding RNAs and other RBPs. MiR-203 directly targets the 3'-UTR of MSI2 mRNA and inhibits the translation of MSI2 leading to cell cycle arrest; miR-143/miR-107 are two p53-targeted tumor suppressive miRNAs that directly bind to MSI2 mRNA and prevent its expression in solid tumor cells[93].

Role of MSI2 in Normal Hematopoiesis and Leukemia

MSI2 is expressed in the hematopoietic system preferentially in the more immature cells, while its expression is progressively downregulated along with the increasing differentiation of precursor cells into more mature lineages[98,108]. MSI1 is barely not expressed in the hematopoietic system.

MSI2 negatively regulates the translation of Numb mRNA in normal hematopoietic stem cells (HSCs). During HSC asymmetric division, one of the two daughter cell maintains the HSC self-renewing property to replenish the stem cell compartment, whereas the other daughter cell becomes a non–self-renewing progenitor and progressively acquires a more mature phenotype. During this process, MSI2 is gradually downregulated, and vice versa Numb is upregulated. Numb is involved in the early stages of development because it inhibits Notch and Hedgehog signaling via E3-mediated ubiquitination; in particular, Notch intracellular domain (NICD) and the zinc finger transcription factor GLI are degraded by proteasome. By binding and inhibiting Numb mRNA, MSI2 allows the aberrant activation of Notch signaling pathway, and subsequently the maintenance of the self-renewing capacity and the undifferentiated state of HSCs[105,109].

Some authors have investigated the role of MSI2 in the HSC. Ito et al. observed that the disruption of MSI2 expression via gene trap causes a marked decrease in the frequency of hematopoietic stem and

progenitor cells. Hope et al. reported that MSI2 acts as positive regulator of asymmetric division and HSC function; indeed, MSI2 downregulation impairs the in vivo repopulating potential of HSCs[110]. Also, Kharas et al. found that the long-term and short-term repopulating ability of LSK (Lin-SCF-c-Kit- triple negative) cells in which MSI2 was knocked down was dramatically impaired. Interestingly, Kharas et al observed an increased number of LSK cells when MSI2 is overexpressed in doxycycline-inducible MSI2 transgenic mice, but they have not detected change in the replating potential of progenitors, suggesting that ectopic MSI2 expression was not responsible for an aberrant self-renewal[98]. In contrast, other studies observed an increase long-term engraftment after overexpression of MSI2 in primary bone marrow cells via retroviral transduction. The discrepant results obtained in different studies could be due to the different strategy used for MSI2 overexpression[102,109].

MSI2 attenuated the mRNA of the Aryl Hydrocarbon Receptor (AHR) by binding some components of this signaling pathway, like CYP1B1 (Cytochrome P450 1B1 Oxidase) and HSP90, and by blocking their transduction. AHR is a transcriptional factor and nuclear receptor that regulates pathways involved in HSC self-renewal/differentiation regulation in normal hematopoiesis and in acute myeloid leukemia[111]. In particular, AHR-HSP90 binding is important for the formation of the AHR complex because prevents the AHR degradation, therefore, downregulation of HSP90 protein reduces the AHR signaling; instead CYP1B1 is a direct target of both AHR and

MSI2. Therefore, through the regulation of AHR pathway, MSI2 maintains the self-renewal in early progenitors and HSCs and HSPC expansion; indeed, when MSI2 was overexpressed, there was an early progenitors expansion[112].

MSI2 was also found to be involved in human leukemia, as it regulates the expression of crucial genes with a pivotal role in the process of leukemogenesis.

The first article correlating MSI2 with hematopoietic malignancies was published in 2003 by Barbouti et al. in which it was reported that MSI2 was fused with HOXA9 in two individuals with blast crisis chronic myelogenous leukemia (CML)[100].

By generating a mouse model, in which the animals were transplanted with HSCs transduced with either BCR-ABL alone or with BCR-ABL together with Nup98-HoxA9 fusion genes (associated with accelerated phase / blast crisis leukemia), Ito et al. showed that MSI2 expression was increased when CML progressed from (latent) chronic phase to a more aggressive accelerated phase or blast crisis. In particular they demonstrated that expression of NUP98-HOXA9 fusion protein induced MSI2 expression, which, in turn, suppressed cell differentiation via Numb downregulation, thus sustaining an immature state of leukemic cells typical of blast crisis.

Furthermore, by disrupting the MSI2 gene by gene trap, the authors observed an inhibition of blast crisis CML propagation and a

significant improvement of survival. In agreement with this, they found that MSI2 expression was significantly higher in blast crisis compared with chronic phase CML patients. In addition, they identified MSI2 as an early indicator of poor prognosis, as a higher MSI2 level correlated with an increased relapse risk in both chronic and accelerated phase CML, thus reinforcing the prognostic impact of MSI2.

Moreover, Kharas et al. observed a high expression of MSI2 in human myeloid leukemia (AML) and CML-BC cell lines and demonstrated that the depletion of MSI2 with lentiviral shRNA system blocked proliferation, increased apoptosis and induced differentiation with NUMB overexpression. The gene expression profiles of several leukemic cell lines with MSI2 knockdown reveled an increased expression of differentiation markers and a decreased expression of genes involved in proliferation and survival like Wnt, Ras-Mapk and c-Myc pathways.

Furthermore, similarly to what was observed in CML, the higher expression of MSI2 directly correlated with poor outcome also in AML patients[98].

Several other studies pointed out the role of MSI2 in myeloid leukemia and gave further insights onto the gene targets directly regulated by MSI2. Through the inhibition of NUMB mRNA translation MSI2 regulates Notch, Hedgehog and P53 (p53) signaling. MSI2 also modulates cell growth by cell proliferation regulation, as it

was observed that the knockdown of MSI2 led to cell cycle arrest in G0/G1 phase in AML cell line by increasing the expression of cyclin-dependent kinase inhibitor 1 (p21) and decreasing the expression of cyclin D1 and cyclin dependent kinase 2 (CDK2). In addition, MSI2 silencing induced a modest apoptosis in AML cells by downregulating the anti-apoptotic B-cell CLL/Lymphoma 2 (Bcl-2) and upregulating the pro-apoptotic BCL2 associated X protein (Bax). Also the level of cleaved PARP, an apoptosis-related protein, increased when MSI2 was silenced[113].

Another study demonstrated that MSI2 knockdown led to the inactivation of ERK/MAPK and p38/MAPK pathways in AML cell line, but no changes in the phosphorylation of AKT was observed [114].

Tetraspanin 3, a member of the Tetraspanin family of transmembrane proteins, was identified as a direct target of MSI2 in AML. Tspan3 has a critical role in AML because it is involved in AML propagation, chemokine (SDF-1) responsiveness, cell migration, microenvironmental interaction and localization in the niche[115].

In 2017 Hattori et al demonstrated that MSI2 direct bound to FMS-like tyrosine kinase 3 (FLT3) mRNA transcript and positively regulated its protein expression. FLT3 is a gene encodes a class III receptor tyrosine kinase (RTK) that plays important roles in the proliferation, differentiation and survival of hematopoietic stem and progenitor cells (HSPCs) and its mutations is one of the most frequent genetic alterations in AML. MSI2 regulated the FLT3 expression in human

AML and in BC-CML and knockdown of MSI2 led to downregulation of FLT3 and impaired leukemia cell growth[116]. Another direct target of MSI2 in AML is the branched-chain ammino acid aminotransferase 1 (BCAT1), an enzyme involved in ammino acid metabolism which catalyzes the production of BCAAs from glutamate (BCKA). BCAT1 is more highly expressed in BC-CML than in CP-CML and high BCAT1 expression levels in AML patients is correlated with poor outcome. MSI2 was found to directly bind to BCAT1 mRNA and promote BCAT1 translation. Indeed, MSI2 knockdown led to a reduced BCAT1 expression, mTORC1 activation and phospho-S6K, which were restored by either BCAT1 over-expression or BCAA supplementation[117].

Sticking evidences were provided for the involvement of MSI2 in MLL rearranged AML. By high-throughput sequencing and cross-linking immunoprecipitation (HITS-CLIP)[118] Park et al. identified the mRNAs directly bound by MSI2 in a leukemia cell line (K562) in which MSI2 was ectopically overexpressed, and they found that direct mRNA targets of MSI2 were associated with the MLL-AF9 self-renewal signature. In addition, functional studies were performed to demonstrate that HOXA9, c-Myc, and Ikzf2, three transcription factors very important for MLL::AF9+ AML development and maintenance, were indeed directly regulated by MSI2[99].

More recently, the same group of Michael Kharas adapted the HyperTRIBE method using a RBP fused to a catalytic domain of

Drosophila RNA editing enzyme ADAR (Adenosine Deaminase Acting on RNA enzyme) to identify the mRNA targets of MSI2 in mammalian normal hematopoietic or leukemic stem cells. RBP-ADAR marks the binding sites with a nearby A-to-G editing on the RBP RNA targets. By using this approach, the authors demonstrated that MSI2 targets differed during differentiation from HSC to multipotent progenitors (MPPs), thus leading to the hypothesis that MSI2-dependent posttranslational regulation of mRNA targets is cell context specific. Importantly, the authors also demonstrated that the RNA binding activity of MSI2 was significantly higher in LSCs compared with normal HSPCs[119], thus suggesting that MSI2 has a greater impact in leukemic cells compared to normal hematopoietic cells.

In the context of lymphoid malignancies MSI2 has been recently found to have a relevant role in CLL and B-lymphoma[120,121].

With regards to acute lymphoblastic leukemia only, very few studies are available in literature, which reported an increased expression of the MSI2 in B-ALL patients compared to bone marrow cells derived from healthy donors. Moreover, these studies clearly showed the existence of a strong correlation between high levels of MSI2 expression and a poor outcome in B-ALL patients (both adults and pediatric cases)[122-124]. These data support the hypothesis that MSI2 is a prognostic marker for B-ALL patients and provide the rational for investigating the potential role of MSI2 in the pathogenesis of B-ALL. However, to date, functional data are still missing.

Preliminary Results (from previous study from our Lab) showed that MSI2 might be involved in MLL leukemogenesis because it was one of the genes downregulated after I-BET151 treatment of MLL::AF4+ cells[39]. For this reason, we decided to better investigate the functional role of MSI2 in particular in MLLr infant ALL.

MSI2 as a Putative Therapeutic Target

MSI2 and MSI family proteins can represent a promising therapeutic target for human cancer. Indeed, some small molecule inhibitors for MSI1 and MSI2 have been discovered in the last years. Here follows a review of the most important studies, with a particular focus on leukemia.

Clingman and colleagues reported the results of a screening of compounds targeting MSI1 by using a fluorescence polarization (FP) competition assay to search for compounds that would disrupt the binding of MSI proteins to a short fluorescein-labeled RNA. They found that the Oleic Acid and several other ω-9 monounsaturated fatty acids inhibited MSI1 binding to RNA by binding the RRM domain. As the RRM domains is identical in MSI1 and MS2, the compounds inhibiting MSI1 presumably also target MSI2. In addition, they discovered that MSI1 promoted the expression of stearoyl-CoA desaturase (SCD), an enzyme involved in the long chain monounsaturated fatty acids production, when oleic acid levels were low; therefore Musashi-1 acts as a 'nutrient sensor' by regulating the fatty acid metabolism[125]. Indeed, SCD was also found among the

mRNA targets directly bound and regulated by MSI2 in the HITS-CLIP database of Park et al.[99].

Lan and colleagues screened a set of 2000 compounds disrupting the binding of MSI1 to its consensus RNA binding site by using the fluorescence polarization (FP) competition assay. The best candidate compound active against MSI1 was (−)-gossypol, a natural product extracted from cottonseed. The authors observed that this compound decreased the Notch/Wnt signaling in colon cancer cells, induced apoptosis/autophagy in cancer cell lines in vitro and inhibited tumor growth of human colon cancers in a xenograft model. The compound (−)-gossypol, which has already completed Phase IIb clinical trials for prostate cancer, is an inhibitor of the anti-apoptotic Bcl-family proteins (Bcl-xL, Bcl-2, and Mcl-1)[126]. Later, through an additional screening, the same group identified a more potent and specific inhibitor of MSI1 and MSI2, the Gossypolone (GN, a derivative of Gossypol), and used PEGylated liposomes to improve the bioavailability and the biocompatibility of this compound. GN bound to MSI1-RBD1 and caused a decrease in cell growth and an induction of the apoptosis and autophagy in colon cancer cell lines[127]. This studies clearly demonstrated a correlation between the effect of an anti-Bcl-2 compound (and its derivative) on MSI2 inhibition.

More recent, in a very interesting study, the authors used the mass spectroscopy (MS) analysis of traditional herbal medicines to find new MSI2 RRM1 antagonists. 262 molecules came out from the MS

analysis and the subsequential docking studies of these identified five compounds as the most promising antagonist of MSI2: Methotrexate (M3) used for some types of cancer, psoriasis or rheumatoid arthritis; Phthalylsulfathiazole (M5), a broad-spectrum antibiotic for bowel surgery and infections of the colon; Phosphoric acid (M7), toxic chemical used to sterilize certain surgical instruments; b-Carotene (M8), red-orange pigment found in plants and fruits; and rescinnamine (M9), angiotensin-converting enzyme inhibitor used as an antihypertensive drug[128].

In the context of leukemia, a drug discovery study from Kharas' group identified the small molecule Ro 08–2750 as a selective inhibitor of MSI2. The authors screened a library of 6208 compounds potentially active against recombinant MSI1 and MSI2 and through biochemical assays they confirmed that Ro 08-2750 directly bound MSI2 RRM1 and selectively inhibited its function by competing for RNA-binding.

The MSI2 inhibitor Ro 08-2750 was used in pre-clinicals studies for AML and CLL. Treatment with this compound induced differentiation and apoptosis and decreased the translation of MSI2 targets (TGFBR1, c-MYC, SMAD3, CDKN1A) in human myeloid leukemia cells. In vivo Ro 08-2750 administration every 3 days for 19 days after transplantation with MLL::AF9+ leukemia cells was well tolerated without overt toxicity and caused a significant decrease of c-MYC levels, spleen weights and white blood cells count. However, there

was no change in leukemia progression with or without Ro treatment and this is the main limit of this study[129].

Ro 08-2750 administration to primary blasts from patients affected by CLL reduced the number of leukemic B and myeloid cells while spared the normal B cells and the T cells. Ro 08-2750 showed an efficacy preferentially on cycling and actively dividing leukemic B cells in which it determined an increase of apoptosis and cell cycle arrest. In addition, mice transplanted with CLL cells were treated with Ro 08-2750 twice a week for 21 days and showed a significant decrease in spleen weights, total white blood cells, and leukemic B lymphocytes without overt toxicity. Moreover, the authors found that Ro was selective for leukemia cells without affecting HSCs or non-lymphoid/myeloid progenitors[120].

Very recently, another study from Kharas' group reported that MSI2 and TP53 were both involved in the resistance to Protein Arginine Methyltransferase 5 (PRMT5) inhibitor (GSK-591) in B-cell lymphoma and they tested the effect of GSK-591 treatment in combination with Ro 08-2750 or Venetoclax. Ro 08-2750 was found to act synergistically with GSK-591 and the co-treatment induced anti-proliferative activity and cell cycle arrest in lymphoma cells by blocking c-MYC and BCL-2 translation[121].

AIM OF THE THESIS

The topic of my PhD was specifically focused on MLLr B-ALL in infants, with the main purposes to:

- Investigate the functional role of the RNA-binding Musashi-2 potentially involved in MLLr B-ALL, as a novel druggable target for therapy.
- Shed light onto the mechanisms possibly involved in drug resistance (in particular Glucocorticoid-resistance) typically associated to infants with MLLr ALL.
- Identify novel compounds potentially active in patients with high-risk B-ALL leukemia.

The biological mechanisms involved in the pathogenesis and disease progression of infant MLLr leukemia are not completely understood so far; therefore, the identification of potentially druggable genes involved in MLL leukemogenesis is crucial to shed light onto the mechanism of disease presentation and progression, as well as to develop novel therapeutic strategies. The study presented in Chapter 2 was fully dedicated to unraveling the functional role of the RNA-binding protein MSI2 in infant MLLr ALL, which was the main project of my PhD thesis. In this study, we specifically aimed at:

- generating a human MLL::AF4+ ALL cell line with MSI2 knock-out by using the CRISPR/CAS9 genome editing technology;

- addressing whether the lack of MSI2 in MLLr ALL cells has an impact on cell growth, leukemogenic potential and response to treatment through the functional study of MSI2 KO cells in vitro and in vivo;
- evaluating the anti-leukemic effect of targeting MSI2 by using a small compound inhibitor (Ro 08-2750), alone or in combination with other drugs.

Additionally, in Chapter 3 it is reported the generation of a RNA interference mouse model of patient-derived xenograft in vivo to target MSI2 in MLLr infant ALL primary patient's sample, and some preliminary data are reported.

Finally, Chapter 4 describes a second study in which I was primarily involved during my PhD, where we applied a high-thruput drug screening platform in order to test the efficacy of selected compounds to target high-risk childhood B-ALL, including infant MLLr ALL cases. This study was specifically aimed at:

- establishing a high-through-put drug screening approach as a useful tool for drug testing of primary-derived patients' samples.
- identifying compounds potentially active in a cohort of high-risk subgroups of pediatric B-ALL, or specifically active for MLLr infant ALL patients

- further validating the efficacy of novel compounds identified with the drug screening and correlating the drug response property with the clinical features.

References

1 Celotti, F. *Patologia generale e Fisiopatologia*. (2013).

2 Kebriaei, P., Anastasi, J. & Larson, R. A. Acute lymphoblastic leukaemia: diagnosis and classification. *Best practice & research. Clinical haematology* **15**, 597-621, doi:10.1053/beha.2002.0224 (2002).

3 Pui, C. H. Childhood leukemias. *The New England journal of medicine* **332**, 1618-1630, doi:10.1056/NEJM199506153322407 (1995).

4 Greaves, M. F., Chan, L. C., Furley, A. J., Watt, S. M. & Molgaard, H. V. Lineage promiscuity in hemopoietic differentiation and leukemia. *Blood* **67**, 1-11 (1986).

5 Lim, J. Y., Bhatia, S., Robison, L. L. & Yang, J. J. Genomics of racial and ethnic disparities in childhood acute lymphoblastic leukemia. *Cancer* **120**, 955-962, doi:10.1002/cncr.28531 (2014).

6 Juliusson, G. & Hough, R. Leukemia. *Progress in tumor research* **43**, 87-100, doi:10.1159/000447076 (2016).

7 Greaves, M. Infection, immune responses and the aetiology of childhood leukaemia. *Nature reviews. Cancer* **6**, 193-203, doi:10.1038/nrc1816 (2006).

8 Armstrong, S. A. & Look, A. T. Molecular genetics of acute lymphoblastic leukemia. *Journal of clinical oncology : official journal of the American Society of Clinical Oncology* **23**, 6306-6315, doi:10.1200/JCO.2005.05.047 (2005).

9 Greaves, M. A causal mechanism for childhood acute lymphoblastic leukaemia. *Nature reviews. Cancer* **18**, 471-484, doi:10.1038/s41568-018-0015-6 (2018).

10 Andersson, A. K. *et al.* The landscape of somatic mutations in infant MLL-rearranged acute lymphoblastic leukemias. *Nature genetics* **47**, 330-337, doi:10.1038/ng.3230 (2015).

11 Gilliland, D. G., Jordan, C. T. & Felix, C. A. The molecular basis of leukemia. *Hematology. American Society of Hematology. Education Program*, 80-97, doi:10.1182/asheducation-2004.1.80 (2004).

12 Biondi, A., Cimino, G., Pieters, R. & Pui, C. H. Biological and therapeutic aspects of infant leukemia. *Blood* **96**, 24-33 (2000).

13 El Chaer, F., Keng, M. & Ballen, K. K. MLL-Rearranged Acute Lymphoblastic Leukemia. *Current hematologic malignancy reports* **15**, 83-89, doi:10.1007/s11899-020-00582-5 (2020).

14 Forgione, M. O., McClure, B. J., Eadie, L. N., Yeung, D. T. & White, D. L. KMT2A rearranged acute lymphoblastic leukaemia: Unravelling the genomic complexity and heterogeneity of this high-risk disease. *Cancer letters* **469**, 410-418, doi:10.1016/j.canlet.2019.11.005 (2020).

15 Winters, A. C. & Bernt, K. M. MLL-Rearranged Leukemias-An Update on Science and Clinical Approaches. *Frontiers in pediatrics* **5**, 4, doi:10.3389/fped.2017.00004 (2017).

16 Greaves, M. F. & Wiemels, J. Origins of chromosome translocations in childhood leukaemia. *Nature reviews. Cancer* **3**, 639-649, doi:10.1038/nrc1164 (2003).

17 Mori, H. *et al.* Chromosome translocations and covert leukemic clones are generated during normal fetal development. *Proceedings of the National Academy of Sciences of the United States of America* **99**, 8242-8247, doi:10.1073/pnas.112218799 (2002).

18 Taub, J. W. & Ge, Y. The prenatal origin of childhood acute lymphoblastic leukemia. *Leukemia & lymphoma* **45**, 19-25, doi:10.1080/1042819031000149403 (2004).

19 Greaves, M. In utero origins of childhood leukaemia. *Early human development* **81**, 123-129, doi:10.1016/j.earlhumdev.2004.10.004 (2005).

20 Khabirova, E. *et al.* Single-cell transcriptomics reveals a distinct developmental state of KMT2A-rearranged infant B-cell acute lymphoblastic leukemia. *Nature medicine* **28**, 743-751, doi:10.1038/s41591-022-01720-7 (2022).

21 Symeonidou, V. *et al.* Defining the fetal origin of MLL-AF4 infant leukemia highlights specific fatty acid requirements. *Cell reports* **37**, 109900, doi:10.1016/j.celrep.2021.109900 (2021).

22 Rice, S. *et al.* A human fetal liver-derived infant MLL-AF4 acute lymphoblastic leukemia model reveals a distinct fetal gene expression program. *Nature communications* **12**, 6905, doi:10.1038/s41467-021-27270-z (2021).

23 Cimino, G. *et al.* ALL-1 gene at chromosome 11q23 is consistently altered in acute leukemia of early infancy. *Blood* **82**, 544-546 (1993).

24 Tkachuk, D. C., Kohler, S. & Cleary, M. L. Involvement of a homolog of Drosophila trithorax by 11q23 chromosomal translocations in acute leukemias. *Cell* **71**, 691-700, doi:10.1016/0092-8674(92)90602-9 (1992).

25 Gu, Y. *et al.* The t(4;11) chromosome translocation of human acute leukemias fuses the ALL-1 gene, related to Drosophila trithorax, to

the AF-4 gene. *Cell* **71**, 701-708, doi:10.1016/0092-8674(92)90603-a (1992).

26 Yu, B. D., Hess, J. L., Horning, S. E., Brown, G. A. & Korsmeyer, S. J. Altered Hox expression and segmental identity in Mll-mutant mice. *Nature* **378**, 505-508, doi:10.1038/378505a0 (1995).

27 Rasio, D., Schichman, S. A., Negrini, M., Canaani, E. & Croce, C. M. Complete exon structure of the ALL1 gene. *Cancer research* **56**, 1766-1769 (1996).

28 Krivtsov, A. V. & Armstrong, S. A. MLL translocations, histone modifications and leukaemia stem-cell development. *Nature reviews. Cancer* **7**, 823-833, doi:10.1038/nrc2253 (2007).

29 Hsieh, J. J., Ernst, P., Erdjument-Bromage, H., Tempst, P. & Korsmeyer, S. J. Proteolytic cleavage of MLL generates a complex of N- and C-terminal fragments that confers protein stability and subnuclear localization. *Molecular and cellular biology* **23**, 186-194 (2003).

30 Milne, T. A. *et al.* MLL targets SET domain methyltransferase activity to Hox gene promoters. *Molecular cell* **10**, 1107-1117, doi:10.1016/s1097-2765(02)00741-4 (2002).

31 Yu, B. D., Hanson, R. D., Hess, J. L., Horning, S. E. & Korsmeyer, S. J. MLL, a mammalian trithorax-group gene, functions as a transcriptional maintenance factor in morphogenesis. *Proceedings of the National Academy of Sciences of the United States of America* **95**, 10632-10636 (1998).

32 Krivtsov, A. V. *et al.* H3K79 methylation profiles define murine and human MLL-AF4 leukemias. *Cancer cell* **14**, 355-368, doi:10.1016/j.ccr.2008.10.001 (2008).

33 Milne, T. A. *et al.* Multiple interactions recruit MLL1 and MLL1 fusion proteins to the HOXA9 locus in leukemogenesis. *Molecular cell* **38**, 853-863, doi:10.1016/j.molcel.2010.05.011 (2010).

34 Slany, R. K. MLL fusion proteins and transcriptional control. *Biochimica et biophysica acta. Gene regulatory mechanisms* **1863**, 194503, doi:10.1016/j.bbagrm.2020.194503 (2020).

35 He, N. *et al.* Human Polymerase-Associated Factor complex (PAFc) connects the Super Elongation Complex (SEC) to RNA polymerase II on chromatin. *Proceedings of the National Academy of Sciences of the United States of America* **108**, E636-645, doi:10.1073/pnas.1107107108 (2011).

36 Tran, T. M. & Rao, D. S. RNA binding proteins in MLL-rearranged leukemia. *Experimental hematology & oncology* **11**, 80, doi:10.1186/s40164-022-00343-5 (2022).

37 Bernt, K. M. *et al.* MLL-rearranged leukemia is dependent on aberrant H3K79 methylation by DOT1L. *Cancer cell* **20**, 66-78, doi:10.1016/j.ccr.2011.06.010 (2011).

38 Zhang, Y., Chen, A., Yan, X. M. & Huang, G. Disordered epigenetic regulation in MLL-related leukemia. *International journal of hematology* **96**, 428-437, doi:10.1007/s12185-012-1180-0 (2012).

39 Bardini, M. *et al.* Antileukemic Efficacy of BET Inhibitor in a Preclinical Mouse Model of MLL-AF4(+) Infant ALL. *Molecular cancer therapeutics* **17**, 1705-1716, doi:10.1158/1535-7163.MCT-17-1123 (2018).

40 Marschalek, R. MLL leukemia and future treatment strategies. *Archiv der Pharmazie* **348**, 221-228, doi:10.1002/ardp.201400449 (2015).

41 Kotecha, R. S., Gottardo, N. G., Kees, U. R. & Cole, C. H. The evolution of clinical trials for infant acute lymphoblastic leukemia. *Blood cancer journal* **4**, e200, doi:10.1038/bcj.2014.17 (2014).

42 Pieters, R. *et al.* A treatment protocol for infants younger than 1 year with acute lymphoblastic leukaemia (Interfant-99): an observational study and a multicentre randomised trial. *Lancet* **370**, 240-250, doi:10.1016/S0140-6736(07)61126-X (2007).

43 Pieters, R. *et al.* Outcome of Infants Younger Than 1 Year With Acute Lymphoblastic Leukemia Treated With the Interfant-06 Protocol: Results From an International Phase III Randomized Study. *Journal of clinical oncology : official journal of the American Society of Clinical Oncology* **37**, 2246-2256, doi:10.1200/JCO.19.00261 (2019).

44 Brown, P. A. *et al.* FLT3 inhibitor lestaurtinib plus chemotherapy for newly diagnosed KMT2A-rearranged infant acute lymphoblastic leukemia: Children's Oncology Group trial AALL0631. *Leukemia* **35**, 1279-1290, doi:10.1038/s41375-021-01177-6 (2021).

45 Tomizawa D, Miyamura T, Imamura T, et al. A risk-stratified therapy for infants with acute lymphoblastic leukemia: a report from the JPLSG MLL-10 trial. Blood. 2020;136(16):1813-1823. *Blood* **139**, 2848, doi:10.1182/blood.2022016374 (2022).

46 Clesham, K. *et al.* Blinatumomab for infant acute lymphoblastic leukemia. *Blood* **135**, 1501-1504, doi:10.1182/blood.2019004008 (2020).

47 Locatelli, F. *et al.* Effect of Blinatumomab vs Chemotherapy on Event-Free Survival Among Children With High-risk First-Relapse B-Cell Acute Lymphoblastic Leukemia: A Randomized Clinical Trial. *Jama* **325**, 843-854, doi:10.1001/jama.2021.0987 (2021).

48 Britten, O., Ragusa, D., Tosi, S. & Kamel, Y. M. MLL-Rearranged Acute Leukemia with t(4;11)(q21;q23)-Current Treatment Options. Is There a Role for CAR-T Cell Therapy? *Cells* **8**, doi:10.3390/cells8111341 (2019).

49 Liao, W., Kohler, M. E., Fry, T. & Ernst, P. Does lineage plasticity enable escape from CAR-T cell therapy? Lessons from MLL-r leukemia. *Experimental hematology* **100**, 1-11, doi:10.1016/j.exphem.2021.07.002 (2021).

50 Brown, P., Levis, M., McIntyre, E., Griesemer, M. & Small, D. Combinations of the FLT3 inhibitor CEP-701 and chemotherapy synergistically kill infant and childhood MLL-rearranged ALL cells in a sequence-dependent manner. *Leukemia* **20**, 1368-1376, doi:10.1038/sj.leu.2404277 (2006).

51 Driessen, E. M. *et al.* Frequencies and prognostic impact of RAS mutations in MLL-rearranged acute lymphoblastic leukemia in infants. *Haematologica* **98**, 937-944, doi:10.3324/haematol.2012.067983 (2013).

52 Kerstjens, M. *et al.* MEK inhibition is a promising therapeutic strategy for MLL-rearranged infant acute lymphoblastic leukemia patients carrying RAS mutations. *Oncotarget* **8**, 14835-14846, doi:10.18632/oncotarget.11730 (2017).

53 Garrido Castro, P. *et al.* The HDAC inhibitor panobinostat (LBH589) exerts in vivo anti-leukaemic activity against MLL-rearranged acute lymphoblastic leukaemia and involves the RNF20/RNF40/WAC-H2B ubiquitination axis. *Leukemia* **32**, 323-331, doi:10.1038/leu.2017.216 (2018).

54 Cheung, L. C. *et al.* Romidepsin enhances the efficacy of cytarabine in vivo, revealing histone deacetylase inhibition as a promising therapeutic strategy for KMT2A-rearranged infant acute lymphoblastic leukemia. *Haematologica* **104**, e300-e303, doi:10.3324/haematol.2018.192906 (2019).

55 Schafer, E. *et al.* Promoter hypermethylation in MLL-r infant acute lymphoblastic leukemia: biology and therapeutic targeting. *Blood* **115**, 4798-4809, doi:10.1182/blood-2009-09-243634 (2010).

56 Stumpel, D. J. *et al.* Specific promoter methylation identifies different subgroups of MLL-rearranged infant acute lymphoblastic leukemia, influences clinical outcome, and provides therapeutic options. *Blood* **114**, 5490-5498, doi:10.1182/blood-2009-06-227660 (2009).

57 Roolf, C. *et al.* Decitabine demonstrates antileukemic activity in B cell precursor acute lymphoblastic leukemia with MLL

rearrangements. *Journal of hematology & oncology* **11**, 62, doi:10.1186/s13045-018-0607-3 (2018).

58 Schneider, P. *et al.* Decitabine mildly attenuates MLL-rearranged acute lymphoblastic leukemia in vivo, and represents a poor chemo-sensitizer. *EJHaem* **1**, 527-536, doi:10.1002/jha2.81 (2020).

59 Dawson, M. A. *et al.* Inhibition of BET recruitment to chromatin as an effective treatment for MLL-fusion leukaemia. *Nature* **478**, 529-533, doi:10.1038/nature10509 (2011).

60 Fong, C. Y. *et al.* BET inhibitor resistance emerges from leukaemia stem cells. *Nature* **525**, 538-542, doi:10.1038/nature14888 (2015).

61 Rathert, P. *et al.* Transcriptional plasticity promotes primary and acquired resistance to BET inhibition. *Nature* **525**, 543-547, doi:10.1038/nature14898 (2015).

62 Daigle, S. R. *et al.* Selective killing of mixed lineage leukemia cells by a potent small-molecule DOT1L inhibitor. *Cancer cell* **20**, 53-65, doi:10.1016/j.ccr.2011.06.009 (2011).

63 Daigle, S. R. *et al.* Potent inhibition of DOT1L as treatment of MLL-fusion leukemia. *Blood* **122**, 1017-1025, doi:10.1182/blood-2013-04-497644 (2013).

64 Yi, Y. & Ge, S. Targeting the histone H3 lysine 79 methyltransferase DOT1L in MLL-rearranged leukemias. *Journal of hematology & oncology* **15**, 35, doi:10.1186/s13045-022-01251-1 (2022).

65 Campbell, C. T. *et al.* Mechanisms of Pinometostat (EPZ-5676) Treatment-Emergent Resistance in MLL-Rearranged Leukemia. *Molecular cancer therapeutics* **16**, 1669-1679, doi:10.1158/1535-7163.MCT-16-0693 (2017).

66 Grembecka, J. *et al.* Menin-MLL inhibitors reverse oncogenic activity of MLL fusion proteins in leukemia. *Nature chemical biology* **8**, 277-284, doi:10.1038/nchembio.773 (2012).

67 Krivtsov, A. V. *et al.* A Menin-MLL Inhibitor Induces Specific Chromatin Changes and Eradicates Disease in Models of MLL-Rearranged Leukemia. *Cancer cell* **36**, 660-673 e611, doi:10.1016/j.ccell.2019.11.001 (2019).

68 Liu, H. *et al.* Proteasome inhibitors evoke latent tumor suppression programs in pro-B MLL leukemias through MLL-AF4. *Cancer cell* **25**, 530-542, doi:10.1016/j.ccr.2014.03.008 (2014).

69 Benito, J. M. *et al.* MLL-Rearranged Acute Lymphoblastic Leukemias Activate BCL-2 through H3K79 Methylation and Are Sensitive to the BCL-2-Specific Antagonist ABT-199. *Cell reports* **13**, 2715-2727, doi:10.1016/j.celrep.2015.12.003 (2015).

70 Alford, S. E. *et al.* BH3 Inhibitor Sensitivity and Bcl-2 Dependence in Primary Acute Lymphoblastic Leukemia Cells. *Cancer research* **75**, 1366-1375, doi:10.1158/0008-5472.CAN-14-1849 (2015).

71 Khaw, S. L. *et al.* Venetoclax responses of pediatric ALL xenografts reveal sensitivity of MLL-rearranged leukemia. *Blood* **128**, 1382-1395, doi:10.1182/blood-2016-03-707414 (2016).

72 Richter, A. *et al.* Effective tumor cell abrogation via Venetoclax-mediated BCL-2 inhibition in KMT2A-rearranged acute B-lymphoblastic leukemia. *Cell death discovery* **8**, 302, doi:10.1038/s41420-022-01093-3 (2022).

73 Cheung, L. C. *et al.* Preclinical efficacy of azacitidine and venetoclax for infant KMT2A-rearranged acute lymphoblastic leukemia reveals a new therapeutic strategy. *Leukemia*, doi:10.1038/s41375-022-01746-3 (2022).

74 DiNardo, C. D. *et al.* Azacitidine and Venetoclax in Previously Untreated Acute Myeloid Leukemia. *The New England journal of medicine* **383**, 617-629, doi:10.1056/NEJMoa2012971 (2020).

75 DiNardo, C. D. *et al.* Venetoclax Combined With FLAG-IDA Induction and Consolidation in Newly Diagnosed and Relapsed or Refractory Acute Myeloid Leukemia. *Journal of clinical oncology : official journal of the American Society of Clinical Oncology* **39**, 2768-2778, doi:10.1200/JCO.20.03736 (2021).

76 Pieters, R. *et al.* Relation between age, immunophenotype and in vitro drug resistance in 395 children with acute lymphoblastic leukemia--implications for treatment of infants. *Leukemia* **12**, 1344-1348 (1998).

77 Stam, R. W. *et al.* Association of high-level MCL-1 expression with in vitro and in vivo prednisone resistance in MLL-rearranged infant acute lymphoblastic leukemia. *Blood* **115**, 1018-1025, doi:10.1182/blood-2009-02-205963 (2010).

78 Spijkers-Hagelstein, J. A. *et al.* Glucocorticoid sensitisation in Mixed Lineage Leukaemia-rearranged acute lymphoblastic leukaemia by the pan-BCL-2 family inhibitors gossypol and AT-101. *European journal of cancer* **50**, 1665-1674, doi:10.1016/j.ejca.2014.03.011 (2014).

79 Spijkers-Hagelstein, J. A. *et al.* Elevated S100A8/S100A9 expression causes glucocorticoid resistance in MLL-rearranged infant acute lymphoblastic leukemia. *Leukemia* **26**, 1255-1265, doi:10.1038/leu.2011.388 (2012).

80 Spijkers-Hagelstein, J. A., Mimoso Pinhancos, S., Schneider, P., Pieters, R. & Stam, R. W. Src kinase-induced phosphorylation of annexin A2 mediates glucocorticoid resistance in MLL-rearranged

infant acute lymphoblastic leukemia. *Leukemia* **27**, 1063-1071, doi:10.1038/leu.2012.372 (2013).

81 Spijkers-Hagelstein, J. A., Pinhancos, S. S., Schneider, P., Pieters, R. & Stam, R. W. Chemical genomic screening identifies LY294002 as a modulator of glucocorticoid resistance in MLL-rearranged infant ALL. *Leukemia* **28**, 761-769, doi:10.1038/leu.2013.245 (2014).

82 Mousavian, Z., Nowzari-Dalini, A., Stam, R. W., Rahmatallah, Y. & Masoudi-Nejad, A. Network-based expression analysis reveals key genes related to glucocorticoid resistance in infant acute lymphoblastic leukemia. *Cellular oncology* **40**, 33-45, doi:10.1007/s13402-016-0303-7 (2017).

83 Mousavian, Z., Nowzari-Dalini, A., Rahmatallah, Y. & Masoudi-Nejad, A. Differential network analysis and protein-protein interaction study reveals active protein modules in glucocorticoid resistance for infant acute lymphoblastic leukemia. *Molecular medicine* **25**, 36, doi:10.1186/s10020-019-0106-1 (2019).

84 de Groot, A. P. *et al.* Targeting critical kinases and anti-apoptotic molecules overcomes steroid resistance in MLL-rearranged leukaemia. *EBioMedicine* **64**, 103235, doi:10.1016/j.ebiom.2021.103235 (2021).

85 Candelli, T. *et al.* Identification and characterization of relapse-initiating cells in MLL-rearranged infant ALL by single-cell transcriptomics. *Leukemia* **36**, 58-67, doi:10.1038/s41375-021-01341-y (2022).

86 Glisovic, T., Bachorik, J. L., Yong, J. & Dreyfuss, G. RNA-binding proteins and post-transcriptional gene regulation. *FEBS letters* **582**, 1977-1986, doi:10.1016/j.febslet.2008.03.004 (2008).

87 Li, W., Deng, X. & Chen, J. RNA-binding proteins in regulating mRNA stability and translation: roles and mechanisms in cancer. *Seminars in cancer biology* **86**, 664-677, doi:10.1016/j.semcancer.2022.03.025 (2022).

88 Prieto, C. & Kharas, M. G. RNA Regulators in Leukemia and Lymphoma. *Cold Spring Harbor perspectives in medicine* **10**, doi:10.1101/cshperspect.a034967 (2020).

89 Elcheva, I. A. & Spiegelman, V. S. Targeting RNA-binding proteins in acute and chronic leukemia. *Leukemia* **35**, 360-376, doi:10.1038/s41375-020-01066-4 (2021).

90 Kang, D., Lee, Y. & Lee, J. S. RNA-Binding Proteins in Cancer: Functional and Therapeutic Perspectives. *Cancers* **12**, doi:10.3390/cancers12092699 (2020).

91 Nakamura, M., Okano, H., Blendy, J. A. & Montell, C. Musashi, a neural RNA-binding protein required for Drosophila adult external sensory organ development. *Neuron* **13**, 67-81 (1994).

92 das Chagas, P. F., Baroni, M., Brassesco, M. S. & Tone, L. G. Interplay between the RNA binding-protein Musashi and developmental signaling pathways. *The journal of gene medicine* **22**, e3136, doi:10.1002/jgm.3136 (2020).

93 Sun, J., Sheng, W., Ma, Y. & Dong, M. Potential Role of Musashi-2 RNA-Binding Protein in Cancer EMT. *OncoTargets and therapy* **14**, 1969-1980, doi:10.2147/OTT.S298438 (2021).

94 Kudinov, A. E., Karanicolas, J., Golemis, E. A. & Boumber, Y. Musashi RNA-Binding Proteins as Cancer Drivers and Novel Therapeutic Targets. *Clinical cancer research : an official journal of the American Association for Cancer Research* **23**, 2143-2153, doi:10.1158/1078-0432.CCR-16-2728 (2017).

95 Sutherland, J. M. *et al.* Developmental expression of Musashi-1 and Musashi-2 RNA-binding proteins during spermatogenesis: analysis of the deleterious effects of dysregulated expression. *Biology of reproduction* **90**, 92, doi:10.1095/biolreprod.113.115261 (2014).

96 Lin, J. C. *et al.* MSI1 associates glioblastoma radioresistance via homologous recombination repair, tumor invasion and cancer stem-like cell properties. *Radiotherapy and oncology : journal of the European Society for Therapeutic Radiology and Oncology* **129**, 352-363, doi:10.1016/j.radonc.2018.09.014 (2018).

97 Nikpour, P., Emadi-Baygi, M., Mohhamad-Hashem, F., Maracy, M. R. & Haghjooy-Javanmard, S. MSI1 overexpression in diffuse type of gastric cancer. *Pathology, research and practice* **209**, 10-13, doi:10.1016/j.prp.2012.09.008 (2013).

98 Kharas, M. G. *et al.* Musashi-2 regulates normal hematopoiesis and promotes aggressive myeloid leukemia. *Nature medicine* **16**, 903-908, doi:10.1038/nm.2187 (2010).

99 Park, S. M. *et al.* Musashi2 sustains the mixed-lineage leukemia-driven stem cell regulatory program. *The Journal of clinical investigation* **125**, 1286-1298, doi:10.1172/JCI78440 (2015).

100 Barbouti, A. *et al.* A novel gene, MSI2, encoding a putative RNA-binding protein is recurrently rearranged at disease progression of chronic myeloid leukemia and forms a fusion gene with HOXA9 as a result of the cryptic t(7;17)(p15;q23). *Cancer research* **63**, 1202-1206 (2003).

101 Fox, R. G., Park, F. D., Koechlein, C. S., Kritzik, M. & Reya, T. Musashi signaling in stem cells and cancer. *Annual review of cell and*

developmental biology **31**, 249-267, doi:10.1146/annurev-cellbio-100814-125446 (2015).

102 Schuschel, K. *et al.* RNA-Binding Proteins in Acute Leukemias. *International journal of molecular sciences* **21**, doi:10.3390/ijms21103409 (2020).

103 Li, M. *et al.* RNA-binding protein MSI2 isoforms expression and regulation in progression of triple-negative breast cancer. *Journal of experimental & clinical cancer research : CR* **39**, 92, doi:10.1186/s13046-020-01587-x (2020).

104 MacNicol, M. C. *et al.* Evasion of regulatory phosphorylation by an alternatively spliced isoform of Musashi2. *Scientific reports* **7**, 11503, doi:10.1038/s41598-017-11917-3 (2017).

105 Ito, T. *et al.* Regulation of myeloid leukaemia by the cell-fate determinant Musashi. *Nature* **466**, 765-768, doi:10.1038/nature09171 (2010).

106 Fujiwara, T., Zhou, J., Ye, S. & Zhao, H. RNA-binding protein Musashi2 induced by RANKL is critical for osteoclast survival. *Cell death & disease* **7**, e2300, doi:10.1038/cddis.2016.213 (2016).

107 Sutherland, J. M. *et al.* RNA binding protein Musashi-1 directly targets Msi2 and Erh during early testis germ cell development and interacts with IPO5 upon translocation to the nucleus. *FASEB journal : official publication of the Federation of American Societies for Experimental Biology* **29**, 2759-2768, doi:10.1096/fj.14-265868 (2015).

108 de Andres-Aguayo, L., Varas, F. & Graf, T. Musashi 2 in hematopoiesis. *Current opinion in hematology* **19**, 268-272, doi:10.1097/MOH.0b013e328353c778 (2012).

109 Moore, M. A. A cancer fate in the hands of a samurai. *Nature medicine* **16**, 963-965, doi:10.1038/nm0910-963 (2010).

110 Hope, K. J. *et al.* An RNAi screen identifies Msi2 and Prox1 as having opposite roles in the regulation of hematopoietic stem cell activity. *Cell stem cell* **7**, 101-113, doi:10.1016/j.stem.2010.06.007 (2010).

111 Ly, M. *et al.* Diminished AHR Signaling Drives Human Acute Myeloid Leukemia Stem Cell Maintenance. *Cancer research* **79**, 5799-5811, doi:10.1158/0008-5472.CAN-19-0274 (2019).

112 Rentas, S. *et al.* Musashi-2 attenuates AHR signalling to expand human haematopoietic stem cells. *Nature* **532**, 508-511, doi:10.1038/nature17665 (2016).

113 Han, Y. *et al.* Musashi-2 Silencing Exerts Potent Activity against Acute Myeloid Leukemia and Enhances Chemosensitivity to Daunorubicin. *PloS one* **10**, e0136484, doi:10.1371/journal.pone.0136484 (2015).

114 Zhang, H. *et al.* Musashi2 modulates K562 leukemic cell proliferation and apoptosis involving the MAPK pathway. *Experimental cell research* **320**, 119-127, doi:10.1016/j.yexcr.2013.09.009 (2014).
115 Kwon, H. Y. *et al.* Tetraspanin 3 Is Required for the Development and Propagation of Acute Myelogenous Leukemia. *Cell stem cell* **17**, 152-164, doi:10.1016/j.stem.2015.06.006 (2015).
116 Hattori, A., McSkimming, D., Kannan, N. & Ito, T. RNA binding protein MSI2 positively regulates FLT3 expression in myeloid leukemia. *Leukemia research* **54**, 47-54, doi:10.1016/j.leukres.2017.01.015 (2017).
117 Hattori, A. *et al.* Cancer progression by reprogrammed BCAA metabolism in myeloid leukaemia. *Nature* **545**, 500-504, doi:10.1038/nature22314 (2017).
118 Park, S. M. *et al.* Musashi-2 controls cell fate, lineage bias, and TGF-beta signaling in HSCs. *The Journal of experimental medicine* **211**, 71-87, doi:10.1084/jem.20130736 (2014).
119 Nguyen, D. T. T. *et al.* HyperTRIBE uncovers increased MUSASHI-2 RNA binding activity and differential regulation in leukemic stem cells. *Nature communications* **11**, 2026, doi:10.1038/s41467-020-15814-8 (2020).
120 Palacios, F. *et al.* Musashi 2 influences chronic lymphocytic leukemia cell survival and growth making it a potential therapeutic target. *Leukemia* **35**, 1037-1052, doi:10.1038/s41375-020-01115-y (2021).
121 Erazo, T. *et al.* TP53 mutations and RNA-binding protein MUSASHI-2 drive resistance to PRMT5-targeted therapy in B-cell lymphoma. *Nature communications* **13**, 5676, doi:10.1038/s41467-022-33137-8 (2022).
122 Aly, R. M. & Ghazy, H. F. Prognostic significance of MSI2 predicts unfavorable outcome in adult B-acute lymphoblastic leukemia. *International journal of laboratory hematology* **37**, 272-278, doi:10.1111/ijlh.12284 (2015).
123 Mu, Q. *et al.* High expression of Musashi-2 indicates poor prognosis in adult B-cell acute lymphoblastic leukemia. *Leukemia research* **37**, 922-927, doi:10.1016/j.leukres.2013.05.012 (2013).
124 Zhao, H. Z. *et al.* Prognostic significance of the Musashi-2 (MSI2) gene in childhood acute lymphoblastic leukemia. *Neoplasma* **63**, 150-157, doi:10.4149/neo_2016_018 (2016).
125 Clingman, C. C. *et al.* Allosteric inhibition of a stem cell RNA-binding protein by an intermediary metabolite. *eLife* **3**, doi:10.7554/eLife.02848 (2014).

126 Lan, L. *et al.* Natural product (-)-gossypol inhibits colon cancer cell growth by targeting RNA-binding protein Musashi-1. *Molecular oncology* **9**, 1406-1420, doi:10.1016/j.molonc.2015.03.014 (2015).

127 Lan, L. *et al.* Natural product derivative Gossypolone inhibits Musashi family of RNA-binding proteins. *BMC cancer* **18**, 809, doi:10.1186/s12885-018-4704-z (2018).

128 Adeniyi, J. N. *et al.* Unravelling the drugability of MSI2 RNA recognition motif (RRM) protein and the prediction of their effective antileukemia inhibitors from traditional herb concoctions. *Journal of biomolecular structure & dynamics* **40**, 2516-2529, doi:10.1080/07391102.2020.1840442 (2022).

129 Minuesa, G. *et al.* Small-molecule targeting of MUSASHI RNA-binding activity in acute myeloid leukemia. *Nature communications* **10**, 2691, doi:10.1038/s41467-019-10523-3 (2019).

CHAPTER 2

(Manuscript in preparation)

THE FUNCTIONAL ROLE OF MUSASHI-2 IN MLL REARRANGED B-ALL UNCOVERS POTENTIALLY TARGETABLE METABOLIC VULNERABILITIES OF LEUKEMIA

Valsecchi Luigia[1], Procopio Simona[1], Naso Simone[1], Mauri Mario[2], Piazza Rocco Giovanni[2], Watrin Titus[3], Bhatia Sanil[3], Arndt Borkhardt[3], Pasquale Valentina[4], Sarno Jolanda[5], Davis Kara L.[5], Fazio Grazia[1], Palmi Chiara[1], Trentin Luca[6], Bresolin Silvia[6], Sacco Elena[4], Biondi Andrea[1,7], Cazzaniga Giovanni[1,8,*] and Bardini Michela[1,*]

[1]Tettamanti Research Center, Pediatrics, Department of Medicine, University of Milano-Bicocca, Monza, Italy. [2]Hematology, Department of Medicine, University of Milano-Bicocca, Monza, Italy [3]Department of Paediatric Oncology, Haematology and Clinical Immunology, Heinrich-Heine University Dusseldorf, Medical Faculty, Düsseldorf, Germany. [4]Department of Biotechnology and Biosciences, University of Milano-Bicocca, Milan, Italy. [5]Department of Pediatrics, Hematology, Oncology, and Stem Cell Transplant and Regenerative Medicine, Stanford University, Stanford, CA [6]SDB Department, Pediatric Hemato-Oncology, University of Padua, Padua, Italy. [7]Pediatrics, Department of Medicine, University of Milano-Bicocca, Fondazione MBBM/San Gerardo Hospital, Monza, Italy. [8]Medical Genetics, Department of Medicine, University of Milano-Bicocca, Monza, Italy. [*]equal contribution

Abstract

MLL-rearranged B-Cell Precursor Acute Lymphoblastic Leukemia (MLLr BCP-ALL) is a rare but very aggressive disease frequently occurring in infants and associated with poor outcome. MLLr ALL cells are typically resistant to conventional therapy and prone to relapse. The biological mechanisms involved in the pathogenesis and drug resistance of MLLr ALL are not completely understood and the identification of druggable genes is urgently needed to develop novel therapeutic strategies. Herein we found that the RNA-binding protein Musashi-2 (MSI2) has a crucial role in MLLr BCP-ALL, by sustaining the growth and the leukemogenic potential of MLL:AF4+ ALL cells. Also, MSI2 is involved in the resistance to Glucocorticoids, as the lack or the pharmacological inhibition of MSI2 prevents mitochondrial activation upon Glucocorticoid's exposure and impairs mitochondrial respiration. The putative role of MSI2 in the bioenergetic metabolism of leukemia is a novel finding and paves the way for targeting metabolic vulnerabilities of BCP-ALL.

Introduction

Acute Lymphoblastic Leukemia (ALL) with the rearrangement of the KMT2A gene (also known as MLL) occurring in infants (infant MLLr ALL) is a rare but very aggressive disease associated with a poor outcome. Within the last decades two consequent International collaborative treatment protocols have been conceived to enrol infant patients with ALL (the Interfant-99 and Inetrfant-06 Clinical Trials). Nevertheless, the outcome of infant patients did not significantly improve over the years, and patients still suffer from a dismal prognosis (overall survival: 20-40%). Although the intense chemotherapy regimen applied (which combines both lympho- and myelo-specific treatments) initially allows the achievement of low level of minimal residual disease early after induction therapy in the majority of the patients, the early remission is transient and frequently followed by relapse. Compared to other patients older than 1 year, MLLr infant ALL patients are typically resistant to Glucocorticoids (GCs)[1], such as Prednisone and Dexamethasone, which represent one of the most important agents currently used for the treatment of MLLr leukemia[2]. It has been shown that GC-resistance largely contributes to the poor prognosis of infant MLLr ALL, especially in relation to young age at diagnosis[1,3-5], and the response to Prednisone in patients evaluated 8 days after the induction therapy was considered a prognostic indicator in the Interfant-99 Protocol. Given the aggressiveness of MLLr infant ALL and the failure of the current therapies, the identification of novel

druggable genes is urgently needed for the development of novel therapeutic strategies, in order to circumvent the therapy-resistance, prevent disease relapse and ameliorate the overall outcome.

Several studies have shed light onto the pathogenesis of infant MLLr leukemia, however the biological mechanisms underlying the disease progression and therapy-resistance are not completely understood yet. In a previous study, we identified a “core signature” of genes associated with the in vivo leukemia-initiating ability of MLL::AF4+ infant ALL and potentially involved in the disease onset and maintenance of leukemia[6]. Among them, we found the RNA-binding protein Musashi-2 (MSI2), a post-transcriptional regulator of gene expression. Two sequence-specific RNA-recognition motifs (RRM1 and RRM2), at the N-terminus of the gene allow the binding of MSI2 to its mRNA targets, which may either promote or block protein translation. In the hematopoietic system, MSI2 is highly expressed in primitive hematopoietic stem cells (HSCs) and early progenitor cells and its expression progressively decreases along with cell differentiations to mature blood cells. MSI2 has a pivotal role in maintaining the “stemness” of HSCs in normal hematopoiesis by regulating symmetric/asymmetric cell division. In a variety of cancers (solid tumors and leukemia) MSI2 was found to be overexpressed and a prognostic marker, being involved in cell proliferation, differentiation and maintenance of the cancer stem cell pool[7-9]. MSI2 was first reported as fused to HOXA9 gene in chronic myeloid leukemia, and responsible for the disease progression from the initial

chronic phase to the accelerated phase and final blast crisis[10,11]. Although several studies have clearly demonstrated the involvement of MSI2 in myeloid leukemia, including MLL::AF9+ acute myeloid leukemia[12], only a very limited number of studies focused on the role of MSI2 in the context of lymphoid malignancies, like B-cell lymphoma[13] and chronic lymphocytic leukemia[14]. With regards to B-cell precursor (BCP) ALL, the most frequent type of tumor occurring in children, our knowledge about the role of MSI2 is rather limited. The over-expression of MSI2 has been associated with a poorer outcome in both pediatric as well as adult BCP-ALL patients[15-17];however functional data are still missing. We previously found that MSI2 was a putative target of HOXA7/9 transcriptional factors in infant MLLr B-ALL patient-derived xenograft (PDX)[6]. HOXA9 is a master regulator of MLL leukemogenesis, and the transcriptional program sustained by HOXA9 is essential for the maintenance of leukemia. In agreement with our findings, a previous study reported that HOXA9 enhanced MSI2 gene expression in AML[18]. In turn, MSI2 directly binds the mRNA of HOXA9 and promotes its protein translation[12], thus suggesting the existence of a MSI2/HOXA9 autoregulatory axis.

Herein, by using a model of CRISPR-edited MSI2 KO cell line, we demonstrate that MSI2 supports the growth of MLL::AF4+ ALL in vitro, sustains the in vivo leukemogenic potential and it is involved in GC-resistance, thus pointing out a crucial role of this gene in MLLr ALL. Moreover, our study unravels for the first time a novel function

of MSI2 in the regulation of the bioenergetic metabolism of MLL::AF4+ ALL and paves the way for targeting the metabolic vulnerabilities of leukemia as a novel therapeutic approach to treat infants with MLLr ALL.

Results

MSI2 is a candidate marker for MLL::AF4+ B-ALL

To address whether MSI2 is a marker of pediatric BCP-ALL, we retrospectively analyzed the gene expression profile of 375 childhood leukemia samples at disease presentation taken from a previous study, the International Microarray Innovations in Leukemia (MILE) Study[19]. Overall, MSI2 was more expressed in children with BCP-ALL compared to AML counterpart and healthy donor BM samples. Also, with specific regard to MLLr cytogenetic subgroups, MSI2 expression was significantly higher in MLLr BCP-ALL compared to MLLr AML patients (Figure 1A). The mRNA targets directly bound and regulated by MSI2 were first reported in a comprehensive study by Kharas's group by using high-throughput sequencing and cross-linking RNA immunoprecipitation (HITS-CLIP Database)[12]. Notably, the top HITS-CLIP MSI2 target genes (n=221 top-ranking genes with p<0,001) were enriched in the transcriptional signature associated with MLL::AF4+ BCP-ALL patients from MILE study (Figure 1B), as assessed by gene set enrichment analysis (GSEA). These findings provided the rationale that MSI2 may have a relevant role in MLL::AF4+ BCP-ALL and prompted us to investigate further in detail.

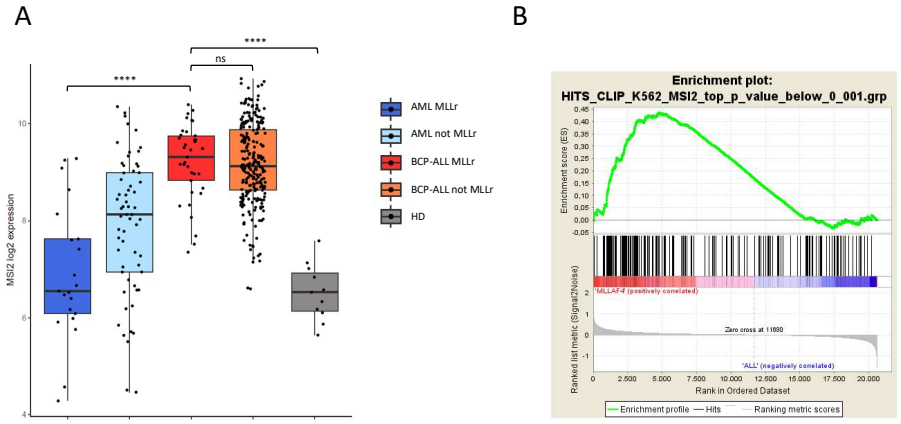

Figure 1: Expression of MSI2 in pediatric leukemia and enrichment analysis of mRNA targets

A. MSI2 expression across pediatric leukemia in a cohort of n=375 patients with childhood leukemia (MILE study)[19]. Patients were classified based on the phenotype of leukemia (AML or BCP-ALL) and based on the presence of MLL gene rearrangement (MLLr). HD: healthy-donor BM samples (normal controls). ns: not significant ****p<0,0001 (Welch t-test). B. GSEA showing enrichment of MLL::AF4+ BCP-ALL associated signature in MILE Study within the HITS-CLIP top ranking genes (n=221 with p<0,001) direct targets of MSI2 from Park et al.[12].

The lack of MSI2 impairs the growth in vitro and the leukemogenic potential in vivo of MLL::AF4+ ALL cells

The human MLL::AF4+ B-ALL cell line SEM was genetically engineered to generate MSI2 knock-out clones (SEM MSI2 KO) by CRISPR/CAS9 genome editing using a pool of guide RNA targeting the RRM1 functional domain (Supplementary Figure 1A-B). As a result of this, an early stop-codon was inserted within the transcript sequence of the

gene in the N-terminus RRM1 domain and the expression of MSI2 protein was completely abolished in MSI2 KO, as confirmed by Western Blot (Supplementary Figure 1C-E). Each individual CRISPR-edited MSI2 KO clone, isolated by limiting dilution (single-cell plating) and expanded in vitro, could be stably maintained in cell culture. The analysis of cell cycle by mass cytometry did not reveal significant differences in the growth of SEM MSI2 KO compared to CNTRL cells in basal condition (Supplementary Figure 2A). However, in a long-term competitive assay in vitro, in which the MSI2 KO and CNTRL cells were mixed and seeded in culture at the initial ratio of 90:10 KO:CNTRL, we observed that the MSI2 KO cells progressively diminished throughout the passages in vitro (from p0 to p20) and eventually extinguished, while the CNTRL cells expressing MSI2 outcompeted them (Figure 2A-C and Supplementary Figure 3). In agreement with this finding, NSG mice transplanted with MSI2 KO cells displayed a reduced tumour load in the bone marrow (BM) and spleen and smaller spleen compared with those transplanted with CNTRL cells 4 weeks after transplantation (Figure 2D-F). Moreover, mice transplanted with MSI2 KO cells showed a prolonged survival compared to those receiving the MSI2-expressing CNTRL cells (Figure 2G). Overall, these data demonstrate that MSI2 is essential to sustain the growth in vitro and the leukemia-initiating capacity in vivo of MLL::AF4+ ALL cells.

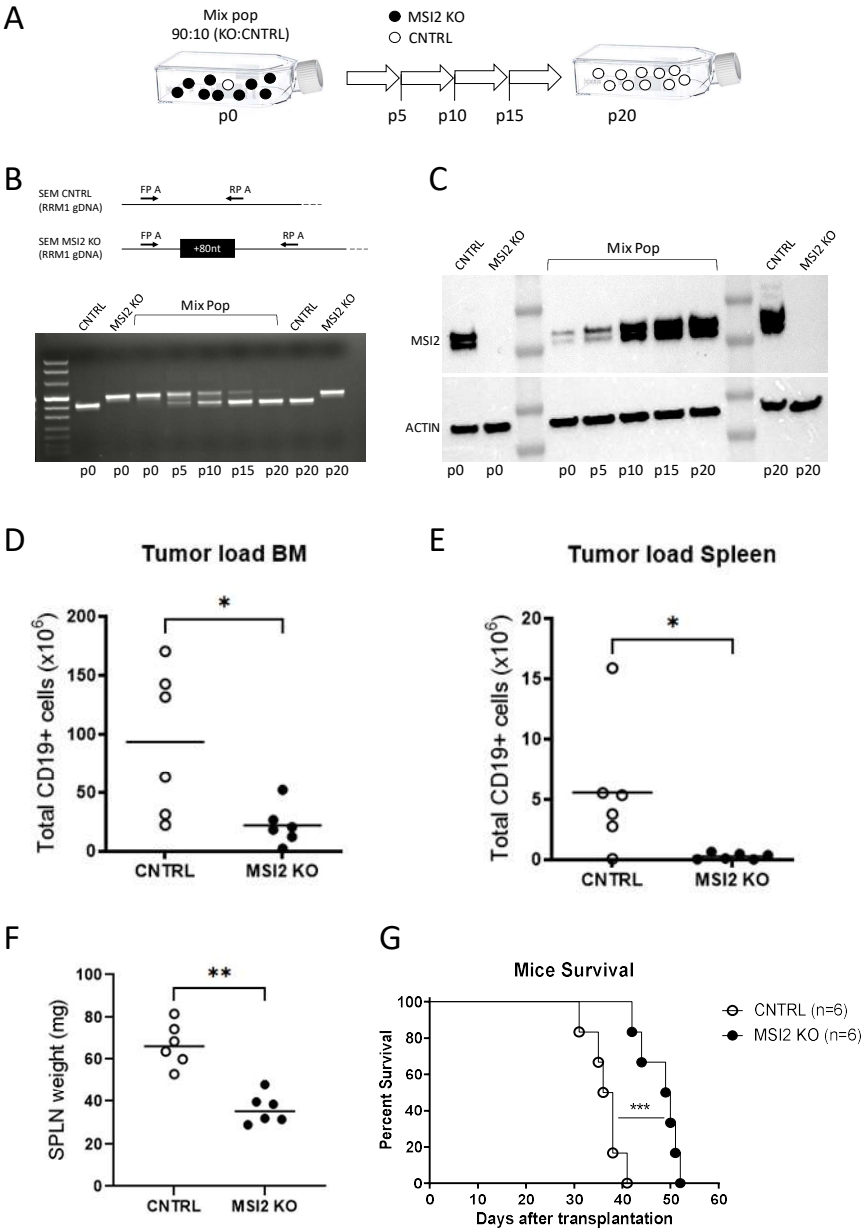
A
Mix pop
90:10 (KO:CNTRL)
MSI2 KO
CNTRL
p0
p5
p10
p15
p20
B
SEM CNTRL
(RRM1 gDNA)
FP A
RP A
SEM MSI2 KO
(RRM1 gDNA)
+80nt
CNTRL
MSI2 KO
Mix Pop
p0 p0 p0 p5 p10 p15 p20 p20 p20
C
MSI2
ACTIN
p0 p0 p0 p5 p10 p15 p20 p20 p20
D
Tumor load BM
Total CD19+ cells (x10^6)
CNTRL
MSI2 KO
E
Tumor load Spleen
F
SPLN weight (mg)
G
Mice Survival
Percent Survival
Days after transplantation
CNTRL (n=6)
MSI2 KO (n=6)

Figure 2: Long-term competitive assay in vitro and xenotransplantation in vivo

A. Experimental scheme. SEM MSI2 KO cells and SEM CNTRL were mixed at the 90:10 ratio (KO:CNTRL), seeded in culture (p0) and maintained for 20 passages in vitro by passing the cells into fresh medium three times a week. Samples were collected at periodical timepoints (from p0 to p20). B. PCR analysis of genomic DNA (gDNA). Specific primer pair designed on the edited region (+80nt) targeted by MSI2 gRNA A (FP A and RP A, upper panel) allow to detect the normal (411bp) and CRISPR-edited (491bp) amplicons, corresponding to SEM CNTRL and MSI2 KO cells, respectively. C. Western blot analysis of MSI2 protein expression of SEM CNTRL and MSI2 KO cells (p0 and p20) and mixed population co-cultured for 20 passages in vitro (from p0 to p20). D-F. Analysis of leukemic engraftment upon xenotransplantation in vivo. NSG mice were transplanted with an equal number of CNTRL or MSI2 KO cells ($2x10^6$ cells/mouse) and culled 4 weeks after transplantation. Graphs reported the total number of hCD19+ leukemic cells (tumor load) detected by FACS analysis in the BM (D) or spleen (E) and the spleen weight (F) of transplanted animals. *p<0,05 **p<0,01 (Mann-Witney test). G. Kaplan-Meier survival curve: mean survival CNTRL=37 days, mean survival MSI2 KO=49,5 days. ***p=0,0005 (Mantel-Cox test).

Genetic ablation or pharmacological inhibition of MSI2 sensitizes MLL::AF4+ cells to Glucocorticoids

The resistance to conventional therapies is the main cause of disease relapse and poor outcome of infants with MLLr ALL. To investigate

whether MSI2 might be involved in therapy-resistance we compared the drug profile of SEM CNTRL and MSI2 KO cells. A high-throughput drug screening was performed by using a manually curated library of 174 selected compounds currently used in clinical trials or in preclinical studies for hematological diseases (Supplementary Table 1A)[20]. The cell viability was assessed with CellTiterGlo 72h after treatment, and the half maximal effective concentration (EC_{50}) for each single compound was determined by using six different doses (ranging from 8nM to 25uM). Unsupervised clustering analysis of the mean drug sensitivity scoring (DSS) obtained from triplicates of each sample nicely showed that the three MSI2 KO clones cluster together (Supplementary Figure 4A). Overall, we observed that the drug profile of SEM MSI2 KO clones were very similar to those of SEM wt or SEM CNTRL cells, with only 20 compounds showing different profiles (Supplementary Figure 4B). Unpaired t-test with Bonferroni correction applied to mean DSS of MSI2-expressing (SEM wt and CNTRL) versus MSI2-depleted (MSI2 KO) samples revealed that only 4 drugs have a statistically different efficacy, namely Dexamethasone, Cytarabine, Prednisolone and Cyclocytidine. Importantly, the One-Way ANOVA statistical analysis of each sample showed that the mean DSS of SEM wt and CNTRL cells was comparable for these 4 drugs (Supplementary Figure 4C), suggesting that the different drug profile observed in MSI2 KO was likely ascribable to the CRISPR-mediated targeting of MSI2. Cytarabine (Ara-C) and Cyclocytidine (the prodrug of Cytarabine) are Pyrimidine analogs. Like other compounds of the Antimetabolite category, these agents exert a very potent and

unspecific cytotoxic effect in all cycling cells, by competing with cytidine/thymidine incorporation and blocking DNA. On the other hand, the Glucocorticoids (GCs) Dexamethasone and Prednisolone (the active form of Prednisone) are less toxic for normal hematopoietic cells (data not shown) and they represent one of the most important chemotherapeutic drugs used in clinics for the treatment of leukemia. Also, infants with MLL::AF4+ ALL were found to be more resistant to GCs compared to pediatric patients older than 1 year at diagnosis with B-ALL. This prompted us to further investigate whether MSI2 could be involved in GC-resistance.

To validate data obtained by high-throughput drug screening, SEM wt, CNTRL and MSI2 KO cells (six individual clones) were treated in vitro with 4 scalar doses of Dexamethasone (Dexa) or MethylPrednisolone (Pred). A cell cycle arrest occurred in MSI2 KO cells after 48h of treatment with Pred, with a reduced percentage of cells in S phase and accumulation of cells blocked in G0/G1, similarly to what observed in RS4;11, an MLL::AF4+ B-ALL human cell line sensitive to GC (Supplementary Figure 2B-C). Notably, the expression of the GC-receptor (NR3C1 or GCR) was unchanged after Prednisone administration and similar in GC-sensitive or GC-resistant cells, as confirmed by Mass Cytometry (Supplementary Figure 2D). Analysis of apoptosis after 72h of treatment demonstrated that, while the SEM wt and CNTRL cells were resistant to treatment, as 60 to 70% of cells were alive at the highest dose (EC_{50} Pred >100µg/ml and EC_{50} Dexa >10µg/ml), MSI2 KO cells were 100-fold more sensitive to GC (EC50

Pred= 0,79 ±0,6 µg/ml; EC50 Dexa 0,09±0,02 µg/ml) (Figure 3A). Notably, treatment of SEM or KOPN8, two cell line resistant to GCs, with the MSI2 inhibitor Ro 08-2750 in combination with Pred or Dexa phenocopied the GC sensitization observed in CRISPR-edited MSI2 KO clones, with Ro 08-2750 and GC showing a synergistic effect (Figure 3B, and Supplementary Figure 5A). The same results were also obtained by using patient-derived xenografts (PDX) samples from two MLLr infant ALL patients treated ex vivo with Ro 08-2750 and GCs (Figure 3C). Overall, our results show that MSI2 is involved in GC resistance of MLL::AF4+ B-ALL, as the genetic ablation or pharmacological inhibition of MSI2 sensitizes MLLr ALL cells to the cytotoxic effects of GC treatment.

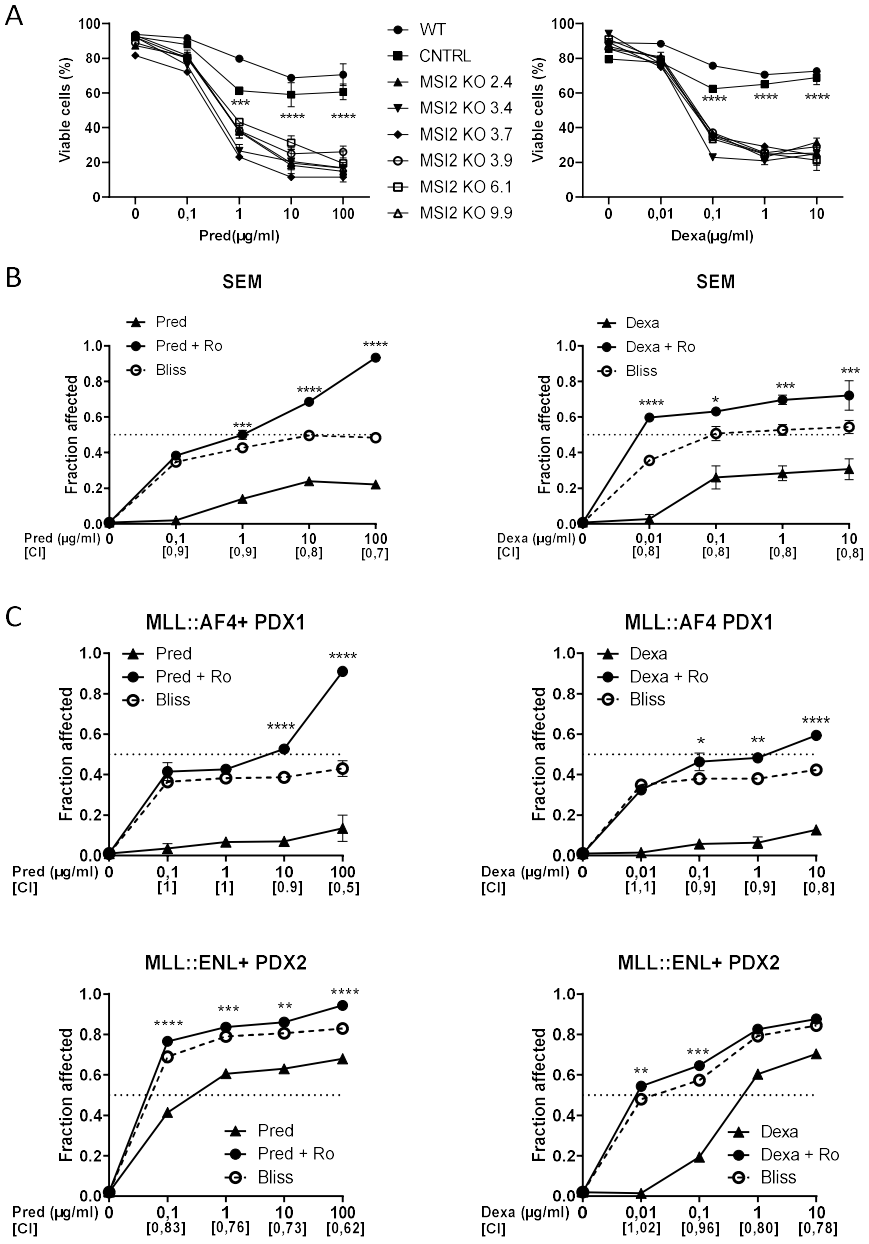
A
Viable cells (%)
Pred(µg/ml)
Dexa(µg/ml)
WT
CNTRL
MSI2 KO 2.4
MSI2 KO 3.4
MSI2 KO 3.7
MSI2 KO 3.9
MSI2 KO 6.1
MSI2 KO 9.9
B
SEM
SEM
Pred
Pred + Ro
Bliss
Dexa
Dexa + Ro
Fraction affected
Pred (µg/ml)
Dexa (µg/ml)
[CI]
C
MLL::AF4+ PDX1
MLL::AF4 PDX1
MLL::ENL+ PDX2
MLL::ENL+ PDX2

Figure 3: Response to GCs treatment and combination study with GC+Ro 08-2750

A. Apoptosis analysis of SEM wt, CNTRL and MSI2 KO treated with four scalar doses of Metyl-Prednisolone (Pred, left) or Dexamethasone (Dexa, right) in vitro. The percentage of viable cells (Annexin V/7-AAD negative) was evaluated by FACS analysis 72h after treatment. MSI2 KO clones: EC_{50} Pred = 0,79±0,6 µg/ml; EC_{50} Dexa = 0,09±0,02 µg/ml (mean±SD calculated on six SEM KO clones: 2.4, 3.4, 3.7, 3.9, 6.1, 9.9). MSI2-expressing cells (SEM wt and CNTRL): EC_{50} Pred > 100µg/ml; EC_{50} Dexa > 10µg/ml. B-C. Combination treatment with GCs (Pred or Dexa, scalar doses) and a constant does of Ro 08-2750 (12µM) on SEM wild-type cell line in vitro (B) or PDX from MLLr infant ALL patients ex vivo (C). Fraction affected: percentage of dead cells (AnnexinV-positive) detected by FACS 72h after treatment (mean of 3 replicates) normalized on the untreated controls. Bliss: Bliss score (open dot, dashed line). CI: combination index. *p<0,05 **p<0,01 ***p<0,001 ****p<0,0001 (Two-way Anova, combo vs Bliss).

MSI2 regulates the bioenergetic metabolism of MLL::AF4+ B-ALL cells

To further dissect the fundamental bases underlying MSI2-dependent GC-resistance/sensitization, we performed confocal analysis and Seahorse XF bioenergetic profiling of CNTRL and MSI2 KO cells, with or without GC administration. Mitochondrial activity was evaluated by confocal microscopy measurement of mitochondrial membrane potential (MMP) and biomass using MitoTracker Red and Green

staining respectively. At steady-state, MSI2 KO cells display a higher MMP compared to controls, while no differences were observed in the mitochondrial mass, indicating a mitochondrial hyperactivity already at basal conditions. As expected, after 24h of treatment with Dexa mitochondria were hyperactivated in CNTRL cells, with an increased MMP compared to the untreated condition. Conversely, in MSI2 KO cells the MMP signal was abolished upon 24h of Dexa exposure, which was not associated with changes in mitochondrial mass, compatible with mitochondrial depolarization triggering cell death (Figure 4A). The bioenergetic profiling assessed by Seahorse XF revealed that the basal ATP, produced by either glycolysis (GlycoATP) or mitochondrial respiration (MitoATP) was similar in CNTRL and MSI2 KO cells in normal conditions (Supplementary Figure 6A). Upon GCs exposure (Dexa or Pred) for 24h, the GlycoATP production decreased in both MSI2 KO and CNTRL cell, due to glycolysis inhibition via c-Myc downregulation (Figure 4B and Supplementary Figure 6B). Notably, while MitoATP was unchanged in CNTRL, it resulted to be severely impaired in MSI2 KO cells upon treatment (Figure 4B). Additional studies using the Seahorse XF Mito Stress Test revealed that both basal and maximal mitochondrial respiration were affected at a higher extent in MSI2 KO cells treated with Dexa compared to CNTRL (Supplementary Figure 6C), leading to a mitochondrial crisis and energy failure. Additionally, we observed that the MSI2 inhibitor Ro 08-2750 acted as Oxphos inhibitor. Indeed, Ro 08-2750 administration for 24h to SEM wt cells (alone or in combination with GCs) dramatically decreased the oxygen

consumption rate (OCR) and affected basal and maximal mitochondrial respiration in treated cells (Figure 4C-D).

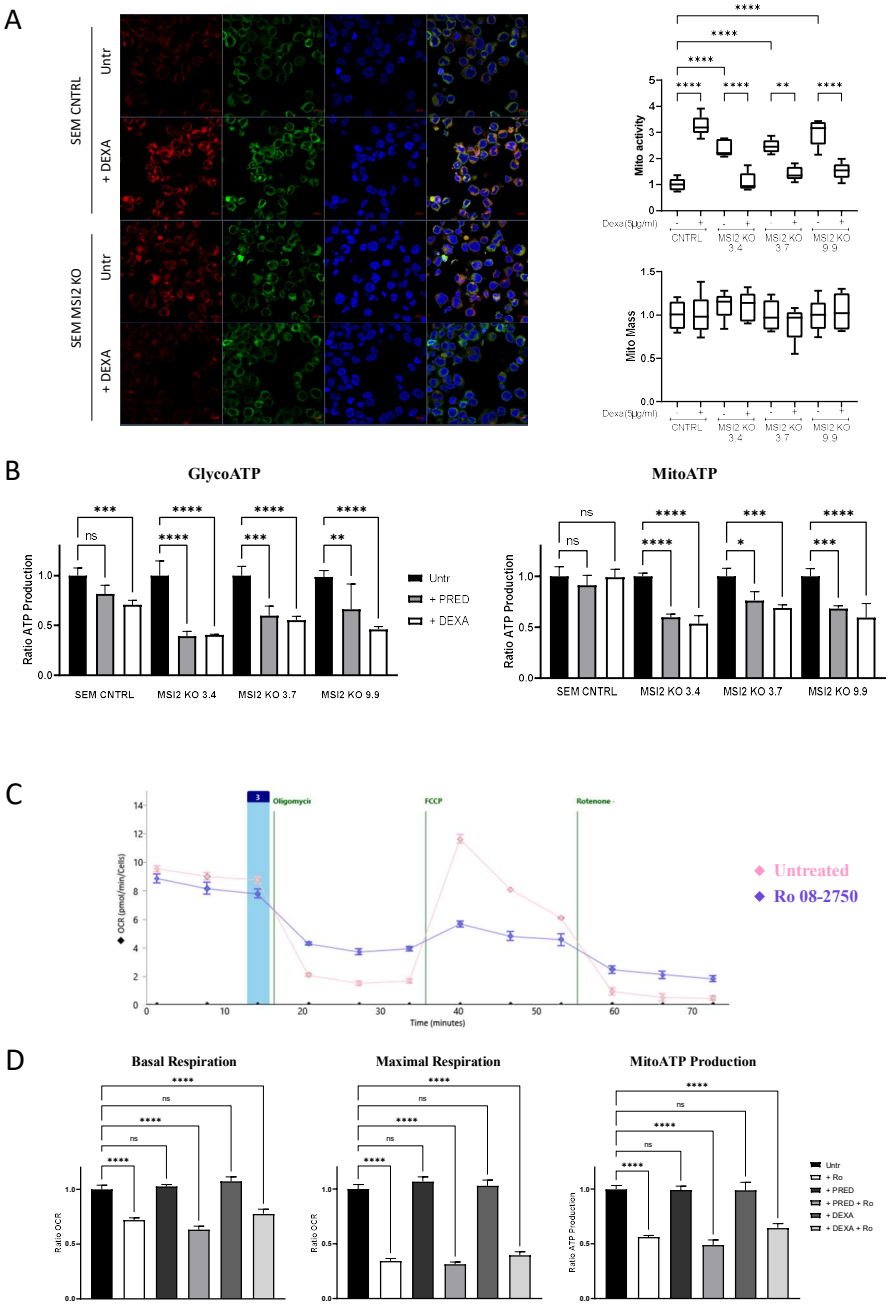

Figure 4: Analysis of mitochondrial activity and bioenergetic profiling upon GC exposure

A. Confocal analysis of mitochondrial membrane potential (MMP) of CNTRL and MSI2 KO cells with or without Dexa for 24h. Red signal = MitoTracker red; green signal = MitoTracker green; blue signal = Hoechst 33342. Images from one representative experiment are shown (left panel). Bar graphs (right panel) reported the quantifications of mitochondrial activity (mean red signal/mean green signal) and mitochondrial mass (mean green signal/mean blue signal) obtained from n=10 images acquired per field (approximately 200 cells/filed) and normalized on untreated CNTRL cells. B. Seahorse XF ATP Rate assay performed after treatment with Pred (50µg/ml) or Dexa (5µg/ml) for 24h. GlycoATP: total ATP produced by glycolysis; MitoATP: total ATP produced by mitochondrial respiration. Bar graph reported the mean values of 6 replicates, normalized on untreated samples. C. Seahorse XF Mito Stress test. Oxygen consumption rate (OCR) profile of SEM wt cells with or without Ro 08-2750 treatment (12µM for 24h). Each sample was analysed in 6 replicates. D. Quantification of basal respiration, maximal respiration and MitoATP obtained by Mito stress test in SEM wt cells after 24h of treatment with Ro 08-2750 (12µM), GCs (Pred 50µg/ml or Dexa 5µg/ml), or a combination of them. Mean OCR was calculated on 6 replicates and normalized on untreated sample. ns: not significant *p<0,05 **p<0,01 ***p<0,001 ****p<0,0001 (One-way Anova)

To address the hypothesis that cells lacking MSI2 are more susceptible to metabolic perturbations, we used the glucose (Glc) analogue 2-DG to inhibit glycolysis. Similarly to what observed for

GCs, MSI2 KO cells were more sensitive to 2-DG administration than CNTRL, as glycolysis inhibition by 2-DG reduced the viability of SEM MSI2 KO cells (with an EC_{50} ranging from 0,27 to 0,34 mM in MSI2 KO cells vs EC_{50} = 1,7 mM in CNTRL) and induced apoptosis (EC_{50} ranging from 0,16 to 0,72 mM in MSI2 KO cells vs EC_{50} = 1,5 mM in CNTRL) (Figure 5A). Also, administration of both 2-DG and Ro 08-2750 was found to be synergistic in SEM wt and KOPN-8 cells, with a detrimental effect on cell viability comparable to that obtained with the Glc analogue alone in MSI2 KO cells (Figure 5B). We hypothesized that metabolic rewiring towards mitochondrial activation may represent not only a physiological adaptation to stress, but also a possible mechanism for therapy resistance of leukemic cells. To provide the proof of principle that Oxphos inhibition can circumvent resistance to GC, we treated SEM wt and KOPN-8 cells with Dexa or Pred in combination with the Oxphos inhibitors Metformin or Tigecycline. Inhibition of mitochondrial respiration with Metformin or Tigecycline increased the anti-leukemic efficacy of GCs treatment alone and combination treatment of Oxphos inhibitors and GCs had a synergic effect, thus phenocopying the effect of Ro 08-2750+GCs combination (Figure 5C and Supplementary Figure 5B). Overall, our findings unravel novel and targetable metabolic vulnerabilities of MLLr ALL; and further in vivo studies using infant MLLr ALL PDX will be necessary in the future to validate this data.

RIP-chip was performed to identify the direct target of MSI2 in MLLr ALL cell lines SEM and RS4;11 (not shown). Gene-expression profiling

was performed in CNTRL vs MSI2 KO cells to identify deregulated pathways. Among them, genes enriched in OXPHOS /Mitochondrial function and GC-resistant associated signature were found (GSEA of RIP-chip and GEP) This data would further corroborate our hypothesis.

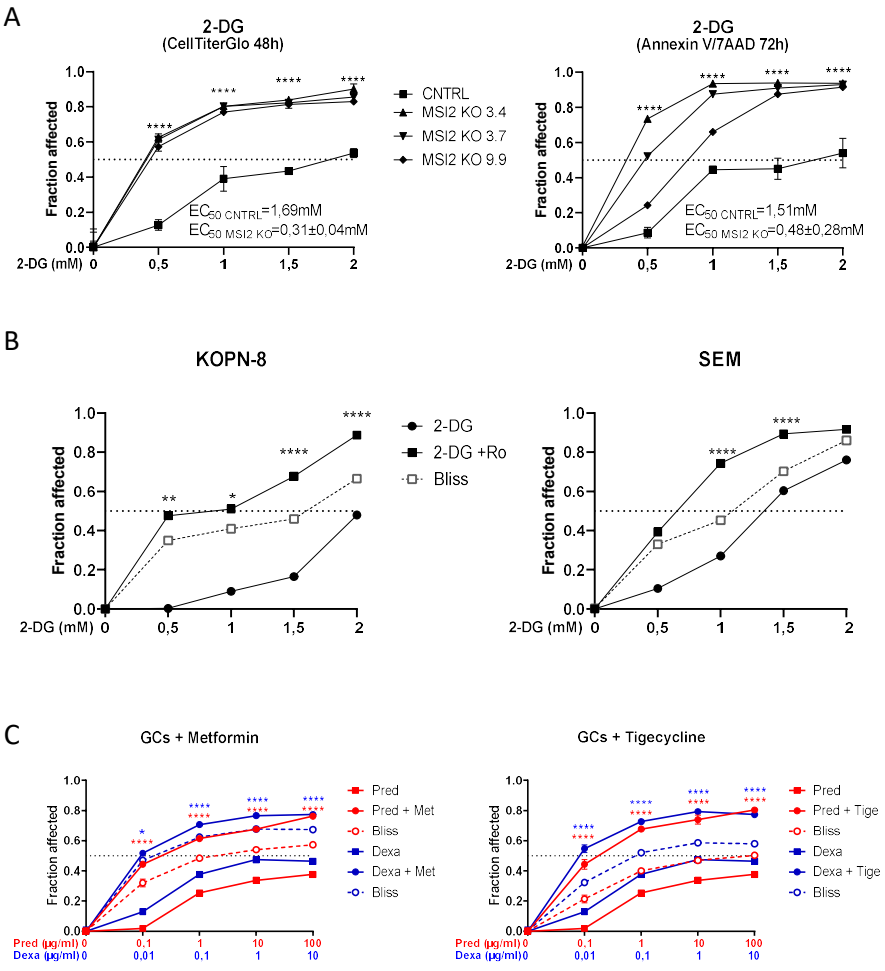

Figure 5: Response to 2-DG administration and effect of GC + Oxphos inhibitors co-treatment

A. Response to 2-DG administration in SEM CNTRL and MSI2 KO. Cell viability was assessed by CellTiterGlo (left panel) or Annexinv7/AAD staining (right panel) at 48h or 72h, respectively. The EC_{50} of CNTRL and MSI2 KO cells (range) is reported. B. Response to 2-DG and Ro 08-2750 co-treatment in MLLr ALL cell lines KOPN-8 (left panel) and SEM (right panel). Different doses of 2-DG were used in combination with a constant (sub-cytotoxic) concentration of Ro 08-2750 (2µM or 12µM for KOPN-8 or SEM cells, respectively). Apoptosis was assessed by FACS analysis of AnnexinV/AAD-positive cells after 72h. C. Anti-leukemic effect of GC and Oxphos inhibitors combination treatment on SEM cells. Scalar doses of Pred (red) or Dexa (blu) were used in combination with a subcytotoxic constant concentration of Metformin (10mM) or Tigecycline (3µM). Cell viability was assessed by CellTiterGlo after 72h. *p<0,05 **p<0,01 ***p<0,001 ****p<0,0001 (Two-way Anova)

The MSI2 inhibitor Ro 08-2750 has a synergistic effect in combination with Venetoclax

To investigate whether the MSI2 inhibitor Ro 08-2750 might have a superior efficacy in combination with other compounds currently used in the clinics for hematopoietic malignancies, we repeated the high-throughput drug screening of our 174 compounds library by using SEM wt cells pre-treated with either Ro 08-2750 or DMSO for

6h (Supplementary Figure 7A). The combination study revealed that 10 compounds, most of whom belonging to the categories of TKi and BTKi, or BCL2 inhibitors, acted synergistically with Ro 08-2750 (Supplementary Figure 7B). Here we focused on ABT-199/Venetoclax (Supplementary Figure 7C), a Phase I Bcl-2 inhibitor which was very recently introduced in clinical trials for infants with MLLr ALL (COG AALL2122) together with Blinatumomab and standard chemotherapy. Independent validation experiments by using three different human MLLr BCP-ALL cell lines in vitro or PDX samples from infants with MLLr ALL ex vivo demonstrated that Ro 08-2750 and Venetoclax have a synergic anti-leukemic effect (Figure 6A-B). Finally, the triple treatment with Ro 08-2750, Venetoclax and Dexa resulted to have a very strong anti-leukemic effects compared to each single drugs alone, and the three drugs acted synergistically both on SEM cell line in vitro as well as in one MLLr PDX ex vivo (Figure 6C). Overall, our findings point out the possibility to combine treatment with Ro 08-2750, Venetoclax and GCs as a promising strategy for infant MLLr ALL patients in the future.

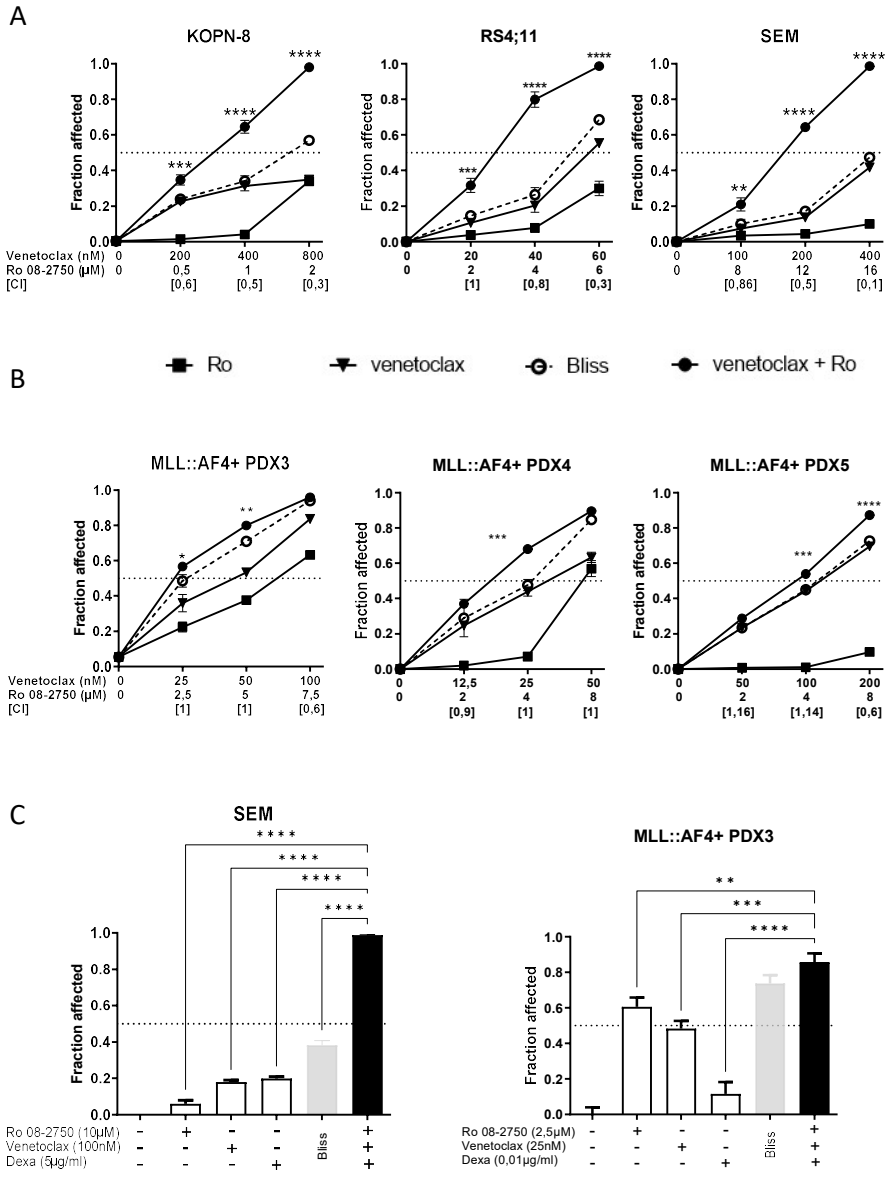

Figure 6: Triple combination with Ro 08-2750, Venetoclax and Dexa

A-B. Combination treatment with Ro 08-2750 and Venetoclax on three MLLr ALL cell lines in vitro (A) and three MLLr infant ALL PDX samples ex vivo (B). Fraction affected: percentage of dead cells (AnnexinV-positive) detected by FACS 72h after treatment (mean of 3 replicates) normalized on the

untreated controls. Bliss: Bliss score (open dot, dashed line). CI: combination index. C. Anti-leukemic effect of Ro 08-2750, Venetoclax and Dexa triple combination in SEM cell line in vitro (left panel; $\Delta[EFF_{combo}$-Bliss]= 0,61) and in one MLLr infant ALL PDX ex vivo (right panel; $\Delta[EFF_{combo}$-Bliss]= 0,12). Cell viability was assessed by AnnexinV/7AAD staining and FACS analysis at 72h. *p<0,05 **p<0,01 ***p<0,001 ****p<0,0001 (Two-way Anova, combo vs Bliss).

Discussion

In this study we demonstrated that the lack of MSI2 in MLL::AF4+ B-ALL impairs the growth in vitro and the capacity to regenerate leukemia in vivo. Also, we found that the genetic depletion or pharmacological inhibition of MSI2 sensitizes MLLr ALL cells to GCs and that the small inhibitor of MSI2, Ro 08-2750, acts synergistically with the Bcl2 inhibitor Venetoclax.

Other studies previously pointed out the involvement of MSI2 in therapy-resistance of human cancers, including solid tumors[8] and hematological malignancies like myeloid leukemia[21] or B-Cell lymphoma[13], which corroborate the prognostic significance of MSI2 in cancers and further validate the use of MSI2 expression as a marker to identify drug-resistant relapse-prone stem cells in leukemia[22]. Herein the functional role of MSI2 in the GC-resistance MLLr B-ALL, through the regulation of the bioenergetic metabolism of leukemic cells, was demonstrated for the first time in this study and it represents the main novelty of our work.

GCs are Corticosteroid hormones exerting multiple and pleiotropic effects on treated cells. In presence of GC, the GC-receptor (NR3C1 or GCR) binds to its ligand and the activated GC-GCR complex is translocated from the cytoplasm to the nucleus, where it may act as a transactivator or transrepressor by recognizing and binding to the DNA responsive elements of specific target genes. Treatment with GC inhibits cell proliferation, suppresses the immune response (by

repressing the pro-inflammatory cytokines expression and signaling cascade) and modulates the cell metabolism (by inhibiting glycolysis, activating the mitochondria and inducing autophagy)[23-27]. Glycolysis inhibition, through c-Myc downregulation which, in turn, downregulates the expression of the Glucose importer GLUT1 on the cell membrane[28], is an indirect effect of GC administration. Our results confirmed that, after GC exposure, glycolysis is inhibited (via c-Myc downregulation) in MLL::AF4+ B-ALL cell lines regardless of MSI2 expression (both in CNTRL and in MSI2 KO). However, in the GC-resistant SEM cell line expressing MSI2, treatment with Pred or Dexa has only a slight effect on cell cycle arrest or apoptosis, as the cells are capable to compensate glycolysis inhibition by hyperactivating the mitochondria. Contrarily, upon GC treatment of MLL-AF4+ cells where MSI2 was genetically depleted or pharmacologically inhibited, the mitochondrial respiration is severely impaired and the membrane potential is lost, which eventually causes a failure of ATP production and energy crisis, leading to cell cycle arrest and cell death. Tumor metabolism is currently emerging as a very important aspect of cancer biology, being involved in cancer cell survival, dissemination and therapy--resistance. Overall, our findings suggest that MSI2 contributes to regulate the bioenergetic metabolism of MLLr B-ALL cells and may have a putative role in the metabolic plasticity of leukemia.

Glycolysis and mitochondrial respiration represent the two main sources of energy for cells. The “Warburg hypothesis” proposes that

cancer cells (highly proliferating and energy demanding) are more dependent to glycolysis compared to normal cells to produce ATP, as they have a higher requirement of energy to self-renew and maintain themselves. Also, it was postulated that malignant cells preferentially rely on glycolysis rather than mitochondrial respiration, even when oxygen is available in the microenvironment (normoxia conditions). However, the mere inhibition of glycolysis is not sufficient to eradicate tumors. The main reason for this is that cancer cells have the capacity to adapt their metabolism to their environmental conditions; they have metabolic plasticity. More specifically, by switching to mitochondria, upon glycolytic suppression the intracellular energy metabolism is reprogrammed toward oxidative phosphorylation (the so-called "Pasteur effect") to obtain the ATP necessary for their survival. Hyperactivation of mitochondria (through enhanced respiration) may indeed represent a possible compensatory mechanism of drug resistance to ensure cellular survival. Besides the classical Warburg hypothesis, more recent studies have indeed demonstrated that tumour cells have increased mitochondrial biogenesis and basal level of oxygen consumption than normal cells[29] and they are highly dependent on oxidative phosphorylation for survival[30].

As a proof of principle that the MSI2-depenent metabolic rewiring of MLLr ALL is a putative mechanism responsible for GC resistance or sensitization, we either used the Glucose analogue 2-DG to block glycolysis in CNTRL and MSI2 KO cell lines, or we co-treated the MSI2-

expressing SEM wild-type cell line with the MSI2 inhibitor Ro 08-2750 together with 2-DG. Our results demonstrated that the ablation or the pharmacological inhibition of MSI2 makes the MLL::AF4+ ALL cells more susceptible to glycolysis blockage. The Seahorse profiling showed that the MSI2 inhibitor Ro 08-2750 exerts its anti-cancer activity by blocking mitochondrial respiration, hence acting as a mitochondrial targeting "Mitocan" compound [31]. Also, the treatment of MLLr ALL cells with other Oxphos inhibitors (Metformin or Tygecycline) in combination with GCs phenocopies the effect of GC-sensitization observed in MLL::AF4+ cells where MSI2 expression was ablated or pharmacologically inhibited. Metformin is a complex I inhibitor, already used in Clinical Trial in CLL (NTC01750567) and ALL (NTC01324180). The FDA-approved Tigecycline is a tetracycline antibiotic which targets leukemia stem cells by inhibiting mitochondrial protein translation, and therefore the respiratory chain electron transport[29]. Emerging evidences correlate mitochondrial functions of leukemic cells with drug response[32]. Further in vivo studies will be required to investigate whether targeting the mitochondria could represent a promising therapeutic option for MLLr infant ALL patients. However, Ro 08-2750 has shown only a limited efficacy in preclinical studies in mice, also due to the poor solubility of this compound in DMSO[14,33]. Investigations of Tigecycline in a phase 1 clinical trial reported no clinical response due to issues with formulation and pharmacokinetics[34]. On the other hand, the use of the Metformin analogue IACS-010759 is more promising and it would represent a better option to target leukemic

cell mitochondria in vivo (in combination with standard chemo and/or Bcl-2 inhibitor). The results of our drug screening and combination studies in vitro and ex vivo revealed that the MSI2 inhibitor Ro 08-2750 acts synergistically with Venetoclax. To further support our findings, a recent study demonstrated that Bcl2 is directly bound and regulated by MSI2 in B-cell lymphoma[13] and mitochondrial functions were found to be related to Venetoclax resistance in both AML[35] as well as in ALL[32]. Moreover, a triple combination treatment with Dexametasone, Ro 082750 and Venetoclax is able to eradicate MLL::AF4+ ALL cell line in vitro and PDX ex vivo.

In conclusion, herein we demonstrated that MSI2 promotes the growth of MLLr ALL, sustains the leukemogenic potential in vivo and it is involved in GC-resistance. Moreover, our study sheds light for the first time onto the functional role of MSI2 in the bioenergetic metabolism of leukemia, uncovers novel metabolic vulnerabilities of ALL and paves the way for targeting the leukemia's reliance/dependency on oxidative phosphorylation as a possible therapeutic approach to treat infants with MLLr ALL.

Methods

Cell lines and compounds

The SEM, RS4;11 and KOPN8 human cell lines, carrying the t(4;11)/MLL::AF4+ or t(11;19)/ MLL::ENL+ translocation respectively, were purchased from DSMZ (https://www.dsmz.de/dsmz) and maintained at 37 °C in a humidified atmosphere at 5% CO2 in RPMI-1640 (Sigma-Aldrich) with the addition of 10% fetal bovine serum (FBS, Sigma-Aldrich), 1% penicillin/streptomycin 100 mg/mL and 1% L-glutamine (both from Cambrex Bio Science). SEM MSI2 KO clones were generated with CRISPR/Cas9 genome editing technology (see Supplementary). Metyl-Prednisolone (Urbason) and Dexametasone (Decadron) were provided from the Pediatric Clinic of the Hospital. Ro 08-2750 was purchased from Tocris (CAS Number 37854-59-4). Venetoclax was purchased from Selleckchem. 2-DG, Metformin and Tigecycline were purchased from Sigma.

In vivo xenotransplantations

SEM CNTRL or MSI2 KO cells were injected into the tail vein of immunodeficient NSG mice ($2x10^6$ cells per mouse). Mice were checked daily and body weight was measured twice a week to score any signs of illness. Bone marrow aspirates was collected periodically to monitor the kinetics of engraftment. Mice were either culled at 4 weeks after transplantation or sacrificed when the overt signs of leukemia appeared for survival experiments. The leukemic

engraftment in the BM, spleen, meningeal plexus and peripheral blood was analyzed by FACS using the anti-human CD45-APC, anti-human CD19-PECy5 (both from BD Biosciences) and anti-mouse CD45-PE (eBioscience). Primary blasts from MLLr infant ALL patients at disease presentation were xenotransplanted in vivo to expand leukemia-initiating cells. BM cells were collected from moribund mice and used for treatment ex vivo.

Analysis of cell viability in response to treatment

MLLr ALL cells were seeded on a 96-wells plate and treated with different concentrations of drugs (in single, or combination). MLL::AF4+ cells were seeded at the concentration of $0,3x10^6$ cells/ml in complete RPMI; while MLLr ALL PDX samples were seeded at $2,4x10^6$ cells/ml in serum-free StemSpan (Stemcell Technologies) supplemented with 1% GlutaMAX (Gibco), 1% Penicillin/Streptomycin (Cambrex, Bio Science), hSCF and hG-CSF recombinant cytokines (10ng/mL, Peprotech). Each sample was analyzed in triplicates. For each compound, the sub-cytotoxic dose (EC25) to be used in combination studies was empirically assessed in preliminary experiments. Cell viability was evaluated 48h and/or 72h after treatment by CellTiterGlo Assay (Promega) and/or FACS analysis of apoptotic cells with AnnexinV/7-AAD staining (Enzo Life Science). The EC50 and Combination Index (CI) were calculated using Compusyn software on the mean values obtained from triplicates. Based on the CI, the drugs were defined as: antagonists (CI>1,2), additives

(0,9<CI<1,1) or synergistic (CI<0,9). The Bliss score was calculated with the following formula: for combination of two drugs Bliss Score=(Fa Drug1 + Fa Drug2) – (Fa Drug1 x Fa Drug2), where Fa is the Fraction affected (percentage of dead cells normalized on untreated controls); for triple combination Bliss Score=(Fa Drug1 + Fa Drug2 + Fa Drug3) – (Fa Drug1 x Fa Drug2) – (Fa Drug1 x Fa Drug3) – (Fa Drug2 x Fa Drug3) – (Fa Drug1 x Fa Drug2 x Fa Drug3)[36]. If the measured effect of drug combination (EFF_{combo}) is higher than the estimated Bliss ($\Delta[EFF_{combo}\text{-Bliss}]>0$) the drugs are synergistic; if it is lower ($\Delta[EFF_{combo}\text{-Bliss}]<0$) the drugs are antagonist; otherwise (if $\Delta[EFF_{combo}\text{-Bliss}]=0$) the drugs are additive.

Confocal microscopy analysis

Mitochondrial mass and membrane potential (MMP) was evaluated with MitoTracker Green and Red CMX staining (Thermo Fisher Scientific), respectively. After 24h of treatment with Dexametasone (5µg/ml), cells were collected ($1x10^6$ cells for each condition), washed and stained with 50nM MitoTrackerTM Red CMXRos and 25nM MitoTrackerTM Green FM (Thermo Fisher Scientific) for 30 minutes in complete medium. Subsequently nuclei were stained with Hoechst 33342 (Thermo Fisher Scientific). Cells were washed twice in PBS, mounted on glass slides with a 90% (v/v) glycerol/PBS solution and analyzed by confocal microscopy. Images were acquired using Zeiss LSM 710 confocal laser-scanning microscope (Zeiss) using a 63x, 1.4 N/A oil-immersion objective. Laser intensities and acquisition

parameters were held constant throughout each experiment. Confocal microscopy fields were analyzed using specific homemade-designed macro with ImageJ (https://imagej.nih.gov/ij/) software. Briefly, mitochondrial size quantification was performed measuring the integrated density (ID) of green signal normalized over the total number if nuclei analyzed and mitochondrial activity was performed measuring the integrated density (ID) of red signal over green signal ratio, after proper manual thresholding. All the data obtained derived from at least ten fields per samples (at least 200 cells each).

Seahorse XF bioenergetic profiling

The bioenergetic profile of SEM CNTRL and MSI2 KO cells was measured with the Seahorse XFe96 analyser (Agilent technology, Santa Clara, CA, USA;). Cells were treated in vitro with GCs (Dexametasone 5 µg/ml or Metyl-Prednisolone 50 µg/ml) or Ro 08-2750 (12 µM) for 24h. The day of the analysis the Seahorse 96-well plates were pre-coated with poly-D-lysine (Sigma-Aldrich, 50 µl/well per 30 min) to allow adhesion of suspension cells. Briefly, cells were washed, counted, resuspended in complete RPMI Seahorse XF assay medium (103575-100 Agilent) supplemented with 10 mM glucose + 2 mM glutamine and seeded on pre-coated plates at a density of 6×10^4 cells per well. The plate was centrifuged (200 rcf without brake for 1 min) to allow cell adhesion and incubated for 1 h at 37°C in absence of CO2. For each sample, the measurement of Oxygen Consumption Rate (OCR) and Extra Cellular Acidification Rate (ECAR) were obtained

from the mean of 6 technical replicates. ATP Rate assay (kit 103591-100, with Oligomycin A 1,5µM and Rotenone/Antimycin A 0,5µM) and Mito Stress test (kit 103015-100, with Oligomycin A 1,5µM, FCCP 2µM and Rotenone/Antimycin A 0,5µM) were performed according to the manufacturer's instructions. The optimal concentrations of Oligomycin A and the uncoupling agent FCCP were previously determined in preliminary experiments by using 2 and 6 different doses, respectively. Seahorse XF analysis was performed at 37°C in absence of CO_2. OCR and ECAR raw values were normalized on the count of nuclei per well evaluated by Hoechst 33342 staining (1µg/mL for 15 min) and Operetta CLS™ imaging, as previously described[37]. Data were analyzed with Wave 2.6.1 software (Agilent), after excluding outliers well data, to obtain cellular bioenergetics. Glycolytic and respiratory parameters were calculated using the following formulas: Basal Mitochondrial Respiration (MitoOCR) = $OCR_{basal} - OCR_{rot/ant}$; Maximal Mitochondrial Respiration = $OCR_{FCCP} - OCR_{rot/ant}$. Proton Efflux rate (PER; pmol H+/min) was calculated from ECAR applying the Buffer Factor of the XF assay medium. Basal glycolysis = $PER_{basal} – PER_{2\text{-}DG}$; Maximal glycolysis = $PER_{rot/ant} – PER_{2\text{-}DG}$. Glycolytic and mitochondrial ATP rates were calculated as following described: ATP-linked respiration (OCR_{ATP}) = $OCR_{basal} – OCR_{oligo}$; mitoATP production rate = OCR_{ATP} x 2 x P/O, where P/O=2,75. MitoPER = mitoOCR x CCF, where CO_2 Contribution Factor CCF=0,61. GlycoATP production rate = glycoPER = PER – mitoPER.

Statistical Analysis

Statistical analysis and graph were analyzed using GraphPad Prism6 (GraphPad Software, Inc.). The in vivo data were analyzed by Mann-Whitney nonparametric statistical test. Survival analysis was performed by Kaplan-Meier survival curve (Log-rank Mantel-Cox test). Data obtained from viability analysis, confocal microscopy and Seahorse profiling were analyzed with One-way or Two-way Anova statistical analysis with Bonferroni's correction for multiple comparisons and data were expressed as mean ± SD.

See also Supplementary Material.

Supplementary

Supplementary Tables and Figures

Supplementary Table 1

	Inhibitor	Drug category and main target
1	5-Azacytidine	Antimetabolites
2	5-Fluorouracil	Antimetabolites
3	6-Mercaptopurine (Monohydrate)	Antimetabolites
4	6-Thioguanine	Antimetabolites
5	Clofarabine	Antimetabolites
6	Cytarabine (Hydrochlorid)	Antimetabolites
7	Cyclocytidine HCL	Antimetabolites
8	Fludarabine (phosphate)	Antimetabolites
9	Nelarabine	Antimetabolites
10	Gemcitabine	Antimetabolites
11	Methotrexate	Antimetabolites
12	Pentostatin	Antimetabolites
13	Cladribine	Antimetabolites
14	Dacarbazine	Antimetabolites/DNA alkylator/crosslinker
15	Vinblastine (sulfate)	Antimitotics
16	Vincristine (sulfate)	Antimitotics
17	Busulfan	Alkylating agents
18	Carmustine	Alkylating agents
19	Cyclophosphamide (Clafen) (Monohydrate)	Alkylating agents
20	Lomustine	Alkylating agents
21	Cisplatin	Alkylating agents
22	Oxaliplatin	Alkylating agents
23	Procarbazine (Hydrochloride)	Alkylating agents
24	Thio-TEPA	DNA alkylator/crosslinker
25	Temozolomide	Alkylating agents
26	Chlorambucil	Alkylating agents
27	Bendamustine (hydrochloride)	Alkylating agents

28	Mechlorethamine hydrochloride	DNA alkylator/crosslinker
29	Epirubicin (hydrochloride)	Topoisomerase inhibitor
30	Etoposide	Topoisomerase inhibitor
31	Idarubicin (hydrochloride)	Topoisomerase inhibitor
32	Mitoxantrone (dihydrochloride)	Topoisomerase inhibitor
33	Teniposide	Topoisomerase inhibitor
34	Daunorubicin (Hydrochloride)	Topoisomerase inhibitor
35	Doxorubicin (hydrochloride)	Topoisomerase inhibitor
36	Amsacrine (Hydochlorid)	Topoisomerase inhibitor
37	Dexamethasone	Glucocorticoid
38	Prednisone	Glucocorticoid
39	Prednisolone (Acetate)	Glucocorticoid
40	Belinostat	HDAC inhibior (HDACi)
41	CI-994 (Tacedinaline)	HDAC inhibior (HDACi)
42	Panobinostat	HDAC inhibior (HDACi)
43	Romidepsin	HDAC inhibior (HDACi)
44	Quisinostat	HDAC inhibior (HDACi)
45	Tubastatin A (Hydrochloride)	HDAC inhibior (HDAC6i)
46	Givinostat (ITF2357)	HDAC inhibior (HDACi)
47	Vorinostat	HDAC inhibior (HDACi)
48	Entinostat	HDAC inhibior (HDACi)
49	Ricolinostat	HDAC inhibior (HDAC6i)
50	Pracinostat	HDAC inhibior (HDACi)
51	Abexinostat	HDAC inhibior (HDACi)
52	EPZ-6438 (Tazemetostat)	EZH2/HMTase inhibitor
53	GSK126	EZH2/HMTase inhibitor
54	GSK343	EZH2/HMTase inhibitor
55	GSK 525762A	Bromodomain inhibitor (BETi)
56	Paclitaxel	Microtubule Ploymerase inhibitor
57	JQ1	Bromodomain inhibitor (BETi)
58	Bortezomib	Proteasome inhibitor
59	MLN-9708 (Citrate)	Proteasome inhibitor
60	Carfilzomib	Proteasome inhibitor
61	Ganetespib	HSP90 inhibitor (HSP90i)
62	PUH71	HSP90 inhibitor (HSP90i)
63	AUY922 (LUMINESPIB)	HSP90 inhibitor (HSP90i)

64	NVP-HSP990	HSP90 inhibitor (HSP90i)
65	EC144	HSP90 inhibitor (HSP90i)
66	PF-04929113	HSP90 inhibitor (HSP90i)
67	BIIB021	HSP90 inhibitor (HSP90i)
68	Alisertib	Aurora Kinase A inhibitor
69	Aurora A Inhibitor I	Aurora Kinase A inhibitor
70	MLN8054	Aurora Kinase A inhibitor
71	MK-5108 (VX-689)	Aurora Kinase A inhibitor
72	Danusertib	Aurora Kinase A inhibitor
73	Barasertib	Aurora Kinase B inhibitor
74	Volasertib	Polo-like Kinase (PLK) inhibitor
75	BI2536	Polo-like Kinase (PLK) inhibitor
76	LEE011 (Ribociclib)	CDK inhibitor (CDKi)
77	LY2835219 (Abemaciclib)	CDK inhibitor (CDKi)
78	Dinaciclib	CDK inhibitor (CDKi)
79	SY-1365-THZ1	CDK inhibitor (CDK7i)
80	Cabozantinib (S-malate)	VEGFR inhibitor
81	Erlotinib	EGFR inhibitor
82	Gefitinib (Hydrochlorid)	EGFR inhibitor
83	Sunitinib (malate)	PDGFR/VEGFR inhibitor
84	Axitinib	VEGFR inhibitor
85	Midostaurin	PKC/VEGFR2/PDGFR/FLT3 inhibitor
86	Foretinib	VEGFR2/c-MET inhibitor
87	Dovitinib	FLT3/PDGFR/VEGFR/c-Kit inhibitor
88	Crenolanib	FLT3/PDGFR inhibitor
89	Pexidartinib	FLT3/c-Kit/CSF1R inhibitor
90	Lestaurtinib	FLT3 inhibitor
91	Quizartinib	FLT3 inhibitor
92	KW-2449	FLT3 inhibitor
93	Pacritinib	FLT3/JAK inhibitor
94	Gilteritinib	FLT3/AXL inhibitor
95	Buparlisib	PI3K inhibitor
96	Idelalisib	PI3K inhibitor
97	Pictilisib GDC-0941	PI3K inhibitor
98	GSK2636771	PI3K/AKT inhibitor

99	Alpelisib	PI3K/AKT inhibitor
100	Dactolisib (BEZ235)	PI3K/mTOR inhibitor
101	GSK2110183 (Afuresertib)	AKT inhibitor
102	Ro 08-2750	NGF/MSI2 inhibitor
103	ARQ-092 (Miransertib)	AKT inhibitor
104	Ipatasertib (GDC-0068)	AKT inhibitor
105	Deforolimus	mTOR inhibitor
106	Everolimus	mTOR inhibitor
107	Rapamycin	mTOR inhibitor
108	Temsirolimus	mTOR inhibitor
109	PF-04691502	PI3K/mTOR inhibitor
110	INK 128 (MLN0128)	mTORC1/2 inhibitor
111	BMS-911543	JAK inhibitor
112	AT9283	JAK inhibitor
113	Baricitinib (phosphate)	JAK inhibitor
114	CYT387 (Momelotinib)	JAK inhibitor
115	Ruxolitinib	JAK inhibitor
116	Tofacitinib (citrate)	JAK inhibitor
117	Fedratinib (TG101348)	JAK/FLT3 inhibitor
118	Gandotinib	JAK mutant (JAK2V617F) inhibitor
119	Tipifarnib	Farnesyl Transferase/Ras inhibitor
120	Lonafarnib	Ras inhibitor
121	Salirasib	Ras inhibitor
122	Dabrafenib (Mesylate)	Raf inhibitor
123	Sorafenib (Tosylate)	Raf inhibitor
124	Regorafenib (Monohydrate)	Raf inhibitor
125	Vemurafenib	Raf inhibitor
126	LGX818 (Encorafenib)	Raf inhibitor
127	Cobimetinib	MEK inhibitor
128	MEK162 (Binimetinib)	MEK inhibitor
129	Selumetinib	MEK inhibitor
130	Trametinib	MEK inhibitor
131	PD0325901	MEK inhibitor
132	PD184352	MEK inhibitor
133	Pimasertib	MEK inhibitor

134	SHP099 (Dihydrochloride)	Ras/ERK inhibitor
135	SCH772984	ERK1/2 inhibitor
136	GDC-0994	ERK inhibitor
137	Losmapimod	p38 MAPK inhibitor
138	Zanubrutinib	BTK inhibitor (BTKi)
139	Tirabrutinib	BTK inhibitor (BTKi)
140	Spebrutinib	BTK inhibitor (BTKi)
141	Ibrutinib	BTK inhibitor (BTKi)
142	Imatinib (Mesylate)	Bcr-Abl inhibitor
143	Radotinib	Bcr-Abl inhibitor
144	Nilotinib (Hydrochlorid)	Bcr-Abl inhibitor
145	Ponatinib	Bcr-Abl/FGFR/FLT3/VEGFR inhibitor
146	Bosutinib	Bcr-Abl/Src kinease inhibitor
147	Dasatinib (Hydrochlorid)	Bcr-Abl/Src kinease inhibitor
148	Rebastinib (DCC-2036)	Bcr-Abl inhibitor
149	Saracatinib	Bcr-Abl inhibitor
150	Bafetinib	Bcr-Abl/Src kinease inhibitor
151	BSI-201 (Iniparib)	PARP inhibitor
152	Olaparib	PARP inhibitor
153	Rucaparib (phosphate)	PARP inhibitor
154	Veliparib (dihydrochloride)	PARP inhibitor
155	ABT-199 (Venetoclax)	Bcl-2 Family inhibitor
156	Obatoclax (Mesylate)	Bcl-2 Family inhibitor
157	Y-27632 (Dihydrochloride)	ROCK inhibitor
158	QNZ (EVP4593)	NF-κB inhibitor
159	Omaveloxolone	NF-κB inhibitor
160	Enasidenib	IDH2 inhibitor
161	Ivosidenib	IDH1 inhibitor
162	Birinapant	XIAP/cIAP1 inhibitor
163	Tariquidar	P-glycoprotein inhibitor
164	Enzastaurin	PKC inhibitor
165	KYA1797K	wnt/beta catenin inhibitor
166	Selinexor	CRM1 inhibitor
167	AZD6738	ATM/ATR inhibitor
168	Omacetaxine Mepesuccinate (Homoharringtonine)	Ribosom Inhibtor

169	Actinomycin D	Antibacterial
170	Bexarotene	Retinoid inhibitor
171	PND-1186	FAK inhibitor
172	Nintedanib (BIBF1120)	LCK inhibitor
173	BAY 80-6946 (Copanlisib)	PI3K inhibitor
174	Palbociclib	CDK inhibitor (CDKi)

Table S1: List of 174 compounds used for high-throughput drug screening

Supplementary Figure 1

A

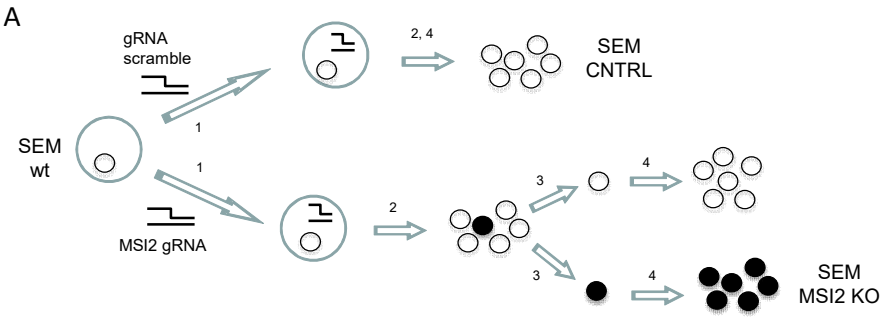

B

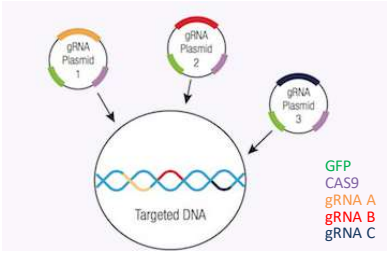

MSI2 gRNA sequence (5'→3'):

gRNA A (sense): ATCCCACTACGAAACGCTCC

gRNA B (antisense): ACCTTGGGTTGCGCTCGACG

gRNA C (sense): TCCTCGTCGAGCGCAACCC

C

SEM CNTRL:

ATCCCACTACGAAACGCTCC ..... TCCTCGTCGAGCGCAACCCAAGGT

(gRNA A) (gRNA B/C)

SEM MSI2 KO:

ATCCCACTACGAAACGC**CAACTTTAACCATCCCTCCAACAGATCAGGTAACTAACATAGCTAGCTAGCCTTTCTGAAATGACCCACCATGCATTTCA**TCC

(gRNA A) TCCTCGTCGAGCGCAACCCAAGGT

(gRNA (B/C)

D

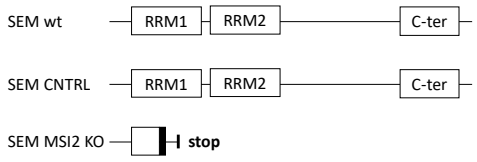

E

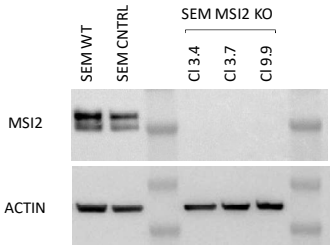

Figure S1: Generation MLL::AF4+ B-ALL cell model with MSI2 knock-out (SEM MSI2 KO)

A. CRISPR/CAS9 genome editing experimental scheme (see also Supplementary Methods). (1) *Transfection*. (2) *Expansion in vitro.* (3) *Clonal Selection.* (4) *Screening* of genomic DNA, mRNA and protein expression. B. gRNA Plasmids and sequences. A pool of three gRNA Plasmids were used for transfection (left panel), each containing the GFP reporter gene, the CAS9 sequence and a gRNA (gRNA A, B or C) targeting first RNA-recognition motif of MSI2 (RRM1) with RNA-binding activity. The 20nt sequence of MSI2 gRNAs is reported (right panel) C: Genomic DNA sequence of MSI2 gene in SEM CNTRL or in SEM MSI2 KO clones. In CRISPR-edited clones, as a result of non-homologous end-joining DNA repair on both alleles, a sequence of 80 random nucleotide sequence (+80nt) was inserted on the region targeted by gRNA A, and one extra cytosine nucleotide (+C) was inserted on the region targeted by gRNA B/C (see also Supplementary Figure 3). D. Structure of MSI2 transcript in SEM wild-type (wt), SEM CNTRL and CRISPR-edited SEM MSI2 KO clones. As a result of CRISPR/CAS9 genome editing, an early stop-codon (stop) was inserted on MSI2 RRM1. E: Western Blot analysis of MSI2 protein expression. An anti-MSI2 antibody recognising the C-terminus of the gene was used to confirm the homozygous depletion of MSI2 in CRISPR-edited SEM MSI2 KO clones.

Supplementary Figure 2

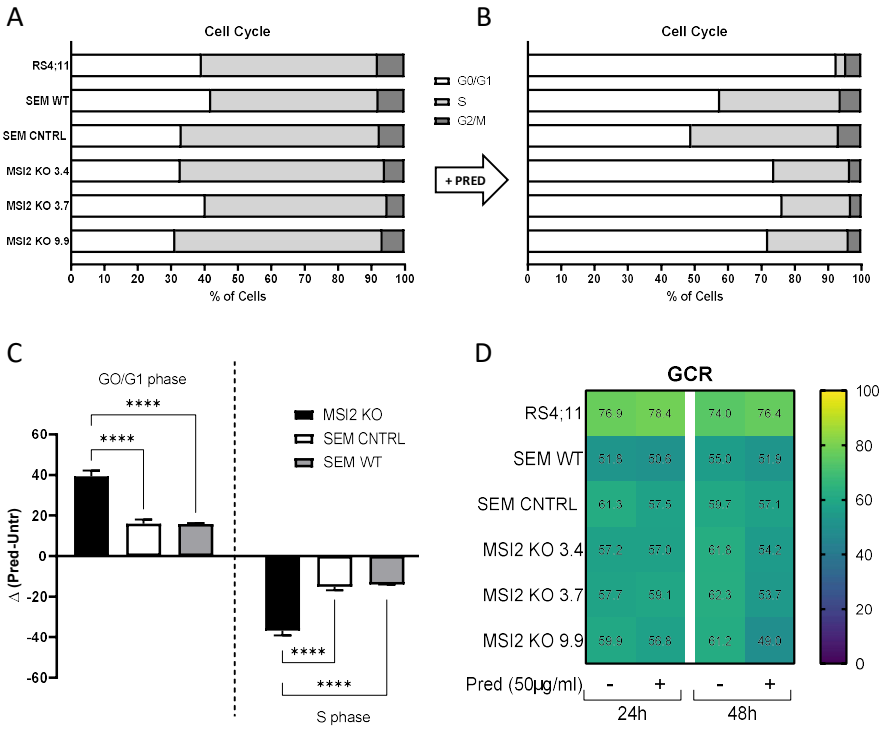

Figure S2: Analysis of cell cycle and GCR expression

A-B. Cell cycle analysis performed by Mass Cytometry (CyTOF) in basal condition (A) and after treatment with 50µg/ml Methyl-Prednisolone for 48h in vitro (B). The percentage of cells in each phase was detected based on cell cycle markers (Cyclin B, pRB and pHH3) and IdU content in live gated cells ($cPARP^-/cCasp3^-$), as previously described[38]. C. Impact of Methyl-prednisolone administration on cell cycle in SEM wt, CNTRL and MSI2 KO clones. Values reported the Delta increase or decrease calculated as the difference between treated and untreated samples. The mean values were calculated on two replicates for SEM wt and CNTRL and by pooling three MSI2 KO individual clones. ****p<0,0001 (One-way Anova). D. Expression of Glucocorticoid receptor (GCR, NR3C1). The heatmap shows the

percentage of live GCR-positive cells with or without Methyl-Prednisolone exposure in vitro (50µg/ml for 24h or 48h). Numbers report the percentage of GCR positive cells gated on live cells ($cPARP^-/cCasp3^-$).

Supplementary Figure 3

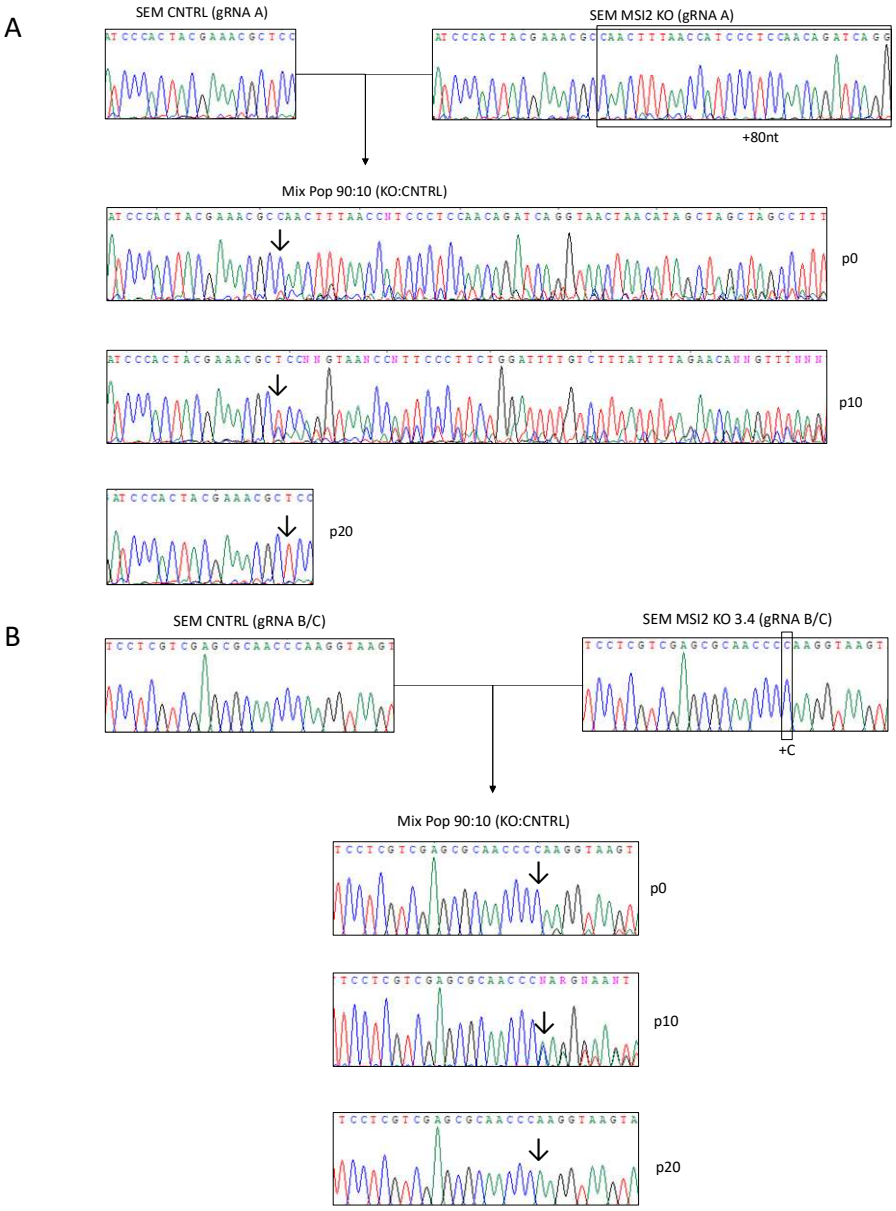

Figure S3: Long-term competitive assay in vitro (supplement to Fig. 2B)

Sanger sequence analysis of MSI2 genomic DNA (gDNA) loci targeted by gRNAs. The gDNA fragments were amplified by PCR using specific primer pairs and sequenced (see also Figure 2B). CRISPR-edited MSI2 KO clones display a (+80nt) random sequence on gRNA A targeted region (panel A) and one extra nucleotide (+C) on gRNA B/C region (panel B) (see also Supplementary Figure 1C). The two single population (CNTRL and MSI2 KO), the mix population 90:10 (KO:CNTRL) at the beginning of the assay (p0) and two representative timepoints (p10 and p20) are shown.

Supplementary Figure 4

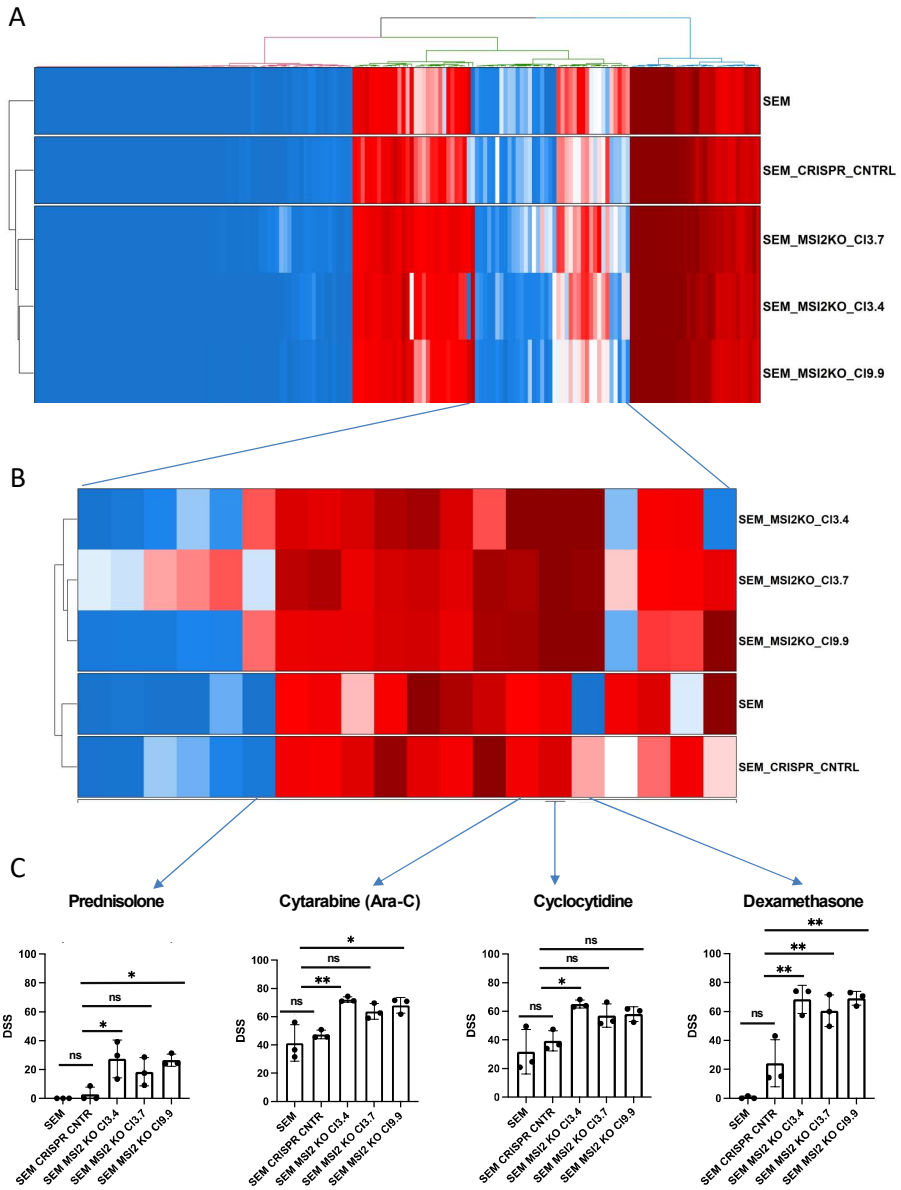

Figure S4: Drug sensitivity profile of SEM MSI2 KO (supplement to Fig. 3)

A. Unsupervised clustering analysis showing of the drug profile of SEM wt, CNTRL and MSI2 KO cells throughout the 174 compounds of the library used for high-throughput drug screening. The reported DSS values were

calculated for each sample as the mean of three replicates. B. Heatmap showing the 20 compounds with a differential profile identified by unpaired t-test statistical analysis ($p<0,05$) in MSI2-expressing (SEM wt and SEM CNTRL in triplicate (n=6)) versus MSI2 KO clones (3.4, 3.7 and 9.9 in triplicate (n=9)). C. Differential drug sensitivity profile of SEM wt, CNTRL and MSI2 KO cells against Dexa, Cytarabine, Prednisolone and Cyclocytidine. *$p<0.05$ **$p<0.01$ ***$p<0.001$ (One-Way Anova multiple t-test with Bonferroni correction).

Supplementary Figure 5

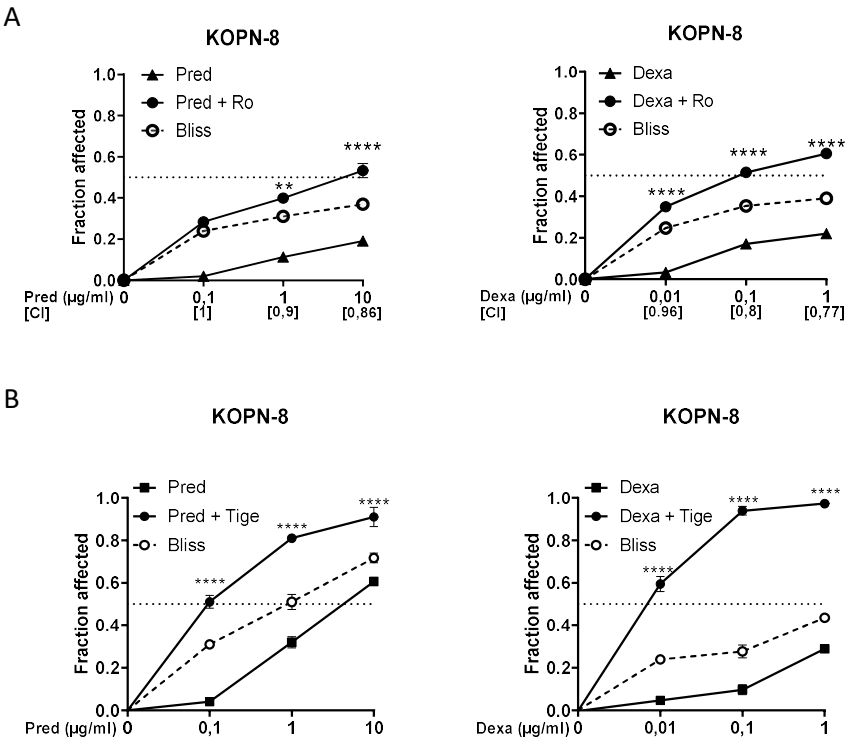

Figure S5: Combination treatment on KOPN8 cell line (supplement to Fig. 3B and Fig. 5C)

A. Scalar doses of Pred (left panel) or Dexa (right panel) were used in combination with a constant sub-cytotoxic concentration of Ro 08-2750 (2µM) in vitro. The Fraction affected was detected by FACS as the percentage of dead cells (AnnexinV-positive) after 72h of treatment (mean of 3 replicates) normalized on the untreated controls. B. Scalar doses of Pred (left panel) or Dexa (right panel) were used in combination with a constant sub-cytotoxic concentration of Tigecycline (3µM) in vitro. The Fraction affected was detected by FACS as the percentage of dead cells (AnnexinV-positive) after 72h of treatment (mean of 3 replicates) normalized on the untreated controls. Bliss: Bliss score (open dot, dashed

line). CI: combination index. **p<0,01 ****p<0,0001 (Two-way Anova, combo vs Bliss).

Supplementary Figure 6

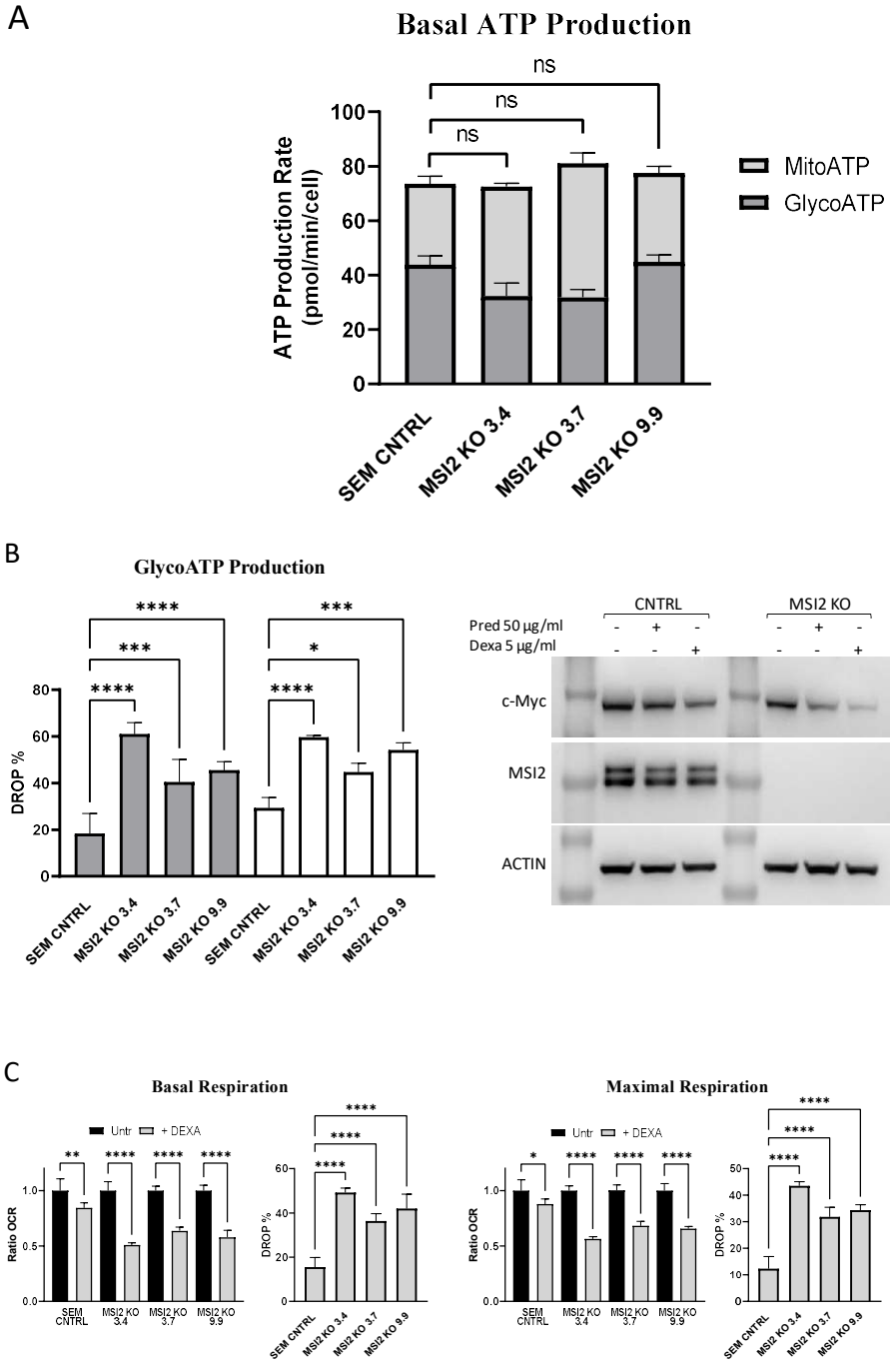

Figure S6: Bioenergetic profiling by Seahorse XF with or without GCs administration (supplement to Fig.4)

A. Seahorse XF ATP Rate assay showing basal ATP production of CNTRL and MSI2 KO cells in normal condition. GlycoATP: total ATP production by glycolysis. Mito ATP: total ATP production by mitochondrial respiration. B. Seahorse XF ATP Rate Assay of CNTRL and MSI2 KO cells after 24h treatment with Dexa or Pred. Drop %: Delta ECAR (Δ_{ECAR}=$ECAR_{GC}$ – $ECAR_{untr}$) x 100. C. Western Blot analysis of c-Myc expression in CNTRL and MSI2 KO cells upon treatment with Dexa or Pred overnight. D. Seahorse XF Mito Stress Test showing basal and maximal mitochondrial respiration of CNTRL and MSI2 KO cells after 24h treatment with Dexa. Ratio OCR: normalized on untreated controls. Drop %: Delta OCR (Δ_{OCR}=OCR_{GC} – OCR_{untr}) x 100. *p<0.05 **p<0.01 ***p<0.001 ****p<0,0001 (One-Way Anova).

Supplementary Figure 7

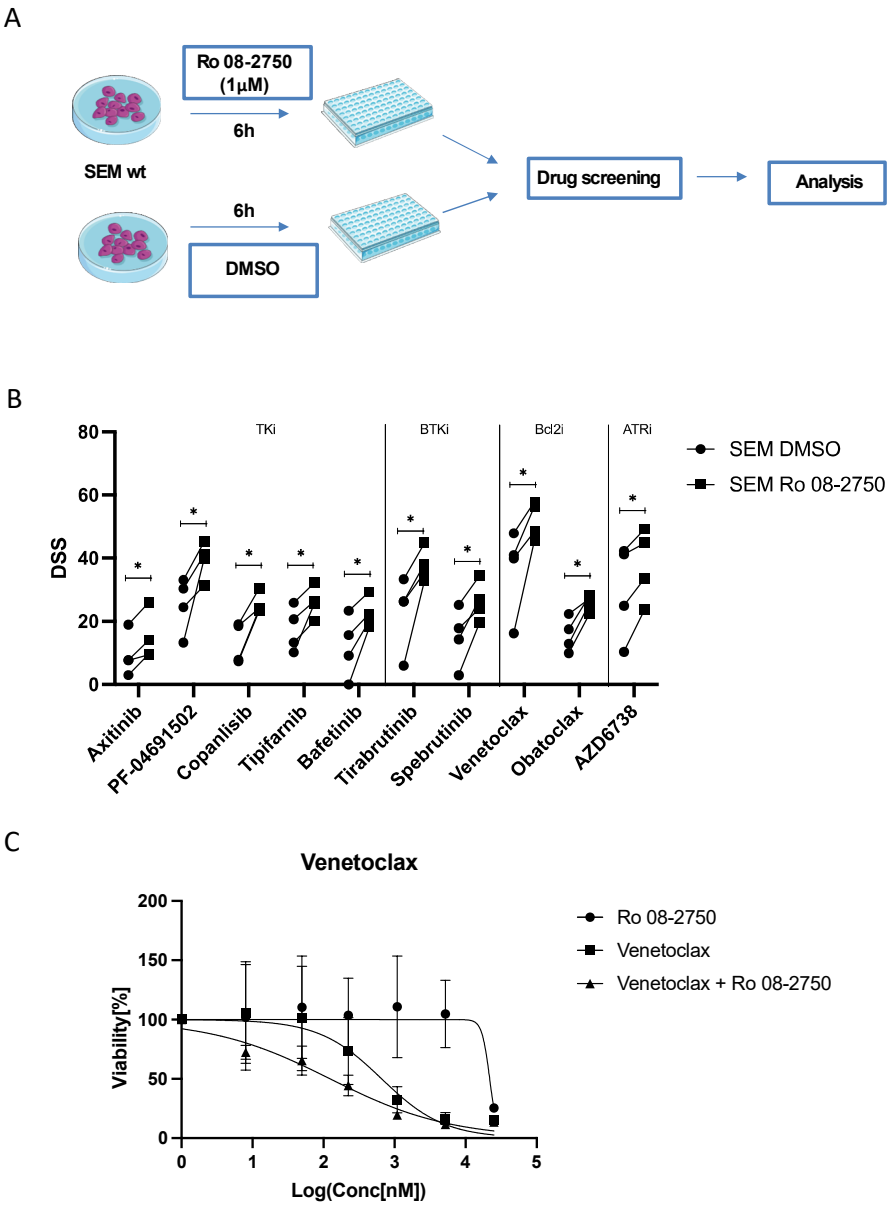

Figure S7: High-throughput drug combination study (supplement to Fig. 6)

A. Experimental scheme (see also Supplementary methods). B. Significant result ($p<0.05$) of a paired t-test without correction for multiple testing of

compounds acting synergistically with Ro 08-2750 in SEM wt cells. Data were obtained from at least 3 biological replicates. C. Combinations study using Ro 08-2750 and Venetoclax. Single drug effects were normalized on DMSO controls, combination effect was normalized on Ro 08-2750 treatment alone. Data were obtained from 3 biological replicates.

Supplementary Methods

CRISPR/CAS9 genome editing

A pool of three expression plasmids each containing the CAS9 sequence, the GFP reporter and a guide RNA (gRNA A, B and C, sequences are provided in Supplementary Figure 1B) targeting the first RNA-recognition motif (RRM1) of MSI2 were purchased from Santa Cruz Biotechnology (sc-404306). A control plasmid (CNTRL) containing a scramble gRNA sequence was used as negative control (sc-418922). SEM cells were plated in antibiotic-free medium in a multi-well plate pre-coated with fibronectin to allow cell adhesion. Cell transfection was performed according to manufacturer instructions using the transfection reagent (sc-395739) and transfection medium (sc-108062). To facilitate cell adhesion and transfection, two centrifugations (1000 rpm for 45min) were applied, one immediately after transfection and another after 3h. After 24h the positively transfected cells (GFP+) cells were FACS sorted and seeded at single cell concentration (1 cell per well) into 96-well

plates. Single clones were expanded in culture and screened to identify CRISPR-edited MSI2 KO clones (see Supplementary Figure 1).

Analysis of MSI2 genome editing

Genomic DNA was extracted using the Wizard Genomic DNA Purification Kit Promega according to the manufacturer's instructions and quantified by Nanodrop. The genomic DNA (gDNA) of MSI2 locus was amplified by PCR using the following primer pairs:

Target	Forward Primer (5'-3')	Reverse Primer (5'-3')
MSI2 A	CCTCTGTTGCCGAATTTCCC	CCTCTGGGGTTACTAGGGGG
MSI2 B/C	ATCTTTTCTCCCAGCCACGC	CCCTCCGAAAGAGTCACAAGG

The PCR products were loaded on a 1,5% agarose gel, purified with the ExoSAP enzymatic PCR Cleanup Reagent (BioLabs) according to the Manufacturer's instructions and analyzed by Sanger sequencing.

Western Blot

Protein lysates were obtained by lysing the cells with commercial buffers RIPA (Sigma R0278) or Laemmli (Sigma S3401). Anti-MSI2 (Abcam, ab76148) and anti-c-MYC (Cell Signaling, #9402) primary antibodies were used for the detection of target protein expression. Anti-actin antibody (Sigma-Aldrich) was used as loading control.

Cell cycle analysis by Mass Cytometry

SEM wt, CNTRL, MSI2 KO (clone 3.4, 3.7 and 9.9) and RS4;11 cells treated with Pred (50µg/ml) for 48h were collected (1X10^6 cells per condition), washed, resuspended in 1ml of filtered cell staining medium (PBS + 0,5% BSA + 0,02% NaN_3) + 10µl of 5-Iodo-2'-deoxyuridine 1mM (cat. n. I7125, Sigma Aldrich, to a final concentration of 10µM IdU). Cells were incubated for 15min at room temperature, then 100µl of filtered PFA 16% was added to each sample (to a final concentration of 1,6% PFA). Cells were incubated for 10 min at room temperature, washed twice in cell staining medium (CSM). Cells were centrifuged 600 rcf for 5 min, supernatant was removed, pellet was resuspended in 100µl cell staining medium, snap-freeze, and stored at -80°C. Samples were thawed and barcoded using 20-plex palladium barcoding plates prepared in-house as described[39]. Cells were stained for surface markers for 30 minutes before being washed with CSM and permeabilized with methanol 100% for 15 minutes at 4C. After 2 washes with CSM, cells were stained for intracellular markers for 30 minutes in 1mL volume. Cells were then washed with CSM and stained with 1:5000 ^{191}Ir/^{193}Ir DNA intercalator (Fluidigm) in PBS with 1.6% PFA overnight at 4C. The following day cells were washed with CSM and ddH_2O, filtered and resuspended in ^{139}La/^{142}Pr/^{59}Tb/^{160}Tm/^{175}Lu normalization beads before being analyzed using a Helios mass cytometer (Fluidigm) at 200 events/sec rate. IMD files were normalized and debarcoded as previously described[39,40] before proceeding to the analysis.

High-throughput Drug Screening

A semi-automated high-throughput drug screening was used for drug screening and drug combination study[20,41]. Briefly, a custom (manually-curated) library of 174 compounds was printed on 1536-wells microplates by d300e Digital Dispenser (Tecan). Compounds list is reported in Supplementary Table 1. Six single doses (8nM, 50nM, 223nM, 1µM, 5µM and 25µM) were used for each compound. All wells were normalized to the volume with DMSO. The apoptosis inducer Staurosporin was used as positive control; DMSO 1% vehicle was used as negative control in 24 wells. SEM wt, CNTRL and three MSI2 KO cells (clone 3.4, 3.7 and 9.9) were seeded at the concentration of 50.000 cells/ml onto library plates by using a Multidrop reagent Dispenser (ThermoFisher). Each sample was analyzed in triplicates. Cell viability was assessed after 72h by CellTiterGlo (Promega) luminescence measurement on a Spark 10M microplate reader (Tecan). The relative inhibition (normalized to DMSO) was calculated as follows:

$$\frac{\text{RLU\{Inhibitor at XnM\}}}{\text{RLU\{mean value of DMSO controls\}}}$$

The EC50 was calculated using GraphPad Prism with the function "log(inhibition) vs normalized response – variable slope". For each drug, the mean Drug Sensitivity Score (DSS) was determined from the three replicates based on the multi parameter AOC-calculation by using R package "DSS" and the function "DSS3"[42].

The Pearson´s correlation coefficient of the three replicates was >0,9 (not shown). Unsupervised clustering analysis was performed with the R package “heatmap3. Data were analysed with unpaired t-test statistical analysis (with $p<0,05$) of MSI2-expressing samples (SEM wt and SEM CNTRL; n=6) Vs MSI2-KO samples (3.4, 3.7 and 9.9 clones; n=9) to identify the compounds with differential drug profile (n=20). All compounds were then analyzed with an unpaired t-test with correction for multiple testing with the Bonferroni-Dunn method to increase reliability of the results (n=4). These compounds were further analyzed with a One-Way ANOVA to verify the differential drug response in SEM wt, CNTRL and each individual MSI2 KO clones. For drug combination screening, SEM wt cells were treated with either the MSI2 inhibitor Ro 08-2750 (1µM) or DMSO. After 6h incubation, the medium was changed, Ro 08-2750 or DMSO was freshly added, and cells were seeded on multi-well plates containing the library of 174 compounds. Cell viability was assessed after 72h as previously described. All samples were tested at least in biological triplicates. The relative Inhibition of the combination treatment was normalized to Ro 08-2750 treatment alone.

References

1 Ramakers-van Woerden, N. L. *et al.* In vitro drug-resistance profile in infant acute lymphoblastic leukemia in relation to age, MLL rearrangements and immunophenotype. *Leukemia* **18**, 521-529, doi:10.1038/sj.leu.2403253 (2004).

2 Pieters, R. *et al.* A treatment protocol for infants younger than 1 year with acute lymphoblastic leukaemia (Interfant-99): an observational study and a multicentre randomised trial. *Lancet* **370**, 240-250, doi:10.1016/S0140-6736(07)61126-X (2007).

3 Dordelmann, M. *et al.* Prednisone response is the strongest predictor of treatment outcome in infant acute lymphoblastic leukemia. *Blood* **94**, 1209-1217 (1999).

4 Pieters, R. *et al.* Relation between age, immunophenotype and in vitro drug resistance in 395 children with acute lymphoblastic leukemia--implications for treatment of infants. *Leukemia* **12**, 1344-1348 (1998).

5 Spijkers-Hagelstein, J. A. *et al.* Glucocorticoid sensitisation in Mixed Lineage Leukaemia-rearranged acute lymphoblastic leukaemia by the pan-BCL-2 family inhibitors gossypol and AT-101. *European journal of cancer* **50**, 1665-1674, doi:10.1016/j.ejca.2014.03.011 (2014).

6 Bardini, M. *et al.* Clonal variegation and dynamic competition of leukemia-initiating cells in infant acute lymphoblastic leukemia with MLL rearrangement. *Leukemia* **29**, 38-50, doi:10.1038/leu.2014.154 (2015).

7 Kharas, M. G. *et al.* Musashi-2 regulates normal hematopoiesis and promotes aggressive myeloid leukemia. *Nature medicine* **16**, 903-908, doi:10.1038/nm.2187 (2010).

8 Kudinov, A. E., Karanicolas, J., Golemis, E. A. & Boumber, Y. Musashi RNA-Binding Proteins as Cancer Drivers and Novel Therapeutic Targets. *Clinical cancer research : an official journal of the American Association for Cancer Research* **23**, 2143-2153, doi:10.1158/1078-0432.CCR-16-2728 (2017).

9 Fox, R. G., Park, F. D., Koechlein, C. S., Kritzik, M. & Reya, T. Musashi signaling in stem cells and cancer. *Annual review of cell and developmental biology* **31**, 249-267, doi:10.1146/annurev-cellbio-100814-125446 (2015).

10 Barbouti, A. *et al.* A novel gene, MSI2, encoding a putative RNA-binding protein is recurrently rearranged at disease progression of chronic myeloid leukemia and forms a fusion gene with HOXA9 as a

result of the cryptic t(7;17)(p15;q23). *Cancer research* **63**, 1202-1206 (2003).

11 Barbouti, A. *et al.* Multicolor COBRA-FISH analysis of chronic myeloid leukemia reveals novel cryptic balanced translocations during disease progression. *Genes, chromosomes & cancer* **35**, 127-137, doi:10.1002/gcc.10099 (2002).

12 Park, S. M. *et al.* Musashi2 sustains the mixed-lineage leukemia-driven stem cell regulatory program. *The Journal of clinical investigation* **125**, 1286-1298, doi:10.1172/JCI78440 (2015).

13 Erazo, T. *et al.* TP53 mutations and RNA-binding protein MUSASHI-2 drive resistance to PRMT5-targeted therapy in B-cell lymphoma. *Nature communications* **13**, 5676, doi:10.1038/s41467-022-33137-8 (2022).

14 Palacios, F. *et al.* Musashi 2 influences chronic lymphocytic leukemia cell survival and growth making it a potential therapeutic target. *Leukemia* **35**, 1037-1052, doi:10.1038/s41375-020-01115-y (2021).

15 Mu, Q. *et al.* High expression of Musashi-2 indicates poor prognosis in adult B-cell acute lymphoblastic leukemia. *Leukemia research* **37**, 922-927, doi:10.1016/j.leukres.2013.05.012 (2013).

16 Aly, R. M. & Ghazy, H. F. Prognostic significance of MSI2 predicts unfavorable outcome in adult B-acute lymphoblastic leukemia. *International journal of laboratory hematology* **37**, 272-278, doi:10.1111/ijlh.12284 (2015).

17 Zhao, H. Z. *et al.* Prognostic significance of the Musashi-2 (MSI2) gene in childhood acute lymphoblastic leukemia. *Neoplasma* **63**, 150-157, doi:10.4149/neo_2016_018 (2016).

18 Ito, T. *et al.* Regulation of myeloid leukaemia by the cell-fate determinant Musashi. *Nature* **466**, 765-768, doi:10.1038/nature09171 (2010).

19 Haferlach, T. *et al.* Clinical utility of microarray-based gene expression profiling in the diagnosis and subclassification of leukemia: report from the International Microarray Innovations in Leukemia Study Group. *Journal of clinical oncology : official journal of the American Society of Clinical Oncology* **28**, 2529-2537, doi:10.1200/JCO.2009.23.4732 (2010).

20 Fazio, G. *et al.* PAX5 fusion genes are frequent in poor risk childhood acute lymphoblastic leukaemia and can be targeted with BIBF1120. *EBioMedicine* **83**, 104224, doi:10.1016/j.ebiom.2022.104224 (2022).

21 Han, Y. *et al.* Musashi-2 Silencing Exerts Potent Activity against Acute Myeloid Leukemia and Enhances Chemosensitivity to

Daunorubicin. *PloS one* **10**, e0136484, doi:10.1371/journal.pone.0136484 (2015).

22 Spinler, K. *et al.* A stem cell reporter based platform to identify and target drug resistant stem cells in myeloid leukemia. *Nature communications* **11**, 5998, doi:10.1038/s41467-020-19782-x (2020).

23 Eberhart, K. *et al.* Glucocorticoid-induced alterations in mitochondrial membrane properties and respiration in childhood acute lymphoblastic leukemia. *Biochimica et biophysica acta* **1807**, 719-725, doi:10.1016/j.bbabio.2010.12.010 (2011).

24 Aoki, S. *et al.* Shift in energy metabolism caused by glucocorticoids enhances the effect of cytotoxic anti-cancer drugs against acute lymphoblastic leukemia cells. *Oncotarget* **8**, 94271-94285, doi:10.18632/oncotarget.21689 (2017).

25 Olivas-Aguirre, M., Torres-Lopez, L., Pottosin, I. & Dobrovinskaya, O. Overcoming Glucocorticoid Resistance in Acute Lymphoblastic Leukemia: Repurposed Drugs Can Improve the Protocol. *Frontiers in oncology* **11**, 617937, doi:10.3389/fonc.2021.617937 (2021).

26 Scheijen, B. Molecular mechanisms contributing to glucocorticoid resistance in lymphoid malignancies. *Cancer drug resistance* **2**, 647-664, doi:10.20517/cdr.2019.29 (2019).

27 Bonapace, L. *et al.* Induction of autophagy-dependent necroptosis is required for childhood acute lymphoblastic leukemia cells to overcome glucocorticoid resistance. *The Journal of clinical investigation* **120**, 1310-1323, doi:10.1172/JCI39987 (2010).

28 Dyczynski, M. *et al.* Metabolic reprogramming of acute lymphoblastic leukemia cells in response to glucocorticoid treatment. *Cell death & disease* **9**, 846, doi:10.1038/s41419-018-0625-7 (2018).

29 Skrtic, M. *et al.* Inhibition of mitochondrial translation as a therapeutic strategy for human acute myeloid leukemia. *Cancer cell* **20**, 674-688, doi:10.1016/j.ccr.2011.10.015 (2011).

30 Weinberg, S. E. & Chandel, N. S. Targeting mitochondria metabolism for cancer therapy. *Nature chemical biology* **11**, 9-15, doi:10.1038/nchembio.1712 (2015).

31 Mani, S., Swargiary, G. & Singh, K. K. Natural Agents Targeting Mitochondria in Cancer. *International journal of molecular sciences* **21**, doi:10.3390/ijms21196992 (2020).

32 Dobson, S. M. *et al.* Relapse-Fated Latent Diagnosis Subclones in Acute B Lineage Leukemia Are Drug Tolerant and Possess Distinct Metabolic Programs. *Cancer discovery* **10**, 568-587, doi:10.1158/2159-8290.CD-19-1059 (2020).

33 Minuesa, G. *et al.* Small-molecule targeting of MUSASHI RNA-binding activity in acute myeloid leukemia. *Nature communications* **10**, 2691, doi:10.1038/s41467-019-10523-3 (2019).

34 Reed, G. A. *et al.* A Phase 1 study of intravenous infusions of tigecycline in patients with acute myeloid leukemia. *Cancer medicine* **5**, 3031-3040, doi:10.1002/cam4.845 (2016).

35 Chen, X. *et al.* Targeting Mitochondrial Structure Sensitizes Acute Myeloid Leukemia to Venetoclax Treatment. *Cancer discovery* **9**, 890-909, doi:10.1158/2159-8290.CD-19-0117 (2019).

36 Goldoni, M. & Johansson, C. A mathematical approach to study combined effects of toxicants in vitro: evaluation of the Bliss independence criterion and the Loewe additivity model. *Toxicology in vitro : an international journal published in association with BIBRA* **21**, 759-769, doi:10.1016/j.tiv.2007.03.003 (2007).

37 Pasquale, V. *et al.* Profiling and Targeting of Energy and Redox Metabolism in Grade 2 Bladder Cancer Cells with Different Invasiveness Properties. *Cells* **9**, doi:10.3390/cells9122669 (2020).

38 Behbehani, G. K., Bendall, S. C., Clutter, M. R., Fantl, W. J. & Nolan, G. P. Single-cell mass cytometry adapted to measurements of the cell cycle. *Cytometry. Part A : the journal of the International Society for Analytical Cytology* **81**, 552-566, doi:10.1002/cyto.a.22075 (2012).

39 Zunder, E. R. *et al.* Palladium-based mass tag cell barcoding with a doublet-filtering scheme and single-cell deconvolution algorithm. *Nature protocols* **10**, 316-333, doi:10.1038/nprot.2015.020 (2015).

40 Finck, R. *et al.* Normalization of mass cytometry data with bead standards. *Cytometry. Part A : the journal of the International Society for Analytical Cytology* **83**, 483-494, doi:10.1002/cyto.a.22271 (2013).

41 Flumann, R. *et al.* An Autochthonous Mouse Model of Myd88- and BCL2-Driven Diffuse Large B-cell Lymphoma Reveals Actionable Molecular Vulnerabilities. *Blood cancer discovery* **2**, 70-91, doi:10.1158/2643-3230.BCD-19-0059 (2021).

42 Yadav, B. *et al.* Quantitative scoring of differential drug sensitivity for individually optimized anticancer therapies. *Scientific reports* **4**, 5193, doi:10.1038/srep05193 (2014).

CHAPTER 3

ADDITIONAL RESULTS: GENERATION OF A RNAi IN VIVO MODEL TO TARGET MSI2 IN MLLr INFANT ALL PRIMARY PATIENTS' CELLS

Introduction

To make the data previously obtained in a cell line model more robust, an in vivo mouse model to target MSI2 in primary patients' blasts is necessary, to mimic more faithfully the complexity in vivo. We generated a constitutive Knock Down using a lentiviral vector system to abrogate the expression of MSI2 in primary leukemic blasts from MLLr infant ALL patients. In a RNA interference (RNAi) model a dsRNA directed against the gene of interest is introduced into cells, then it is cleaved by the nuclease Dicer into double-stranded small interfering RNAs (siRNAs). These siRNAs are assembled into the RNA-induced silencing complex (RISC) which recognizes, binds (by sequence complementarity) and induces the degradation of the target mRNA. For the degradation of the mRNA a second nuclease Ago 2 is required. The siRNAs could be inserted in cells through a vector system and constitutively genetically encoded by expressing a short hairpin RNA (shRNA), consisting of a short target sequence (sense), a short loop region, and the reverse complement of the target sequence (antisense). The polymerase (pol) III drives the transcription in vivo of the shRNA, which is then converted by endogenous nucleases into short RNAs binding the target mRNAs[1]. By using this constitutive knock down model, we aimed to confirm the role of MSI2 in leukemia progression and drug resistance in an in vivo mouse model of PDX.

Results

Cloning and Lentiviral Transduction

The construct constitutively encoding for dsRED, which in its 3'UTR harbors the miR-30 shRNA cassette, was previously generated by cloning into the pCDH lentiviral backbone the PCR amplified dsRED-miR30 fragment under the control of the viral promoter SFFV (Figure 1A)[1,2]. The shRNA sequences control (CNTRL) or the shRNA anti-MSI2 (MSI2 KD) targeting our gene of interest have been synthetized as part of 110 bp ss-DNA oligos (Figure 1B), annealed and cloned into the pCDH-SFFV-dsRED/miR30 vector using XhoI and EcoRI digestion enzymes. The plasmids also contain the ampicillin resistance cassette for the bacterial selection (Figure 1A).

Other two plasmids, each containing the Luciferase gene (the Gaussia Luciferase GLuc or a codon optimized enhanced Firefly Luciferase eFFly, respectively) and a fluorescent marker (either mtagBFP or eGFP, respectively) were previously generated by cloning the amplified coding sequences of mtagBFP (from plasmid pmTagBFP-C1) and eGFP (from DNA fragment synthetized by IDT) into the same vector as above using BamHI and SalI digestion enzymes[2] (Figure 1C). The rational for generating these Luciferase plasmids was to use them to co-transfect the cells together with the dsRED/miR30 shRNA plasmid, in order to allow to discriminate MSI2 KD cells and CNTRL cells and to track the engraftment in mice by in vivo imaging.

To target MSI2, 8 different 110-mer oligonucleotides shRNA constructs were designed by using the splash RNA online tool (http://splashrna.mskcc.org/) (Figure 1D), three of which (#1 to #3) were directed against the canonical full-length isoform (MSI2v1), while five (#4 to #8) targeted the common region shared by both MSI2v1 and MSI2v2 isoforms (Figure 1D). The eight shRNA anti-MSI2 constructs were then cloned into the pCDH dsRED plasmid.

E. coli DH5alpha bacteria were transformed with the shRNA anti-MSI2 or the shRNA CNTRL constructs, and the plasmid obtained (after having been checked for the presence of the shRNA anti-MSI2), were used to produce the viruses using the HEK293T packaging cells[3]. The shRNA CNTRL construct was used as a negative control. Overall, we successfully generated: eight dsRED shRNA anti-MSI2 viruses, one dsRED shRNA CNTRL, one GLuc-mtagBFP and one eFFly-eGFP viruses. The eight dsRED shRNA anti-MSI2 constructs were initially screened to select the three best performing ones (data not shown) to be used to infect the SEM cell line and PDX samples, namely shRNA anti-MSI2 #3 (targeting MSI2v1) and shRNA anti-MSI2 #6 and #7 (targeting MSI2v1+MSI2v2).

A

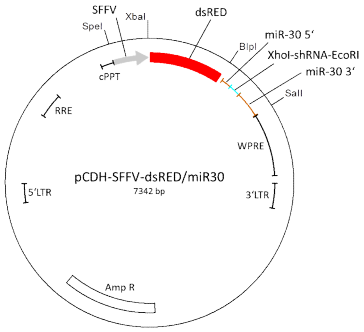

B

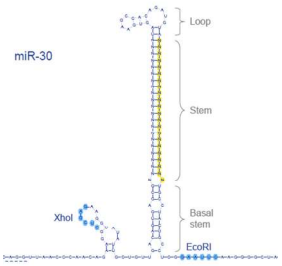

C

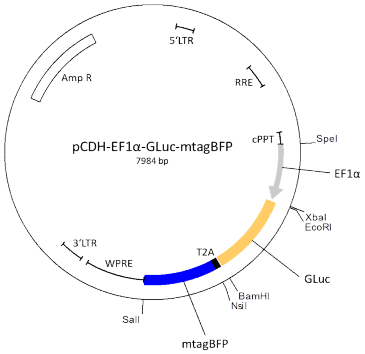

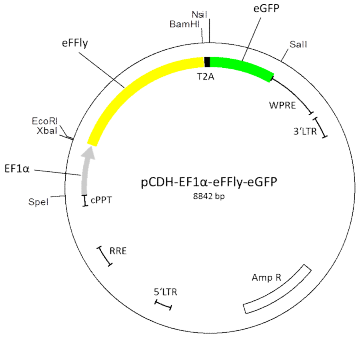

D

shRNA	Strand	Sequences
#1	S	TCGAGAAGGTATATTGCTGTTGACAGTGAGCGCGCATATGAAATTGTTTACAAATAGTGAAGCCACAGATGTATTTGTAAACAATTTCATATGCATGCCTACTGCCTCGG
	AS	AATTCCGAGGCAGTAGGCATGCATATGAAATTGTTTACAAATACATCTGTGGCTTCACTATTTGTAAACAATTTCATATGCGCGCTCACTGTCAACAGCAATATACCTTC
#2	S	TCGAGAAGGTATATTGCTGTTGACAGTGAGCGACATAGTATAATTGTTATATTATAGTGAAGCCACAGATGTATAATATAACAATTATACTATGGTGCCTACTGCCTCGG
	AS	AATTCCGAGGCAGTAGGCACCATAGTATAATTGTTATATTATACATCTGTGGCTTCACTATAATATAACAATTATACTATGTCGCTCACTGTCAACAGCAATATACCTTC
#3	**S**	**TCGAGAAGGTATATTGCTGTTGACAGTGAGCGATAGATGTAAACAGAATTTTAATAGTGAAGCCACAGATGTATTAAAATTCTGTTTACATCTACTGCCTACTGCCTCGG**
	AS	**AATTCCGAGGCAGTAGGCAGTAGATGTAAACAGAATTTTAATACATCTGTGGCTTCACTATTAAAATTCTGTTTACATCTATCGCTCACTGTCAACAGCAATATACCTTC**
#4	S	TCGAGAAGGTATATTGCTGTTGACAGTGAGCGCTCCATGAAATCAATAATAAAATAGTGAAGCCACAGATGTATTTTATTATTGATTTCATGGAATGCCTACTGCCTCGG
	AS	AATTCCGAGGCAGTAGGCATTCCATGAAATCAATAATAAAATACATCTGTGGCTTCACTATTTTATTATTGATTTCATGGAGCGCTCACTGTCAACAGCAATATACCTTC
#5	S	TCGAGAAGGTATATTGCTGTTGACAGTGAGCGACCACCATGAGTTAGATTCCAATAGTGAAGCCACAGATGTATTGGAATCTAACTCATGGTGGGTGCCTACTGCCTCGG
	AS	AATTCCGAGGCAGTAGGCACCCACCATGAGTTAGATTCCAATACATCTGTGGCTTCACTATTGGAATCTAACTCATGGTGGTCGCTCACTGTCAACAGCAATATACCTTC
#6	**S**	**TCGAGAAGGTATATTGCTGTTGACAGTGAGCGCTTCCATGAAATCAATAATAAATAGTGAAGCCACAGATGTATTTATTATTGATTTCATGGAAATGCCTACTGCCTCGG**
	AS	**AATTCCGAGGCAGTAGGCATTTCCATGAAATCAATAATAAATACATCTGTGGCTTCACTATTTATTATTGATTTCATGGAAGCGCTCACTGTCAACAGCAATATACCTTC**
#7	**S**	**TCGAGAAGGTATATTGCTGTTGACAGTGAGCGACCAGCAAGTGTAGATAAAGTAGTAGTGAAGCCACAGATGTATACTTTATCTACACTTGCTGGGTGCCTACTGCCTCGG**
	AS	**AATTCCGAGGCAGTAGGCACCCAGCAAGTGTAGATAAAGTATACATCTGTGGCTTCACTATACTTTATCTACACTTGCTGGTCGCTCACTGTCAACAGCAATATACCTTC**
#8	S	TCGAGAAGGTATATTGCTGTTGACAGTGAGCGCTGCAATGCTGATGTTTGATAATAGTGAAGCCACAGATGTATTATCAAACATCAGCATTGCATTGCCTACTGCCTCGG
	AS	AATTCCGAGGCAGTAGGCAATGCAATGCTGATGTTTGATAATACATCTGTGGCTTCACTATTATCAAACATCAGCATTGCAGCGCTCACTGTCAACAGCAATATACCTTC

Figure 1: Plasmids and shRNA constructs used for lentiviral transduction

A. pCDH-SFFV-dsRED/miR30 vector in which the shRNA anti-MSI2 or the shRNA CNTRL constructs were clones. B. Structure of the short harpin RNAi (shRNA) targeting the gene of interest. C. pCDH plasmids containing the Gaussia Luciferase (GLuc) and the mtagBFP fluorescent marker (left panel), or the codon optimized enhanced Firefly Luciferase (eFFly) and the eGFP reporter (right panel) used for co-transfection with the pCDH-SFFV-dsRED/miR30 vector shown in panel A. D. sequences of the eight shRNA anti-MSI2 constructs (#1 to #8) used to target MSI2 and cloned into the pCDH-SFFV-dsRED/miR30 vector. The sense and antisense sequences targeting MSI2 are written in red. The three shRNA constructs (#3, #6 and #7) selected for infection of SEM cell line and MLLr PDX samples are indicated in bold.

MSI2 was Successfully Targeted in a MLL::AF4+ B-ALL Cell Line by Using a shRNA anti-MSI2 Lentiviral Vector System to Generate SEM MSI2 KD

The MLL::AF4+ B-ALL cell line SEM was lentiviral transduced (overnight, with 8 μg/ml Polybrene), washed three times (24h after transfections), kept in culture (for 4 days after transfection), then FACS-sorted (to purify dsRED+/eGFP+ or dsRED+/mtagBFP+ cells) to obtain SEM CNTRL and SEM MSI2 KD cells (Figure 2A). Co-transductions was performed as follows:

1. dsRED shRNA anti-MSI2 #3 + eFFly-eGFP (hereafter referred as SEM MSI2 KD 3)

2. dsRED shRNA anti-MSI2 #6 + eFFly-eGFP (hereafter referred as SEM MSI2 KD 6)
3. dsRED shRNA anti-MSI2 #7 + eFFly-eGFP (hereafter referred as SEM MSI2 KD 7)
4. dsRED shRNA CNTRL + Gluc-mtagBFP (referred as SEM shRNA CNTRL)

The efficacy of transduction was around 10%. After sorting we obtained a purity of 88-96% dsRED+/mtagBFP+ and dsRED+/eGFP+ cells as shown by FACS analysis (Figure 2B). The cells were checked by Real-Time Quantitative PCR for the expression of MSI2 transcripts (Figure 2C-D) and by Western Blot analysis of MSI2 protein expression (Figure 2E) to validate the efficacy of the shRNA lentiviral system. Indeed, we were able to successfully generate SEM MSI2 KD in which the expression of MSI2 (both mRNA and protein) was strongly silenced (Figure 2C-E) and SEM CNTRL cells. Notably, by using isoform-specific primer pairs (Figure 2D), the RQ-PCR analysis of variant expression revealed that, as expected, shRNA anti-MSI2 #3 construct targeted only the (most represented) canonical full-length MSI2v1, while shRNA anti-MSI2 #6 and #7 constructs targeted both MSI2v1 and the (less represented) short MSI2v1 (Figure 2C).

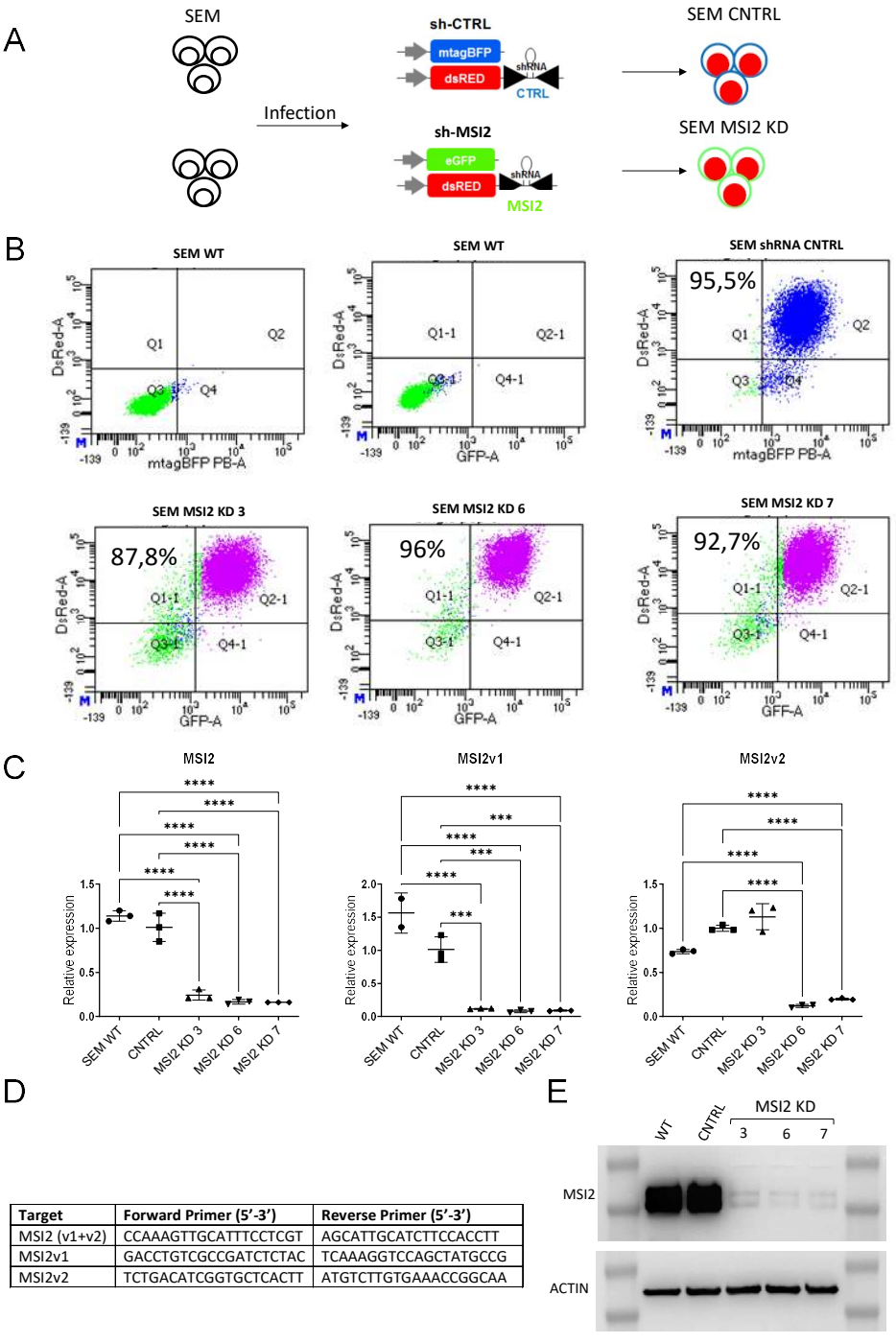

Target	Forward Primer (5'-3')	Reverse Primer (5'-3')
MSI2 (v1+v2)	CCAAAGTTGCATTTCCTCGT	AGCATTGCATCTTCCACCTT
MSI2v1	GACCTGTCGCCGATCTCTAC	TCAAAGGTCCAGCTATGCCG
MSI2v2	TCTGACATCGGTGCTCACTT	ATGTCTTGTGAAACCGGCAA

Figure 2. Validation of the shRNA anti-MSI2 lentiviral vector system in SEM cell line

A. Generation of SEM CNTRL and SEM MSI2 KD by using a shRNA lentiviral vector system. B. FACS analysis of SEM wild-type (wt), and SEM cells infected with shRNA anti-MSI2 or shRNA CNTRL plasmid. Numbers reported refer to the purity of double-positive dsRED+/mtagBFP+ SEM CNTRL or dsRED+/eGFP+ MSI2 KD cells after sorting. C. RQ-PCR Analysis of MSI2 mRNA expression in SEM wt, SEM CNTRL and SEM MSI2 KD cells (#1, #6 and #7). MSI2v1+MSI2v2 isoforms; MSI2v1: canonical (full-length) variant 1 isoform; MSI2v2: short variant 2 isoform. The relative expression was normalized to GAPDH housekeeping gene with the $2^{-\Delta\Delta Ct}$ methods. ***p<0.001 ****p<0,0001 (one-way Anova test). D. Sequence of isoform specific primers pairs used for RQ-PCR targeting either a common region shared by both isoforms of the gene MSI2 (v1+v2) or variant-specific regions (MSI2v1 and MSI2v2). E. Western Blot analysis of MSI2 protein expression confirming the strong silencing of MSI2 in SEM MSI2 KD cells.

Functional Studies: In Vitro Competitive Assay

SEM shRNA CNTRL and MSI2 KD cells were used to perform the first functional study, the long-term competitive assay in vitro. Similarly to what has been done before with CRISPR-edited SEM SMI2 KO and CNTRL cells (see Chapter 2), we mixed the SEM MSI2 KD #3 or #6 with the SEM shRNA CNTRL cells at the initial ratio of 90:10 KD:CNTRL (Figure 3A). We seeded the cells in vitro and maintained them in culture for up to forty passages. The composition of the KD:CNTRL mix population could be easily checked by FACS based on

dsRED+/mtagBFP+ or dsRED+/eGFP+ double positivity. We observed that the SEM MSI2 KD cells slowly but progressively diminished throughout the passages (from p0 to p40), while the SEM shRNA CNTRL cells slightly but consistently increased (Figure 3B). This data confirmed our previous observations in a CRISPR-edited cell line model, and suggested that not only the gene ablation, but also the silencing of MSI2 expression confers a proliferation disadvantage to MLL::AF4+ B-ALL cells.

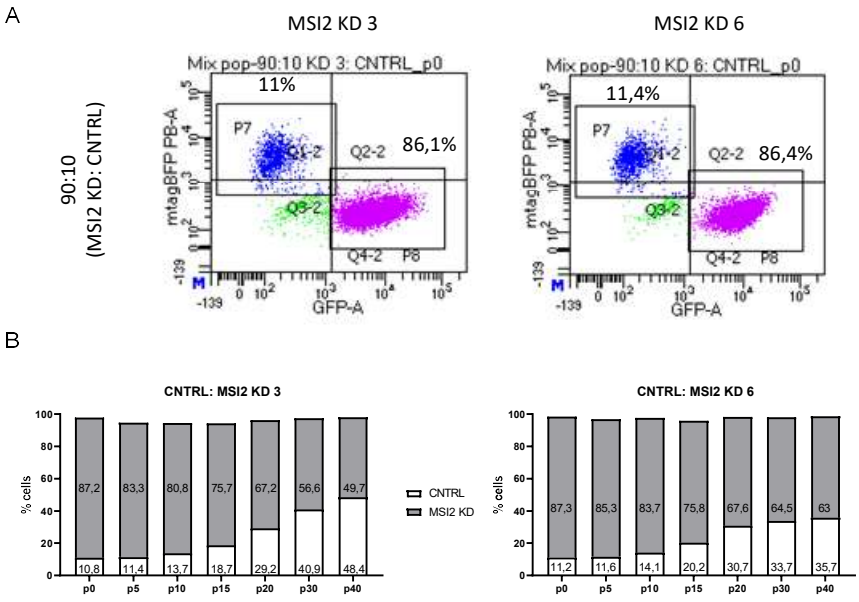

Figure 3: In vitro competitive assay on SEM CNTRL:MSI2 KD

A. FACS analysis of Mix population SEM MSI2 KD 3:CNTRL (left) or SEM MSI2 KD 6:CNTRL (right) at the beginning of the assay (p0) showing the 90:10 KD:CNTRL ratio. dsRED+/mtagBFP+ double positivity marks the SEM CNTRL cells, while dsRED+/eGFP+ double positivity marks the SEM MSI2 KD cells.

B. Proportion of the CNTRL:KD mix population assessed by FACS at periodic timepoints (p0, p5, p10, p15, p20, p30 and p40) showing the increasing outgrowth of SEM CNTRL cells.

Generation of MLLr infant ALL PDX samples with MSI2 KD

The diagnostic samples from three MLLr infant ALL patients were previously transplanted into immunodeficient NSG mice to expand the bulk leukemic samples. Differently to what was done with SEM cells, the PDX cells (freshly isolated from the BM of leukemic mice) were subjected to a double round of transduction: first with either the GLuc/mtagBFP or eFFly/eGFP virus, then with the dsRED shRNA anti-MSI2 or CNTRL virus (Figure 4A). After each round of infection, the PDX cells were maintained in culture for 4 days, FACS-sorted for dsRED/mtagBFP/eGFP positivity and immediately re-injected into serially transplanted NSG mice recipients[3]. This has been done because the efficacy of transduction was very low (approximately in a range of 1-10% of cells, data not shown), so that the re-transplantation into NSG recipient mice allowed the expansion of positively transduced cells. In particular, MLLr PDX1 was infected with the shRNA anti-MSI2 #3 construct, while MLLr PDX2 and PDX3 were infected with the shRNA anti-MSI2 #6 construct. After the double infection we successfully generated (dsRED+/mtagBFP+) MSI2 KD and (dsRED+/eGFP+) CNTRL PDXs as confirmed by FACS analysis (Figure 4B).

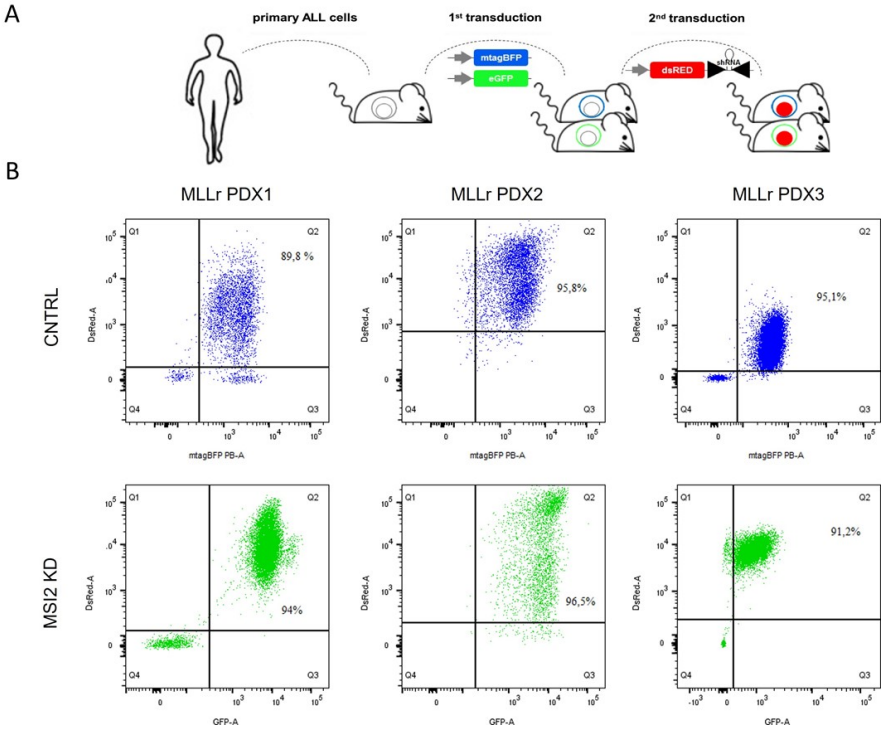

Figure 4: Generation of MLLr ALL PDX samples with MSI2 KD

A. Schematic representation of the generation of three MLLr PDX CNTRL and SEM MSI2 KD by using a shRNA lentiviral vector system B. Numbers reported refer to the purity of double-positive dsRED+/mtagBFP+ MLLr PDX1, PDX2, PDX3 CNTRL or dsRED+/eGFP+ MSI2 KD PDX after sorting and expansion in the mice. The PDX1 was infected with MSI2 KD 3 virus, instead the PDX2 and 3 with the MSI2 KD 6 virus.

Future Directions

The obtained MSI2 knock-down (KD) PDX samples will be used for further functional studies in a mouse model in vivo. This part will be aimed at validating the essential function of MSI2 as a therapeutic target in primary MLLr infant All patients. More specifically, we will:

- perform a competitive assay in vivo (Figure 5A). The PDX control and PDX MSI2 KD will be mixed at 1:1 ratio and re-transplanted into immunodeficient NSG mice to evaluate the impact of MSI2 silencing in the engraftment of primary patients' blast cells. The presence of the luciferase in the plasmids co-transfected (eFFly in PDX MSI2 KD cells and GLuc in PDX CNTRL cells) will offer the great advantage to follow the kinetic of leukemia engraftment in mice by in vivo imaging (BLI: bioluminescence in vivo). On other possibility to check the engrafment is by periodic bone marrow aspiration followed by flow cytometric detection of dsRED/eGFP/mtagBFP fluorescent markers. At the endpoint of analysis, mice will be sacrificed and the bone marrow, spleen, meningeal plexus will be collected for FACS analysis of dsRED/eGFP/mtagBFP fluorescent markers to evaluate the engraftment potential and the ability of PDX MSI2 KD to metastasize and/or to invade the CNS. From this in vivo competitive assay we expect that dsRED+/eGFP PDX MSI2 KD progressively diminished in the bone marrow (and secondary

organs), while the dsRED+/mtagBFP PDX CNTRL expressing MSI2 take over. This data will confirm our hypothesis that MSI2 has a fundamental role in primary blasts from patients with MLLr infant ALL.

- set up a drug treatment mouse model of MLLr infant ALL with MSI2 KD to corroborate our hypothesis that MSI2 has an important role in response to treatment (such as for examples Glucocorticoids response) and represents a candidate therapeutic target (Figure 5B). Mice transplanted with PDX CNTRL or PDX MSI2 KD cells will be treated with Dexamentasone (or other candidate drugs, i.e. Venetoclax, Oxphos inhibitors or other candidate metabolic drugs). Leukemia engraftment will be monitored by BLI and mice survival will be evaluated. From this experiment we expect to address whether targeting of MSI2, combined with drug treatment can efficiently eradicate MLLr infant ALL in vivo.

Additional functional studies, like transcriptomic analysis by RNA sequencing, identification of MSI2 targets by RIP-seq and metabolic studies will be necessary to complete this part. This part will be the topic of my Post-Doctoral studies.

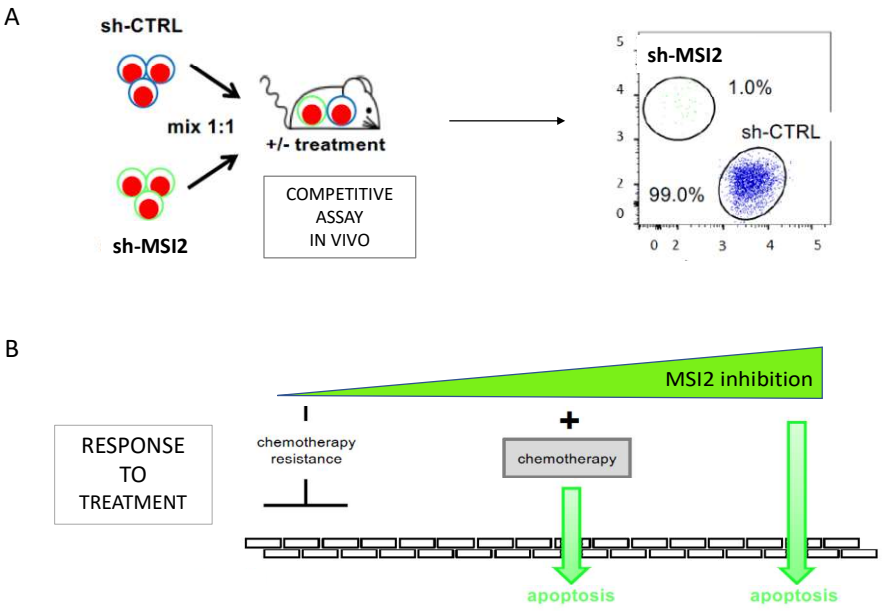

Figure 5: Experimental design for future in vivo studies

A. Schematic representation of the competitive assay in vivo. The dsRED/mtagBFP CNTRL and dsRED/eGFP PDX MSI2 KD derived from each MLLr infant ALL patient will be mixed at 1:1 ratio and transplanted in NSG mice to evaluate the impact of MSI2 silencing on leukemia engraftment and dissemination. B. Schematic representation of the combining effect of MSI2 KD and chemotherapy (as for example GC treatment) in MLLr infant ALL in vivo to assess the impact of MSI2 as a therapeutic target.

References

1 Stegmeier, F., Hu, G., Rickles, R. J., Hannon, G. J. & Elledge, S. J. A lentiviral microRNA-based system for single-copy polymerase II-regulated RNA interference in mammalian cells. *Proceedings of the National Academy of Sciences of the United States of America* **102**, 13212-13217, doi:10.1073/pnas.0506306102 (2005).

2 Carlet, M. *et al.* X-linked inhibitor of apoptosis protein represents a promising therapeutic target for relapsed/refractory ALL. *EMBO molecular medicine* **15**, e14557, doi:10.15252/emmm.202114557 (2023).

3 Carlet, M. *et al.* In vivo inducible reverse genetics in patients' tumors to identify individual therapeutic targets. *Nature communications* **12**, 5655, doi:10.1038/s41467-021-25963-z (2021).

CHAPTER 4

ADDITIONAL RESULTS: PRE-CLINICAL DRUG SCREENING TO TARGET HIGH RISK CHILDHOOD ACUTE LYMPHOBLASTIC LEUKEMIA

Introduction

The ALL with onset in the first year of life (Infant) and with the rearrangement of the MLL gene (MLLr) on the short arm of chromosome 11 (11q21) is a high-risk, rare but very aggressive subtype of leukemia. Infant MLLr ALL is one of the subgroups with the poorest outcome among all cases of pediatric leukemia, with an event free survival (EFS) rate of ~20%– 40% compared to EFS rate of ~80% in children older than one year at diagnosis[1]. MLLr ALL is a unique disease, with peculiar biological and clinical features. It is typically associated to chemotherapy resistance and a high incidence of disease relapse[2]. Therefore, the identification of new active drugs against MLLr infant ALL represents nowadays an urgent unmet need.

In this context we applied a high-throughput (HTP) drug screening using a library of 174 compounds (already used in the clinic and mostly FDA/EMA-approved) to evaluate their anti-leukemic activity in primary blasts from leukemic patients. A cohort of 34 childhood BCP-ALL patient-derived xenograft (PDX) samples was screened on our platform, including 10 infants with MLLr ALL, 9 CRLF2r DS-ALL and 15 PAX5r ALL cases. The screening of compounds which are currently been used in the clinic, and already FDA/EMA approved gives us the great advantage to have the toxicity/pharmacokinetics data available and allows us to identify compounds which potentially could be immediately translatable to the clinic. This reduces the risk of failure in early clinical trials of the drug tested in vitro[3]. This application is

enabling direct and robust conclusions of drug repurposing, an increasingly popular strategy in drug discovery[3].

The majority of the drugs selected for our screening have been tested in both preclinical experiments, clinical trials and observational studies, that have demonstrated antitumor efficacy within a wide range of cancer settings[4].

With specific regards to infant MLLr ALL, a similar approach of high-thruput drug screening was applied by other groups in the past, with the purpose to identify new therapeutic compounds. Here follows a brief review of the main studies available in literature. The group of R. Stam performed an in vitro drug screen of (mostly) clinically approved drugs (3685) on a variety of human ALL cell lines, including three with MLL gene rearrangement, and they reported that 7-Ethyl-10-hydroxycamtothecin (SN-38), the active metabolite of the prodrug Irinotecan, was one of the most active compound at nanomolar concentrations in all ALL cells[5]. In a second high-throughput screening of various drug libraries, comprising 4191 compounds (mostly FDA-approved) performed on two MLLr infant ALL patient samples, the same group identified various drug categories such as BCL-2 inhibitors, histone deacetylase (HDAC) inhibitors, topoisomerase inhibitors, cardiac glycosides, MDM2/p53 inhibitors, microtubule inhibitors, and corticosteroids as active compounds able to reduce the viability of MLLr infant ALL patients. Some of the compounds came up from the screening are known to be effective

against the MLLr infant ALL supporting the validity of the drug screening; instead, other compounds represented indeed novel candidate drug[6], not previously known, like for example the HDACi Panobinostat, whose mechanistic effect was further studied in more details[7]. Finally, Cruickshank et al. also used a high-throughput screening to identify new therapeutic compounds active against infant MLLr ALL. They identified, among all, proteasome inhibitors, histone deacetylase inhibitors, cyclin-dependent kinase inhibitors and, most importantly, they demonstrated the efficacy of Romidespin, another histone deacetylase inhibitor[8].

Methods

In vivo Xenotransplantation

The diagnostic material (BM or PB cells) from 34 patients with BCP-ALL was thawed and transplanted into the tail vein of immunodeficient NSG mice to expand the bulk leukemia. Upon showing the signs of overt leukemia, mice were sacrificed and the BM cells collected to be used for high-throughput drug screening. The BM cells was analyzed by FACS analysis using anti-hCD45, anti-hCD19 and anti-mCD45 antibodies, to check the percentage of engraftment (above 90% for all patients)

High-throughput Drug Screening

The 1536-well plates were pre-coated by Tecan d300 Dispenser with a custom library comprising 174 compounds (of which 100 FDA/EMA approved, see Chapter 2 Supplementary Table 1) under a 6-point specified concentration range from 8nM to 25uM (in a randomized mode). DMSO and Staurosporin were used as negative and positive control of cell death induction, respectively. The BM cells freshly collected from leukemic mice were seeded by Thermo Multidrop reagent Dispenser at the concentration of $1{,}5x10^6$ cells/ml. The cell viability after 3-day culture was evaluated using CellTiter-Glo assay (Promega) on Tecan SPARK 10M microplate reader, according to the manufacturer's instructions. The proportion of luminescence detected by metabolically active cells marked by ATP production

indicate cell viability (Supplementary Figure 1A). Each sample was analyzed in one replicate. Seven BCP-ALL cell lines (carrying the same mutations as the PDX samples analyzed) and 14 healthy samples (healthy lymphoblastoid B-cell lines: n=5, hematopoietic stem cells (HSCs): n=3, T cells: n=3, PBMCs: n=3) were also screened on the platform.

Data Analysis and Statistics

For each drug the quantitative drug sensitivity score (DSS)was computed as previously described[9]. The DSS from 41 BCP-ALL samples (n=34 PDXs + n=7 cell lines) was used to generate a heatmap by R studio using the integration of the packages “pheatmap” and “ComplexHeatmap” with parameters of euclidean distance measurement and ward. For clustering Euclidean distance measurement and the ward. D clustering method was used both for the samples screened (column dendrogram) as well as for the compounds included (row dendrogram). Principal component analysis (PCA) was performed for the leukemic samples upon the compounds (n=153) with the most variable response using the R studio package “stats”. A t distributed stochastic neighbor embedding (tSNE) plot was constructed under the R package “Rtsne” by using the DSS of the evaluated leukemic samples (perplexity=50, exaggeration factor=15; max iterations=1000). The supervised heatmap on selected standard therapy compounds (n=13) currently

used in clinical protocols for pediatric BCP-ALL was created with the same parameters mentioned above.

For each ALL cohort, the drug response against the healthy controls was analyzed by Mann Whitney U-tests statistical analysis in GraphPad Prism6 (GraphPad Software, Inc.). Mean rank difference and statistical significance (p-value) for each compound were visualized by volcano plots using the R package "EnhancedVolcano". Compounds with a p-value<0.05 and a positive mean rank difference were selected to intersect a Venn diagram (using the tool http://bioinformatics.psb.ugent.be/webtools/Venn/) for the identification of the common compounds active against the three different BCP-ALL subgroups. To select the most effective and less toxic compounds (n=9), more stringent criteria were applied by setting the median DSS in ALL patients > 50 and median DSS of healthy controls <10 cut-offs. Data visualization was performed in R studio using the package "ggplot2".

Analysis of cell viability and apoptosis in response to Venetoclax treatment

Nine BCP-ALL PDX samples (CRLF2r DS-ALL n=3, MLLr ALL n=3 and PAX5r ALL n=3) were used to validate the efficacy of Venetoclax treatment ex vivo. The BM cells (fresh or frozen samples) collected from moribund mice were seeded at the concentration of $2{,}4x10^6$ cells/ml in serum-free StemSpan (Stemcell Technologies) supplemented with 1% GlutaMAX (Gibco), 1% Penicillin/Streptomycin

(Cambrex, BioScience), 10ng/mL hSCF and 10ng/mL hG-CSF recombinant cytokines (Peprotech), with or without ABT-199/Venetoclax (Selleckchem). The broad dose range to be used for each PDX sample was previously assessed in preliminary experiments. Each sample was tested in triplicate by using four doses of Venetoclax. The cell viability was evaluated 72h after treatment by CellTiterGlo luminescence Assay (Promega) and by FACS analysis of apoptotic cells after AnnexinV/7-AAD staining (Enzo Life Science). The EC50 values were calculated using Compusyn software on the mean values obtained from triplicates normalized on untreated samples. Data analysis was performed using GraphPad Prism6 (GraphPad Software, Inc.).

Results and Discussion

High-throughput drug screening of BCP-ALL PDX samples and cell lines

An high-throughput (HT) drug screening using a custom library of 174 compounds (Supplementary Figure 1) was performed on 34 samples of pediatric BCP-ALL PDX, 7 human B-ALL cell lines (Supplementary Table 1) and 14 healthy control samples (Supplementary Table 2). The clinical characteristics of BCP-ALL patients screened is reported in Table 1.

Characteristic		Number	Percentage
Sex	Male	18	52,9
	Female	16	47,1
Age at diagnosis (years)	<1	11	32,4
	1 to <10	19	55,9
	≥10	4	11,8
Final Risk	High	10	29,4
	Medium	15	44,1
	Standard	8	23,5
	Low	1	2,9
Response to Predinsolone	PPR	5	14,7
	GPR	29	85,3
Subgroup	CRLF2r DS-ALL	9	26,5
	MLLr ALL	10	29,4
	PAX5r ALL	15	44,1

Table 1: Clinical characteristics of the patients.

Unsupervised clustering analysis of the DSS score of all compounds (n=174) among all BCP-ALL samples (n=41, of which 34 ALL patients + 7 cell lines) was not able to segregate cases according to their disease subgroup or other clinical and biological parameters (like gender, final risk stratification, incidence of relapse, response to prednisone) (Figure 1A). It is also to be noted an absence of clustering of PDX-samples and cell lines, which highlights the similarity of leukemic cell lines with primary patients' material. Similar findings were also observed on PCA analysis (Figure 1B) of all BCP-ALL samples using the compounds with the most variable response (n=153). Interestingly, a very profound clustering of patients sensitive to a plethora of compounds was observed, comprising cases from a variety of clinical characteristics, mostly of them are MLLr or PAX5, while only one CRLF2 (Figure 1A, left branch).

On the other side, the differential profile of the compounds included was explained by differences in efficacy (Figure 2A, y-axis) as well as specificity towards the samples tested (Figure 2A, x-axis). Indeed, some compounds were very efficient and acted in many samples, other were very active but specifically for only a few samples or had no effect. According to this, the compounds cluster based on their drug category defined by common mechanism of action (Figure 2B). Observations coming from the integration of these facts highlighted for example Topoisomerase inhibitors with very high efficacy and minimum variance across the leukemic samples (Figure 2 light green dots), while the opposite trend was seen for the majority of

PI3K/mTOR inhibitors (Figure 2 purple dots). On the other hand, all HSP90 inhibitors (Figure 2 blue dots) presented an intermediate sensitivity and a high variation across the samples, which is also observed for the majority of HDAC inhibitors (Figure 2 orange dots). Antimetabolites (Figure 2 light pink dots) were an example of compounds with a wide range of sensitivity under low variance, in agreement with their nonspecific mechanism of action as interfering with the synthesis of DNA constituent. Finally, compounds belonging to MAPKi (Figure 2 light green dots) and BCR-ABLi classes (Figure 2 pink dots) were indicative of low sensitivity and low variance between the patients.

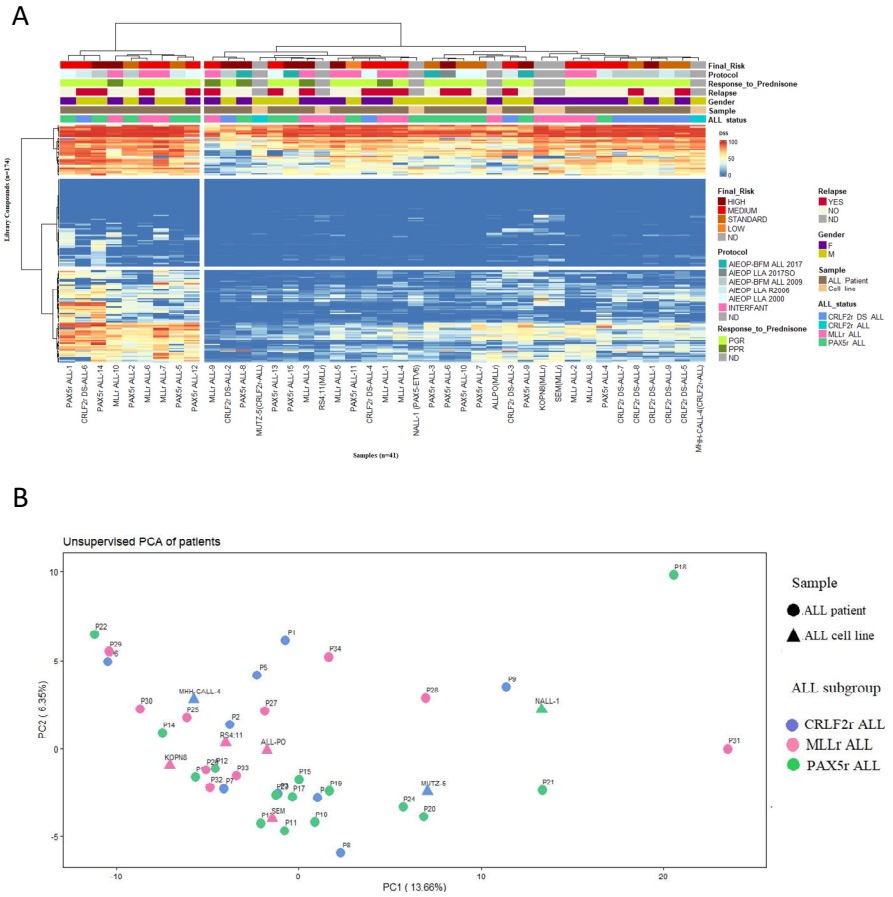

Figure 1: High-throughput (HT) drug screening of BCP-ALL PDX and cell lines

A. Heatmap showing the Drug Sensitivity Score (DSS) of the compounds (n=174, in rows) across the BCP-ALL samples for which drug screening assay was performed (n=41 in total: ALL patients n=34 and cell lines n=7, in columns). Drug efficacy is color-coded according to DSS (from blue=0 to red=100). Heatmap annotation comprises a series of labels of biological and clinical characteristics reported in legend. B. Principal component analysis (PCA) performed for the 41 BCP-ALL samples (n=34 PDXs + n=7 cell lines) upon the most variable response (n=153 compounds). A color code defines

the BCP-ALL subgroup while shape indicates the material (either PDXs or cell lines).

A

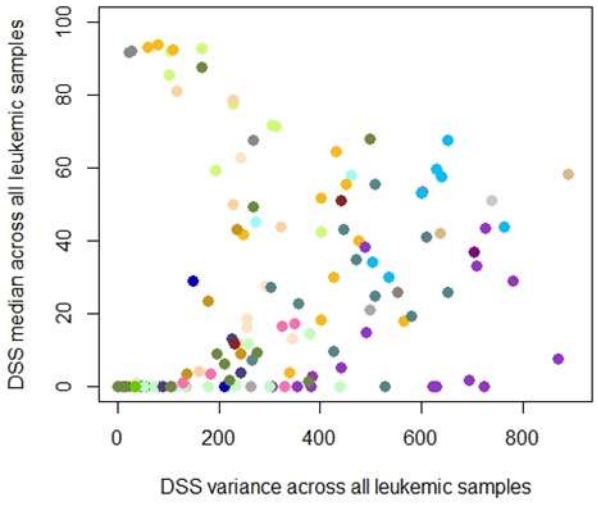

B

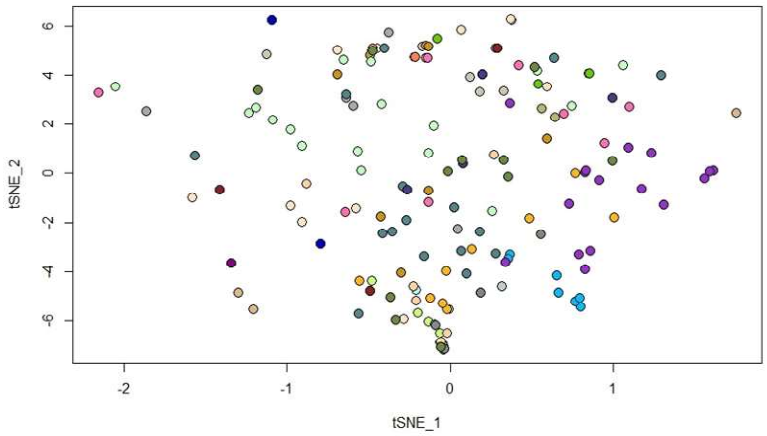

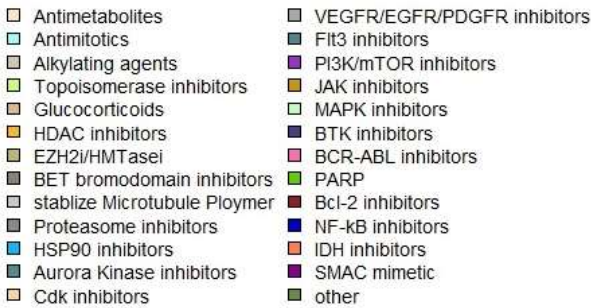

Figure 2: Clustering of compounds on BCP-ALL PDX and cell lines

A. Scatter plot summarizing the median DSS (y-axis) and the variance in DSS (x-axis) across the 41 BCP-ALL samples. Color-coded based on drug category defined by common mechanism of action. B. t-distributed stochastic neighbor embedding (tSNE) plot illustrating the drug sensitivity profile of the 174 compounds across the 41 BCP-ALL samples. Each dot represents a compound, colored by drug category defined by common mechanism of action, as reported in the legend.

In a supervised approach, we sought to dissect the response of BCP-ALL patients to compounds currently used in clinical protocol for first-line treatment of pediatric leukemia. Also in this case, the hierarchical clustering analysis of the profile of standard chemotherapy drugs was not able to discriminate the patients with regard to their disease subgroup or any other clinical and biological feature (Figure 3). However, concerning the drug sensitivity pattern of these compounds (row dendrogram), we were able to identify drugs with minimal to zero response for all BCP-ALL cases (like Prednisone, 6-Thioguanine, Cyclophosphamide, 6-Mercaptopurine, Methotrexate), drugs with enhanced efficacy in all samples (as Bortezomib, Daunorubicin, Doxorubicin) and most interestingly agents with an intense differential sensitivity profile across the patient samples tested (like Dexamethasone, Vinblastine, Vincristine, Cytarabine, Etoposide).

Figure 3: Clustering analysis of standard chemotherapy drugs

Heatmap showing the Drug Sensitivity Score (DSS) of compounds currently used as standard chemotherapy in clinical protocol for pediatric ALL patients (n=13, in rows) across the ALL PDX samples analyzed (n=34, in columns). Drug efficacy is color-coded according to DSS (in a color scare from blue=0 to red=100). Labels of biological and clinical characteristics is reported in legend.

Identification of active compounds on BCP-ALL samples

To identify compounds selectivity targeting BCP-ALL samples, while sparing normal cells, we analyzed the drug profile of a cohort of 14 healthy control samples obtained by healthy volunteers (Supplementary Table 2). This samples comprises different types of cells recapitulating the healthy hematopoietic compartment. By applying Mann Whitney U-test between the drug responses of each three ALL subtype and the healthy controls, we were able to identify compounds with a statistically significant difference (Figure 4A). More specifically, 73/174 compounds were shown to have a higher efficacy in MLLr-ALL PDXs versus the healthy cells, while 77/174 and 82/174 were more efficient in CRLF2r or PAX5r-ALL, respectively. At this step, we thought to investigate the overlap in drugs coming as effective and non-toxic from the three independent comparisons by intersecting them in a Venn diagram. Interestingly we found that most compounds (n=59 out of 77) obtained from the three individual

statistical analysis were common between the three ALL subgroups (Figure 4B). Drug categories of these common 59 compounds are shown in Supplementary Figure 2. To have a deeper idea on the difference in DSS between ALL samples and healthy cells, we plotted these 59 compounds in terms of median DSS of leukemia and median DSS in healthy cells (Figure 4C). To further identify a more limited number of candidate compounds which have a strong activity against leukemia, but not toxic on normal cells we applied a more stringent cut-off by selecting only compounds with a median DSS in ALL PDXs > 50 and a median DSS in healthy cells <10 (highlighted in blue in Figure 4C). This strategy led to the identification of 9 compounds, the Bcl-2 inhibitor ABT-199 (Venetoclax), the HSP90 inhibitors AUY922 (Luminespib), EC144, PF-04929113, NVP-HSP990, the BET bromodomain inhibitor JQ1, the microtubule polymer stabilizer Paclitaxel, the glucocorticoid Dexamethasone and the antimitotic Vincristine. Some of these nine compounds are already in clinic for the treatment of BCP-ALL, like Dexamethasone and Vincristine, two agents included in the classical chemotherapy already used in the current clinical protocols for pediatric patients with ALL[10]. For other drugs, like for example the Bromodomain inhibitor JQ1, preclinical studies have been already published showing the efficacy of BETi in a subgroup of patients with MLLr leukemia[11,12], thus further enhancing the robustness of our drug screening platform and strategy of data analysis to efficiently identify active compounds. Of these 9 compounds identified, it is to be noted that only ABT-199 (Venetoclax) and Paclitaxel (besides Dexamethasone and Vincristine)

are already approved by FDA or EMA for CLL[13] and ovarian and breast cancer respectively. In summary, out of the 174 compounds included in the HTP library, we identified 9 candidates, which clearly present a statistically significant higher efficacy in all the three ALL subgroup compared to healthy cell cohort (Figure 5A).

More importantly, we then moved on evaluating the response of these nine compounds within the samples of the healthy cell cohort, to delineate their sensitivity upon the different components of the healthy hematopoietic system (Figure 5B). By this approach, it became evident that the majority of compounds leave the populations of T cells and PBMCs unaffected, with the major effect seen in hematopoietic stem cells (HSCs) followed by B-cells in some cases (represented as healthy B-cell lymphoblastoid cell lines). Of note, ABT-199 (Venetoclax) and Dexamethasone were the two compounds with the most “safety profile”, as they showed a very limited effect in all the different type of healthy-donor control cells, and most importantly they spared the normal (CD34+) HSC compartment (Figure 5B).

A

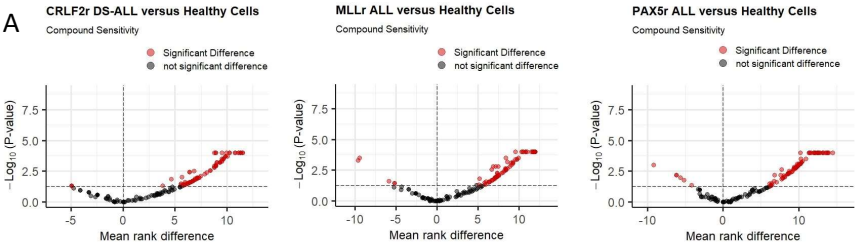
CRLF2r DS-ALL versus Healthy Cells
Compound Sensitivity
Significant Difference
not significant difference
−Log10 (P-value)
Mean rank difference
MLLr ALL versus Healthy Cells
Compound Sensitivity
Significant Difference
not significant difference
−Log10 (P-value)
Mean rank difference
PAX5r ALL versus Healthy Cells
Compound Sensitivity
Significant Difference
not significant difference
−Log10 (P-value)
Mean rank difference

B

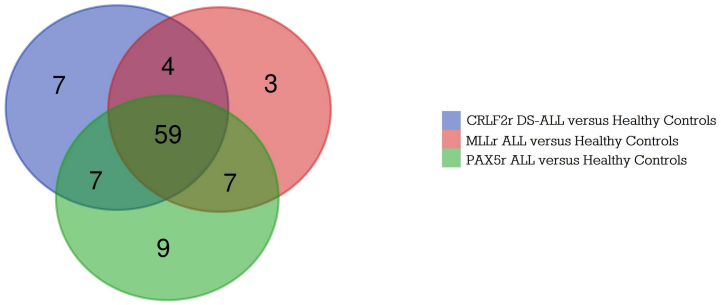
7
4
3
59
7
7
9
CRLF2r DS-ALL versus Healthy Controls
MLLr ALL versus Healthy Controls
PAX5r ALL versus Healthy Controls

C

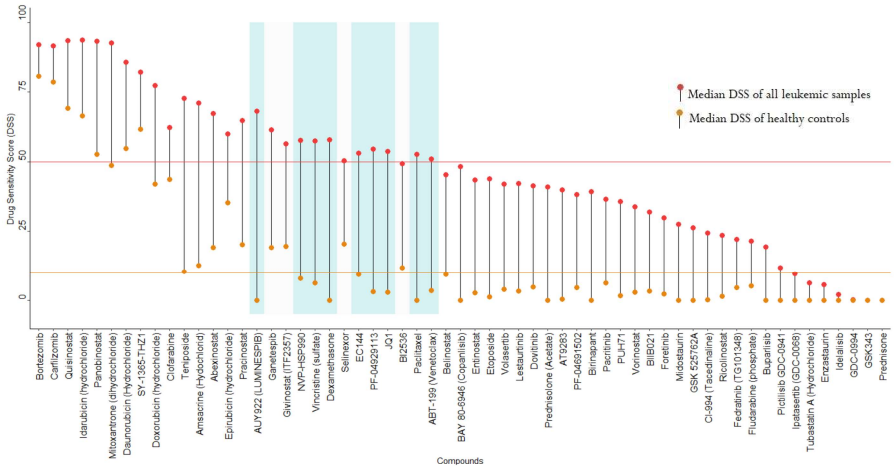
Drug Sensitivity Score (DSS)
Median DSS of all leukemic samples
Median DSS of healthy controls
Bortezomib
Carfilzomib
Quisinostat
Idarubicin (hydrochloride)
Panobinostat
Mitoxantrone (dihydrochloride)
Daunorubicin (hydrochloride)
SY-1365-THZ1
Doxorubicin (hydrochloride)
Cladribine
Teniposide
Amsacrine (Hydrochlorid)
Alvespimycin
Epirubicin (hydrochloride)
Pracinostat
AUY922 (LUMINESPIB)
Ganetespib
Givinostat (ITF2357)
NVP-HSP990
Vincristine (sulfate)
Dexamethasone
Selinexor
EC144
PF-04929113
JQ1
BI2536
Paclitaxel
ABT-199 (Venetoclax)
Belinostat
BAY 80-6946 (Copanlisib)
Entinostat
Etoposide
Volasertib
Lestaurtinib
Dovitinib
Prednisolone (Acetate)
AT9283
PF-04691502
Bfinapant
Pacritinib
PLK-r71
Vorinostat
BIIB021
Foretinib
Midostaurin
GSK 525762A
Ci-994 (Tacedinaline)
Ricolinostat
Fedratinib (TG101348)
Fludarabine (phosphate)
Buparlisib
Pictilisib GDC-0941
Ipatasertib (GDC-0068)
Tubastatin A (Hydrochloride)
Enzastaurin
Idelalisib
GDC-0994
GSK343
Prednisone
Compounds

Figure 4: Identification of candidate active compounds in BCP-ALL PDXs

A. Volcano plots relative to the Mann-Whitney U-test statistical analysis of each individual ALL patient cohort (CRLF2r DS-ALL n=9, PAX5r ALL n=15, MLLr ALL n=10) versus the healthy cells (total n=14; healthy lymphoblastoid B-cell lines: n=5, hematopoietic stem cells-HSCs: n=3, T cells: n=3, PBMCs: n=3). The compounds with p value<0.05 and a positive mean rank difference are highlighted in red. B. Venn diagram intersecting the compounds identified by statistical significance of Mann-Whitney U-test in each ALL subgroup (blue: CRLF2r DS-ALL n=9, pink: MLLr ALL n=10, green: PAX5r ALL n=15) versus the healthy controls (n=14). C. Graph depicting the difference drug profile of the 59 common compounds (red dots: median DSS in BCP-ALL PDXs; orange dots: median DSS in healthy controls). Compounds that fulfil the criteria of a median DSS of ALL patients > 50 and median DSS of healthy cells <10 are highlighted in blue (n=9).

A

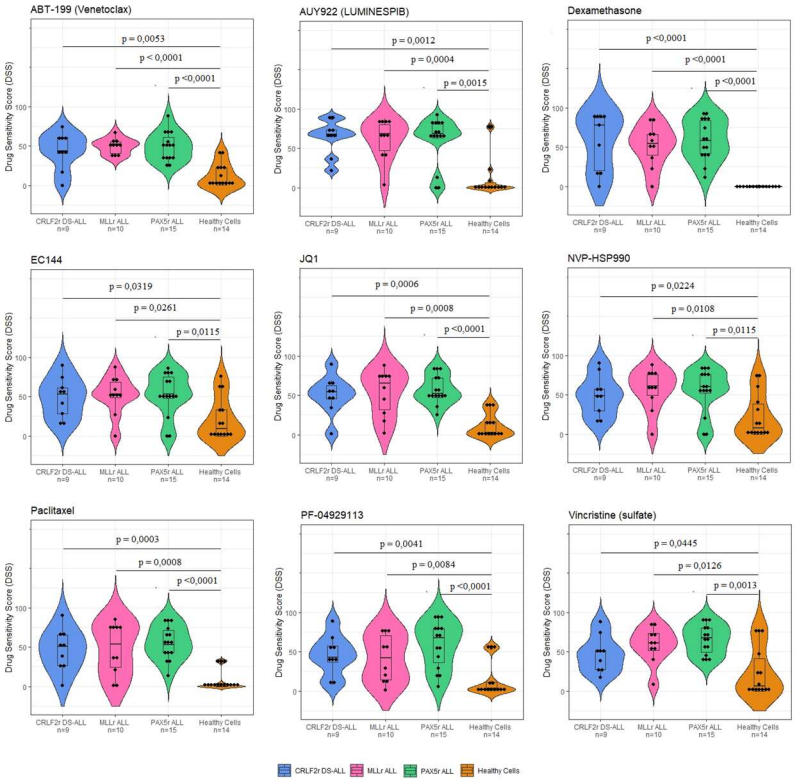
ABT-199 (Venetoclax)
p = 0,0053
p < 0,0001
p <0,0001
AUY922 (LUMINESPIB)
p = 0,0012
p = 0,0004
p = 0,0015
Dexamethasone
p <0,0001
p <0,0001
p <0,0001
EC144
p = 0,0319
p = 0,0261
p = 0,0115
JQ1
p = 0,0006
p = 0,0008
p <0,0001
NVP-HSP990
p = 0,0224
p = 0,0108
p = 0,0115
Paclitaxel
p = 0,0003
p = 0,0008
p <0,0001
PF-04929113
p = 0,0041
p = 0,0084
p <0,0001
Vincristine (sulfate)
p = 0,0445
p = 0,0126
p = 0,0013
Drug Sensitivity Score (DSS)
CRLF2r DS-ALL n=9
MLLr ALL n=10
PAX5r ALL n=15
Healthy Cells n=14

B

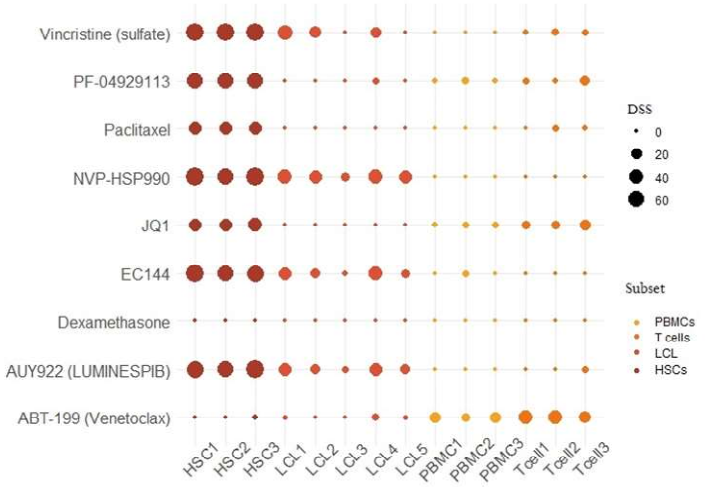
Vincristine (sulfate)
PF-04929113
Paclitaxel
NVP-HSP990
JQ1
EC144
Dexamethasone
AUY922 (LUMINESPIB)
ABT-199 (Venetoclax)
HSC1
HSC2
HSC3
LCL1
LCL2
LCL3
LCL4
LCL5
PBMC1
PBMC2
PBMC3
Tcell1
Tcell2
Tcell3
DSS
0
20
40
60
Subset
PBMCs
T cells
LCL
HSCs

Figure 5: Drug profile of BCP-ALL PDXs and healthy donor control cells

A. Violin plots reporting the distribution of the DSS score in PDX samples from the three ALL subgroups (blue: CRLF2r DS-ALL n=9, pink: MLLr ALL n=10, green: PAX5r ALL n=15) and healthy samples (orange, n=14). The 9 compounds fulfilling the stringent criteria reported in Figure 3C are reported. Mann-Whitney t-test applied. B. Dotplot illustrating the drug sensitivity of the different healthy-donor control subpopulations (healthy lymphoblastoid B-cell lines: n=5, hematopoietic stem cells-HSCs: n=3, T cells: n=3, PBMCs: n=3). Size of the dots reflects magnitude of DSS sensitivity score while color intensity is indicative of each cell subgroup represented in the healthy cohort.

Validation studies of Venetoclax therapeutic effect

Venetoclax has recently emerged as a promising compound for the treatment of patients with different kind of hematopoietic malignancies, like CLL, lymphoma, AML[14], ALL[13] and recently also for MLLr infant ALL[15-17]. Venetoclax, is a BH3-mimetic selectively inhibiting the anti-apoptotic B-cell lymphoma/leukemia 2 (BCL2) protein[15]. Venetoclax was also found as one of the most active compounds in all the three cohort of BCP-ALL from our drug screening study and resulted as the most “safe” drugs as not affecting healthy controls. As a proof of principle, we validated the anti-leukemic effect of Venetoclax treatment in ALL samples. Nine PDX were treated ex vivo (3 PDX for each ALL subgroup) with 4

different doses of Venetoclax. In this setting, we sought to assess the effect of Venetoclax treatment on cell viability by using a metabolic assay (Cell Titer Glo) as well as the apoptosis by Annexin/7AAD staining. As shown in Figure 6, Venetoclax was able to induce apoptosis and decrease cell viability in all 9 PDX samples at very low nanomolar concentrations, as indicated by the calculated IC50 values. The cytostatic (inhibition of cell proliferation) and cytotoxic (apoptosis induction) effect of the drug were very similar in PDX samples. Accordingly, we observed that the anti-leukemic effect of Venetoclax was highly specific for ALL samples, as we were not able to observe apoptotic cell death on healthy lymphoblastoid B-cell lines treated with Venetoclax (Supplementary Figure 3), even when using a broader dose range. Our data demonstrate that Venetoclax is a very active compounds against BCP-ALL while sparing the normal cells, thus further pointing out the potential clinical application of this compound to eradicate leukemia in patients.

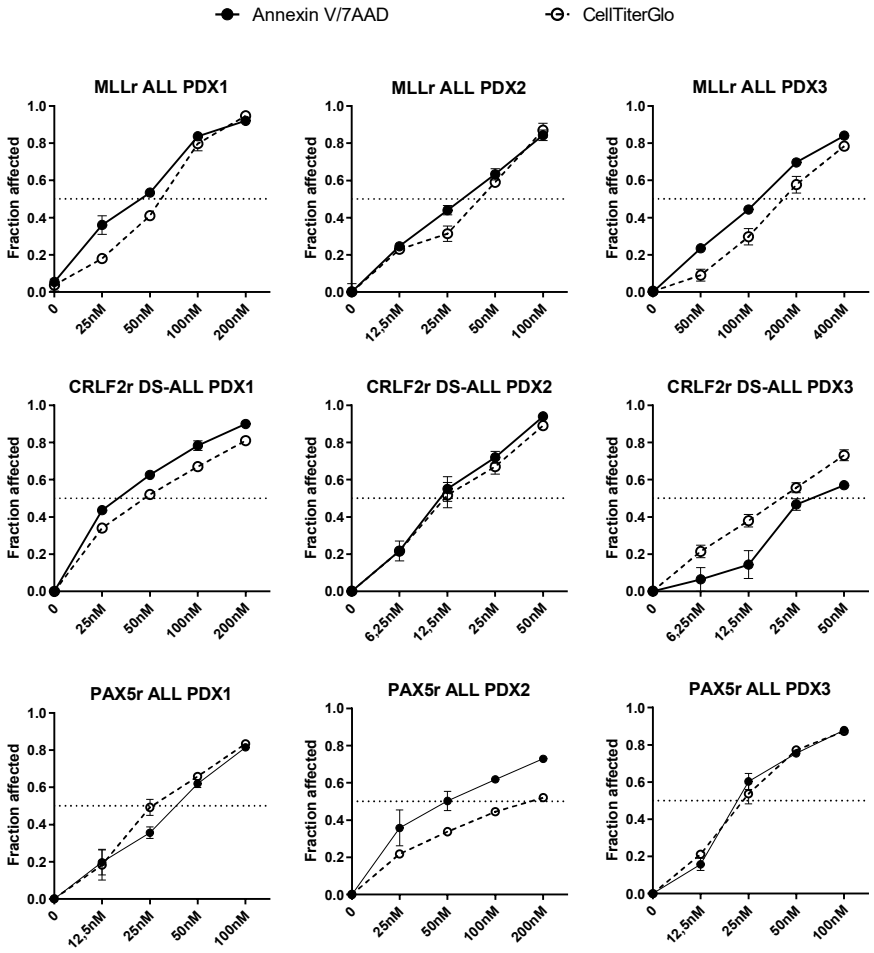

	IC50 AnnV/7AAD (nM)	IC50 CellTiterGlo (nM)
MLLr PDX1	39	53
MLLr PDX2	32	34
MLLr PDX3	112	173
CRLF2r DS PDX1	32	48
CRLF2r DS PDX2	12	14
CRLF2r DS PDX3	36	20
PAX5r PDX1	36	29
PAX5r PDX2	54	157
PAX5r PDX3	27	25

Figure 6: Validation studies of Venetoclax treatment ex-vivo

Cell viability and apoptosis analysis of nine PDX samples (three MLLr infant ALL, three CRLF2r DS-ALL, three PAX5r ALL) treated ex vivo with four scalar doses of Venetoclax. The percentage of dead cells and cell viability were

evaluated by CellTiterGlo luminescence assay (dashed line) or by FACS analysis of Annexin/7AAD staining (continuous line) 72h after treatment. Fraction affected: percentage of dead cells (mean of three replicates) normalized on the vehicle. EC50s written in the table were calculated using Compusyn software on the mean values obtained from triplicates.

Supplementary Figures and Tables

Supplementary Figure 1

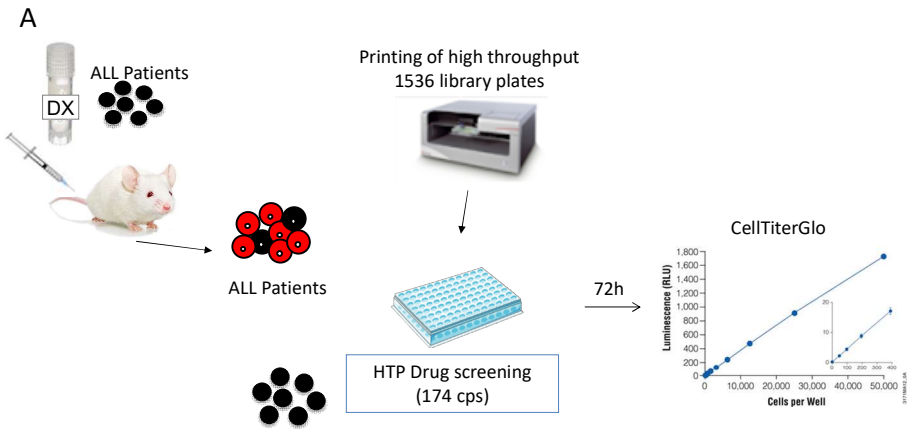

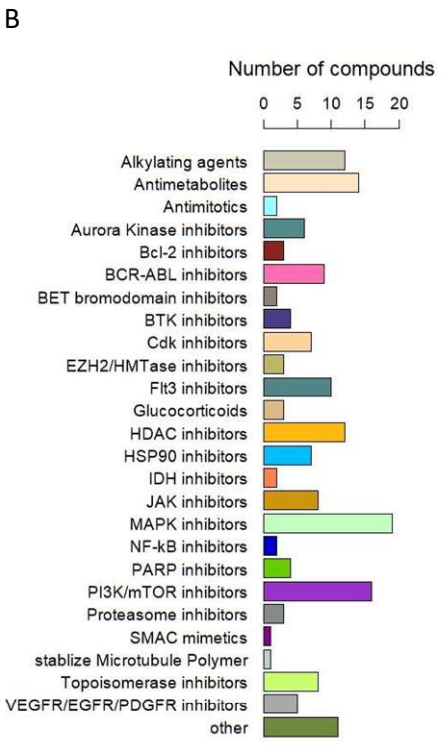

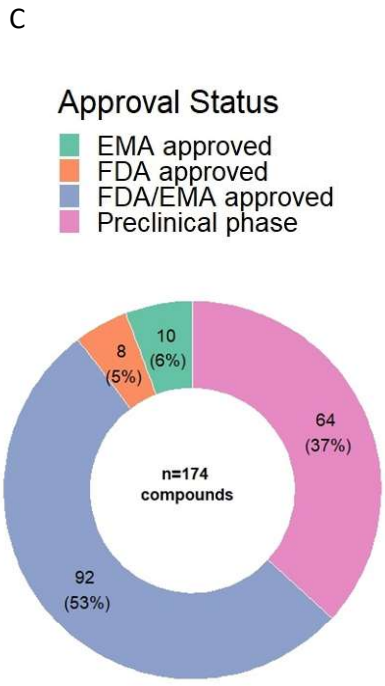

Figure S1: High-throughput (HT) drug screening platform and compound library

A. Experimental workflow. B. Drug categories C. Approval status of the drugs of the custom library

Supplementary Table 1

ALL Subgrup	n. PDX	Cell lines
CRLF2r DS-ALL	9	MUTZ-5, MHH-CALL-4
MLLr ALL	10	ALL-PO, KOPN8, RS4;11, SEM
PAX5r ALL	15	NALL-1
Total	34	7

Table S1: BCP-ALL Samples.

Supplementary Table 2

Healthy Contrl Cohort	Number
Lymphoblastoid cell lines (LCL)	5
T cells from healthy donor	3
PBMCs from healthy donor	3
HSCs from healthy donor	3

Table S2: Control Samples.

Supplementary Figure 2

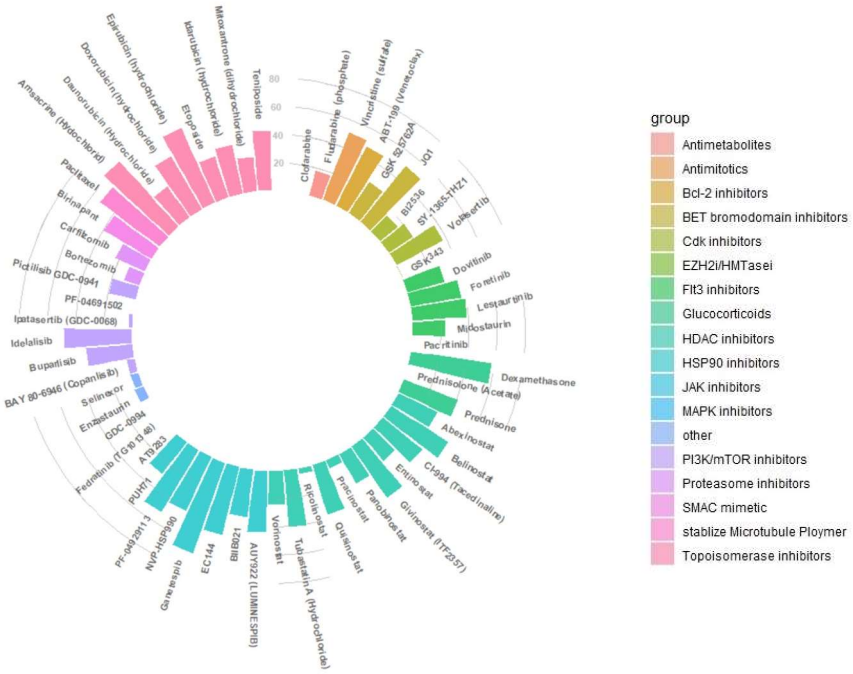

Figure S2: Drugs specific for ALL samples

Drug categories of the common 59 compounds active against BCP-ALL PDX samples.

Supplementary Figure 3

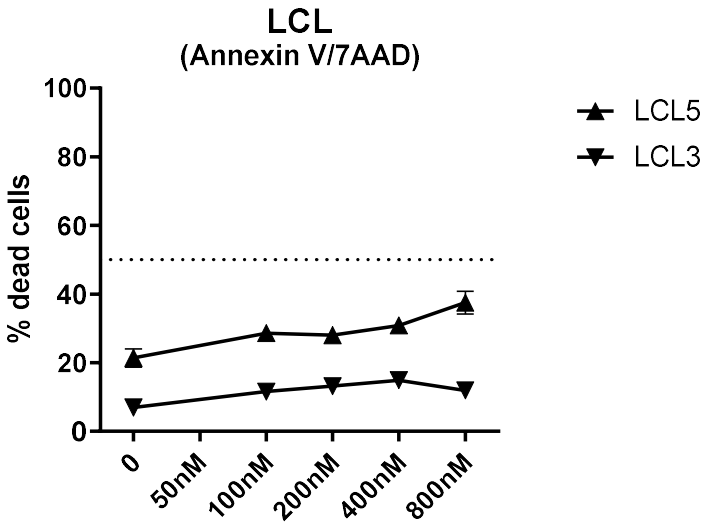

Figure S3: Treatment of LCL with Venetoclax in vitro

Apoptosis analysis of two lymphoblastoid cell lines (LCL) treated with scalar doses of Venetoclax in vitro. The percentage of dead cells (AnnexinV-positive) was evaluated by FACS analysis assay 72h after treatment. Data shown represent the median of three replicas for each dose.

References

1 Pieters, R. *et al.* Outcome of Infants Younger Than 1 Year With Acute Lymphoblastic Leukemia Treated With the Interfant-06 Protocol: Results From an International Phase III Randomized Study. *Journal of clinical oncology : official journal of the American Society of Clinical Oncology* **37**, 2246-2256, doi:10.1200/JCO.19.00261 (2019).

2 Pieters, R. *et al.* Relation between age, immunophenotype and in vitro drug resistance in 395 children with acute lymphoblastic leukemia--implications for treatment of infants. *Leukemia* **12**, 1344-1348 (1998).

3 Sleire, L. *et al.* Drug repurposing in cancer. *Pharmacological research* **124**, 74-91, doi:10.1016/j.phrs.2017.07.013 (2017).

4 Fazio, G. *et al.* PAX5 fusion genes are frequent in poor risk childhood acute lymphoblastic leukaemia and can be targeted with BIBF1120. *EBioMedicine* **83**, 104224, doi:10.1016/j.ebiom.2022.104224 (2022).

5 Kerstjens, M. *et al.* Irinotecan Induces Disease Remission in Xenograft Mouse Models of Pediatric MLL-Rearranged Acute Lymphoblastic Leukemia. *Biomedicines* **9**, doi:10.3390/biomedicines9070711 (2021).

6 Wander, P. *et al.* High-Throughput Drug Library Screening in Primary KMT2A-Rearranged Infant ALL Cells Favors the Identification of Drug Candidates That Activate P53 Signaling. *Biomedicines* **10**, doi:10.3390/biomedicines10030638 (2022).

7 Garrido Castro, P. *et al.* The HDAC inhibitor panobinostat (LBH589) exerts in vivo anti-leukaemic activity against MLL-rearranged acute lymphoblastic leukaemia and involves the RNF20/RNF40/WAC-H2B ubiquitination axis. *Leukemia* **32**, 323-331, doi:10.1038/leu.2017.216 (2018).

8 Cheung, L. C. *et al.* Romidepsin enhances the efficacy of cytarabine in vivo, revealing histone deacetylase inhibition as a promising therapeutic strategy for KMT2A-rearranged infant acute lymphoblastic leukemia. *Haematologica* **104**, e300-e303, doi:10.3324/haematol.2018.192906 (2019).

9 Yadav, B. *et al.* Quantitative scoring of differential drug sensitivity for individually optimized anticancer therapies. *Scientific reports* **4**, 5193, doi:10.1038/srep05193 (2014).

10 Pui, C. H. & Evans, W. E. Treatment of acute lymphoblastic leukemia. *The New England journal of medicine* **354**, 166-178, doi:10.1056/NEJMra052603 (2006).
11 Dawson, M. A. *et al.* Inhibition of BET recruitment to chromatin as an effective treatment for MLL-fusion leukaemia. *Nature* **478**, 529-533, doi:10.1038/nature10509 (2011).
12 Bardini, M. *et al.* Antileukemic Efficacy of BET Inhibitor in a Preclinical Mouse Model of MLL-AF4(+) Infant ALL. *Molecular cancer therapeutics* **17**, 1705-1716, doi:10.1158/1535-7163.MCT-17-1123 (2018).
13 Alford, S. E. *et al.* BH3 Inhibitor Sensitivity and Bcl-2 Dependence in Primary Acute Lymphoblastic Leukemia Cells. *Cancer research* **75**, 1366-1375, doi:10.1158/0008-5472.CAN-14-1849 (2015).
14 DiNardo, C. D. *et al.* Venetoclax Combined With FLAG-IDA Induction and Consolidation in Newly Diagnosed and Relapsed or Refractory Acute Myeloid Leukemia. *Journal of clinical oncology : official journal of the American Society of Clinical Oncology* **39**, 2768-2778, doi:10.1200/JCO.20.03736 (2021).
15 Benito, J. M. *et al.* MLL-Rearranged Acute Lymphoblastic Leukemias Activate BCL-2 through H3K79 Methylation and Are Sensitive to the BCL-2-Specific Antagonist ABT-199. *Cell reports* **13**, 2715-2727, doi:10.1016/j.celrep.2015.12.003 (2015).
16 Khaw, S. L. *et al.* Venetoclax responses of pediatric ALL xenografts reveal sensitivity of MLL-rearranged leukemia. *Blood* **128**, 1382-1395, doi:10.1182/blood-2016-03-707414 (2016).
17 Cheung, L. C. *et al.* Preclinical efficacy of azacitidine and venetoclax for infant KMT2A-rearranged acute lymphoblastic leukemia reveals a new therapeutic strategy. *Leukemia*, doi:10.1038/s41375-022-01746-3 (2022).

CHAPTER 5

SUMMARY, COCLUSIONS AND FUTURE PERSPECTIVES

During all my PhD our studies aimed to find a novel therapeutic approach for treating patients with the MLLr infant acute lymphoblastic leukemia (MLLr infant ALL), a rare but very aggressive disease. These patients suffer of a dismal prognosis even if they are enrolled in specific treatment protocols, but these have not led to improvements in the poor outcome and the overall survival in infants is still remain around 20%[1]. In addition, in the last decades many researchers try to find new genes or pathways involved in the leukemogenesis in order to inhibit these as a therapy[2]; therefore many novel compound were developed against infant MLLr ALL and some of these have been also tested in clinical trials, like for example the Menin inhibitors[3] or the Histone deacetylase inhibitor[4], but without promising results. For this reason, the finding of new therapeutic strategy for this high-risk subgroup of leukemia patients is urgently needed. In addition, one of the main reason of this very poor outcome is the development of resistance to current chemotherapy[5] and there are many studies that investigated the possible mechanism involved in it in order to overcome the resistance and ameliorate the outcome[6-8].

Specifically, in my PhD I focused on unravelling the function of a novel gene involved in the pathogenesis of the disease and potentially targetable: Musashi-2 (MSI2), in particular investigating its role in Glucocorticoid-resistance, and on testing compounds already in clinic developed for other disease and potentially acting on leukemia.

Since the biological mechanisms involved in the pathogenesis of MLLr infant ALL are not completely understood, the identification of genes involved in the leukemogenesis could represent a way to better elucidate the processes occurring in the development and the progression of the pathology. We focused in particular on MSI2 because it is well known its important role in normal hematopoiesis, in myeloid leukemia, both acute[9,10] and chronic[11], in chronic lymphoblastic leukemia[12] and there is also a study that showed the involvement of MSI2 in MLLr AML[13]. About acute lymphoblastic leukemia there are only very few studies which reported an increased expression of the MSI2 in B-ALL patients compared to bone marrow cells derived from healthy donors and showed the existence of a strong correlation between high levels of MSI2 expression and a poor outcome in B-ALL patients (both adults and pediatric cases)[14-16]. In addition, our laboratory has previously discovered that MSI2 was one of the genes downregulated after I-BET151 treatment of MLL::AF4+ cells[17].

By retrospectively analyzing the gene expression profile of a large cohort of Italian pediatric patients affected by BCP-ALL, we observed that the expression levels of MSI2 were higher in MLLr ALL compared to MLLr AML cases and healthy donor. Given the proven importance of MSI2 in AML, these data reinforce our hypothesis that this gene might have a crucial role in ALL as well and prompted us to better investigate the role of MSI2 in the MLLr ALL.

By successfully generating a human MLL::AF4+ ALL cell line with *MSI2* knock-out by using the CRISPR/CAS9 genome editing, we demonstrated that the absence of MSI2 caused a proliferation disadvantage in vitro and an impaired leukemia-initiating capacity and a lower disease burden in vivo in a xenotransplantation mouse model. However, the most relevant and new result that we obtained is the involvement of MSI2 on the Glucocorticoid resistance through the regulation of the bioenergetic profile. Indeed, we had observed that the absence or the pharmacological inhibition of MSI2 sensitized the MLLr ALL cell lines to Prednisolone and Dexametasone by affecting the mitochondrial respiration and the mitochondrial energy production. GCs act on the glycolytic metabolism of the cells by reducing the expression of the proto-oncogene c-Myc[18] and consequently downregulating the glucose transporter GLUT1[19]; as also confirmed by our results that indicated a reduction of c-Myc expression after GCs exposure both on control cells expressing MSI2 and in the MSI2 KO cells. However, the leukemic cells were able to escape from the apoptotic effect induced by GCs because they underwent a metabolic adaptation system in which they hyperactived the mitochondria to compensate the block of the energy production from glycolysis. Instead, when MSI2 is absent or inhibited, also the mitochondria were impaired and the cells were not able to survive in stress condition, like after GCs exposure. Indeed, Although the Warburg hypothesis proposes that malignant cells reply on glycolysis and are less dependent on oxidative phosphorylation for survival, more recent studies indicated that

some tumors are highly dependent on oxidative phosphorylation for survival[20]. Notably, various studies have shown that tumor cells have increased mitochondrial biogenesis and basal level of oxygen consumption than normal cells[21]. In addition, it was also demonstrated that between the pathways associated with GC resistance in MLLr infant ALL there were electron transport chain, protesome, tRNA-aminoacyl biosynthesis and peroxisome signaling pathways[7]. Importantly, our study points out new possible therapeutic strategy to overcome the GCs resistance: targeting the metabolic vulnerabilities of the leukemic cells. Indeed, we demonstrated that the block of mitochondria with Metformin and Tigecycline sensitized the MLLr ALL cell lines to glucocorticoids comparable to what happen when we treated the cells with the MSI2 inhibitor Ro 08-2750. Indeed, we confirmed that MSI2 is involved in GC resistance by regulating the mitochondria metabolism and we pay the way for a new possible combination therapy adding to the standard chemotherapy backbone new Oxphos inhibitor already used in clinic. Indeed, Metformin is a Bioguanide that inhibits the complex I of electron transport chain and blocks mitochondrial respiration causing a reduction of cell viability[22]. Metformin is already used in Clinical Trial in CLL (NTC01750567) and ALL (NTC01324180). Tigecycline is a FDA-approved tetracycline antibiotic inhibiting mitochondrial ribosomes and therefore inhibiting the translation of the subunits of all electron chain complex[23]. Tigecycline is already used in Clinical Trial in CML (NCT02883036) and AML (NCT01332786).

In conclusion, in the first and main part of this study we demonstrated that the lack of MSI2 in MLL::AF4+ B-ALL impairs the growth in vitro and the capacity to regenerate leukemia in vivo. Also, we found that the genetic depletion or pharmacological inhibition of MSI2 sensitizes MLLr ALL cells to GCs probably due to the impairment of the bioenergetic metabolism of leukemic cells (mitochondrial respiration and ATP production) (Figure 1); in addition, the small inhibitor of MSI2, Ro 08-2750, acts synergistically with the Bcl2 inhibitor Venetoclax.

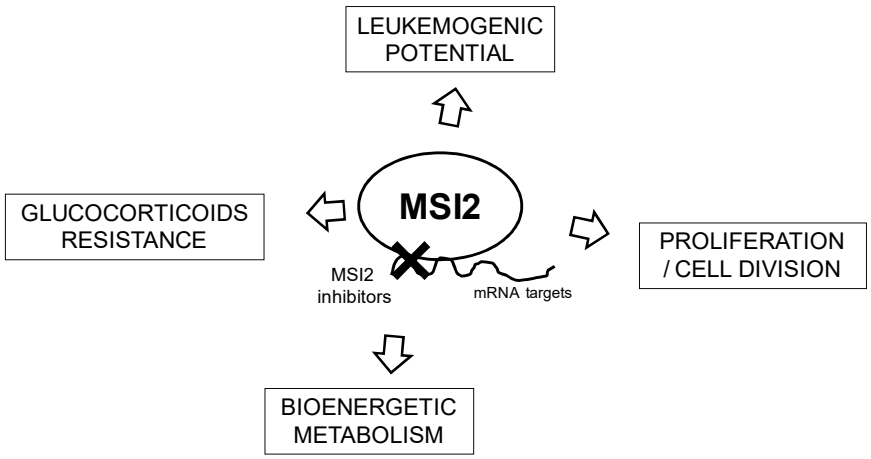

Figure 1: MSI2 has a crucial role for MLL::AF4+ infant ALL.

Subsequentially, we tried to make the data on the role of MSI2 in MLLr infant ALL obtained in a cell line model more robust; therefore, we targeted MSI2 in MLLr ALL PDXs by using a lentiviral vector system. For this part of the project, I had only some preliminary date in which we successfully generated the MSI2 KD SEM cells using different constructs against MSI2 in order to select the best

performers; then we infected also three MLLr PDX with these best performers and we will use this sample to more functional studies. First of all we will set up a competitive assay in vivo taking advantage from the presence of the Luciferase and fluorescent marker into the plasmid used for the virus production; in addition we will perform in vivo treatment with specific compounds of interest (such as for examples the Glucocorticoids) to evaluate the drug response profile of MSI2 KD cells.

In the second part of my PhD I was involved in a collaborative study aimed at identifying novel compounds potentially active against "high-risk" childhood B-ALL. In this study, we applied a high-thruput drug screening platform by using a library of 174 compounds (already used in the clinic and mostly FDA/EMA-approved) to screen a cohort of 34 childhood B-ALL patient-derived xenograft samples, including 10 infants with MLLr ALL, 9 CRLF2r DS-ALL and 15 PAX5r ALL. This approach of testing compound already in clinic for other disease has been already used in other studies with the aim of find new therapies for MLLr infant ALL[24,25]. The main advantage of the 'drug repurposing' is the fact that the data on toxicity and pharmacokinetics of the compound are already available; therefore the preclinical studies for the safety of the compound are not needed[26]. From this study came out both drug acting in all three cohort of high-risk leukemia and others promising selectively targeting MLLr infant ALL. The more important result of the study is that we found and tested a drug screening able to discover new drug acting on ALL PDX and give the

rational for subsequential functional analysis. Many compounds found to be the best performers are known as agents already use in leukemia, like for example Venetoclax (ABT-199), Dexametasone and Vincristine, thus confirm the high-throughput screening applied in our study as a powerful tool to identify active compounds. We focused on Venetoclax and we validated its efficacy to target different subgroups of pediatric B-ALL (while sparing normal cells) because ABT-199 is in use or emerging in some preclinical studies as a drug for the treatment of patients with CLL, AML, early T cell progenitor leukemia, Myc-driven B cell lymphomas and ALL[27]. In addition, Venetoclax has been used in combination with many other compounds in some preclinical studies; Tregnano et al. tested the synergistic effect of Venetoclax with I-BET151 or Sunitinib in MLLr AML[28]; Benito et al observed that combination of ABT-199 with DOT1L inhibitors or standard induction chemotherapeutic agents was synergistic in vitro in MLL::AF4 cells[29]. Regarding in particular the MLLr infant ALL, the COG started a new clinical trial (2122) in which they will combine ABT-199 with Blinatumomab and standard chemotherapy. A very important study that straighten our results and can combine every part of my PhD is that of Erazo et al in which the authors demonstrated the BCL2 is a direct target of MSI2 in B-cell lymphoma and the treatment with Ro 082750 reduced the expression of BCL2[30].

In the future further studies will be directed to:

- Corroborate the pivotal role of MSI2 in primary patients with MLLr infant ALL and validate this gene as a therapeutic marker. This was done by using our RNAi mouse model of PDX in vivo which we successfully generated and validate in SEM cell line.
- Further investigate the involvement of MSI2 in drug resistance, not only GCs but also Venetoclax or other compounds with a putative synergistic effect identified in our combination study (like TKi or BTKi Antimetabolite agents), in order to identify potentially active combination treatments for future clinical application.
- Better elucidate the emerging role of MSI2 in the metabolism of leukemia, by performing metabolomic analysis and/or Seahorse metabolic profiling. The metabolic changes of MLLr ALL cells will be investigated not only after drug administration (like GCs or other compound of interest) but also under stress conditions (like for example hypoxia or nutrient deprivation) to confirm our hypothesis that MSI2 actually plays an important role when leukemic cells are exposed to a metabolic pressure or under stress conditions. Specifically, we will investigate in more in details the function of MSI2 within the mitochondria, as we observed that MSI2 is indeed expressed not only in the cytoplasm, but also in the mitochondrial compartment. Electron microscopy analysis will correlate the expression of MSI2 with the ultrastructure of mitochondrial cristae, while further functional studies will

address whether MSI2 is involved in biogenies, function and fitness of mitochondria.

- Further explore the possibility to exploit the newly discovered metabolic vulnerabilities of leukemic cells to target MLLr infant ALL. In particular we will target the mitochondrial respiration by using Oxphos inhibitors in vivo, like for example by using Tigecycline or the new generation Bioguanide IACS-01075 (an analogue of Metformin) as a strategy to increase the response to Dexamethasone and/or Venetoclax treatment. Combination treatment or triple treatment of mice in vivo will be done.
- Validate in vivo the novel compounds selectively targeting MLLr infant ALL patients emerged from the high throughput drug screening, perform the functional studies to shed light onto their mechanism of actions, and integrate the drug profile with transcriptome data to predict the response to treatment.

References

1 Pieters, R. *et al.* Outcome of Infants Younger Than 1 Year With Acute Lymphoblastic Leukemia Treated With the Interfant-06 Protocol: Results From an International Phase III Randomized Study. *Journal of clinical oncology : official journal of the American Society of Clinical Oncology* **37**, 2246-2256, doi:10.1200/JCO.19.00261 (2019).

2 El Chaer, F., Keng, M. & Ballen, K. K. MLL-Rearranged Acute Lymphoblastic Leukemia. *Current hematologic malignancy reports* **15**, 83-89, doi:10.1007/s11899-020-00582-5 (2020).

3 Krivtsov, A. V. *et al.* A Menin-MLL Inhibitor Induces Specific Chromatin Changes and Eradicates Disease in Models of MLL-Rearranged Leukemia. *Cancer cell* **36**, 660-673 e611, doi:10.1016/j.ccell.2019.11.001 (2019).

4 Cheung, L. C. *et al.* Romidepsin enhances the efficacy of cytarabine in vivo, revealing histone deacetylase inhibition as a promising therapeutic strategy for KMT2A-rearranged infant acute lymphoblastic leukemia. *Haematologica* **104**, e300-e303, doi:10.3324/haematol.2018.192906 (2019).

5 Pieters, R. *et al.* Relation between age, immunophenotype and in vitro drug resistance in 395 children with acute lymphoblastic leukemia--implications for treatment of infants. *Leukemia* **12**, 1344-1348 (1998).

6 Spijkers-Hagelstein, J. A. *et al.* Glucocorticoid sensitisation in Mixed Lineage Leukaemia-rearranged acute lymphoblastic leukaemia by the pan-BCL-2 family inhibitors gossypol and AT-101. *European journal of cancer* **50**, 1665-1674, doi:10.1016/j.ejca.2014.03.011 (2014).

7 Mousavian, Z., Nowzari-Dalini, A., Rahmatallah, Y. & Masoudi-Nejad, A. Differential network analysis and protein-protein interaction study reveals active protein modules in glucocorticoid resistance for infant acute lymphoblastic leukemia. *Molecular medicine* **25**, 36, doi:10.1186/s10020-019-0106-1 (2019).

8 Candelli, T. *et al.* Identification and characterization of relapse-initiating cells in MLL-rearranged infant ALL by single-cell transcriptomics. *Leukemia* **36**, 58-67, doi:10.1038/s41375-021-01341-y (2022).

9 Kharas, M. G. *et al.* Musashi-2 regulates normal hematopoiesis and promotes aggressive myeloid leukemia. *Nature medicine* **16**, 903-908, doi:10.1038/nm.2187 (2010).

10 Minuesa, G. *et al.* Small-molecule targeting of MUSASHI RNA-binding activity in acute myeloid leukemia. *Nature communications* **10**, 2691, doi:10.1038/s41467-019-10523-3 (2019).
11 Ito, T. *et al.* Regulation of myeloid leukaemia by the cell-fate determinant Musashi. *Nature* **466**, 765-768, doi:10.1038/nature09171 (2010).
12 Palacios, F. *et al.* Musashi 2 influences chronic lymphocytic leukemia cell survival and growth making it a potential therapeutic target. *Leukemia* **35**, 1037-1052, doi:10.1038/s41375-020-01115-y (2021).
13 Park, S. M. *et al.* Musashi2 sustains the mixed-lineage leukemia-driven stem cell regulatory program. *The Journal of clinical investigation* **125**, 1286-1298, doi:10.1172/JCI78440 (2015).
14 Aly, R. M. & Ghazy, H. F. Prognostic significance of MSI2 predicts unfavorable outcome in adult B-acute lymphoblastic leukemia. *International journal of laboratory hematology* **37**, 272-278, doi:10.1111/ijlh.12284 (2015).
15 Mu, Q. *et al.* High expression of Musashi-2 indicates poor prognosis in adult B-cell acute lymphoblastic leukemia. *Leukemia research* **37**, 922-927, doi:10.1016/j.leukres.2013.05.012 (2013).
16 Zhao, H. Z. *et al.* Prognostic significance of the Musashi-2 (MSI2) gene in childhood acute lymphoblastic leukemia. *Neoplasma* **63**, 150-157, doi:10.4149/neo_2016_018 (2016).
17 Bardini, M. *et al.* Antileukemic Efficacy of BET Inhibitor in a Preclinical Mouse Model of MLL-AF4(+) Infant ALL. *Molecular cancer therapeutics* **17**, 1705-1716, doi:10.1158/1535-7163.MCT-17-1123 (2018).
18 Buentke, E. *et al.* Glucocorticoid-induced cell death is mediated through reduced glucose metabolism in lymphoid leukemia cells. *Blood cancer journal* **1**, e31, doi:10.1038/bcj.2011.27 (2011).
19 Dyczynski, M. *et al.* Metabolic reprogramming of acute lymphoblastic leukemia cells in response to glucocorticoid treatment. *Cell death & disease* **9**, 846, doi:10.1038/s41419-018-0625-7 (2018).
20 Weinberg, S. E. & Chandel, N. S. Targeting mitochondria metabolism for cancer therapy. *Nature chemical biology* **11**, 9-15, doi:10.1038/nchembio.1712 (2015).
21 Skrtic, M. *et al.* Inhibition of mitochondrial translation as a therapeutic strategy for human acute myeloid leukemia. *Cancer cell* **20**, 674-688, doi:10.1016/j.ccr.2011.10.015 (2011).

22 Panina, S. B., Pei, J. & Kirienko, N. V. Mitochondrial metabolism as a target for acute myeloid leukemia treatment. *Cancer & metabolism* **9**, 17, doi:10.1186/s40170-021-00253-w (2021).

23 de Beauchamp, L., Himonas, E. & Helgason, G. V. Mitochondrial metabolism as a potential therapeutic target in myeloid leukaemia. *Leukemia* **36**, 1-12, doi:10.1038/s41375-021-01416-w (2022).

24 Kerstjens, M. *et al.* MEK inhibition is a promising therapeutic strategy for MLL-rearranged infant acute lymphoblastic leukemia patients carrying RAS mutations. *Oncotarget* **8**, 14835-14846, doi:10.18632/oncotarget.11730 (2017).

25 Wander, P. *et al.* High-Throughput Drug Library Screening in Primary KMT2A-Rearranged Infant ALL Cells Favors the Identification of Drug Candidates That Activate P53 Signaling. *Biomedicines* **10**, doi:10.3390/biomedicines10030638 (2022).

26 Sleire, L. *et al.* Drug repurposing in cancer. *Pharmacological research* **124**, 74-91, doi:10.1016/j.phrs.2017.07.013 (2017).

27 Alford, S. E. *et al.* BH3 Inhibitor Sensitivity and Bcl-2 Dependence in Primary Acute Lymphoblastic Leukemia Cells. *Cancer research* **75**, 1366-1375, doi:10.1158/0008-5472.CAN-14-1849 (2015).

28 Tregnago, C. *et al.* Novel Compounds Synergize With Venetoclax to Target KMT2A-Rearranged Pediatric Acute Myeloid Leukemia. *Frontiers in pharmacology* **12**, 820191, doi:10.3389/fphar.2021.820191 (2021).

29 Benito, J. M. *et al.* MLL-Rearranged Acute Lymphoblastic Leukemias Activate BCL-2 through H3K79 Methylation and Are Sensitive to the BCL-2-Specific Antagonist ABT-199. *Cell reports* **13**, 2715-2727, doi:10.1016/j.celrep.2015.12.003 (2015).

30 Erazo, T. *et al.* TP53 mutations and RNA-binding protein MUSASHI-2 drive resistance to PRMT5-targeted therapy in B-cell lymphoma. *Nature communications* **13**, 5676, doi:10.1038/s41467-022-33137-8 (2022).